Modelling and simulation of solar heating systems

Mørck, Ove C; Korsgaard, Vagn

Publication date:
1985

Document Version
Publisher's PDF, also known as Version of record

MODELLING AND SIMULATION OF SOLAR HEATING SYSTEMS

Ove C. Mørck

October 1985

THERMAL INSULATION LABORATORY
TECHNICAL UNIVERSITY OF DENMARK
report no. 170

Knowledge starts with practical experience, and theoretical knowledge gained through practical experience must therefore turn back to practical experience.

Mao-Tse-Tung.

PREFACE

Solar energy utilization will be of steadily increasing importance for the supply of the world's energy demand in the future. Of solar energy's applications, the conversion to heating energy for use in buildings seems to be one of the most simple and straightforward. However, optimum strategies for the design, construction and operation of solar heating systems are essential to accelerate the use of this technology, in order to be prepared for the future.

Modelling and simulation is one of the research and development activities needed to develop optimum strategies for efficient use of solar energy. As the speed capacity of micro-computers increase, simulation programs will gain ground as design tools in the coming years.

In this document I have summarized the work I have been conducting on modelling and simulation of solar heating systems, active as well as passive. During the past four years I have been engaged in international cooperation within the solar research programmes of the Commission of the European Communities (CEC) and the International Energy Agency (IEA). As part of this engagement I have undertaken a number of different activities covering various aspects of modelling and simulation of solar heating systems. With a few exceptions, the work presented here has been conducted in this context.

The theme of the presentations is the process of model development, validation and use. The intension and hope is that by emphasizing the process, the documents will prove useful to future modellers.

ACKNOWLEDGEMENTS

This document forms the principal part of my dissertation for the Danish Ph.D. degree "Licentiatus Technices". Sub-dissertations are the two reports entitled "Common Solar Simulation and Validation in Europe (Jørgensen, 1982a) and "Simulation Program Validation using Domestic Hot Water System Data" (Jørgensen, 1982b). A summary of these reports is included in Chapter 4 of this document. The study has been conducted at the Thermal Insulation Laboratory at the Technical University of Denmark with Professor Vagn Korsgaard as tutor.

My work at the Thermal Insulation Laboratory has been funded by the Danish Ministry of Energy and the Commission of the European Communities. I acknowledge my indebtedness to these organizations.

The primary inspiration for my work stems from the international research projects in which I have been engaged, and I feel indebted to the many colleagues and friends I have met through these activities. I also appreciate the many fruitful discussions with my colleagues at the Thermal Insulation Laboratory. Especially, I want to thank Peder Vejsig Pedersen and Ole Balslev-Olesen for the friendly and creative atmosphere in the office we share. I also wish to thank Preben Nordgaard Hansen for his gentle reminders at the right moments to keep me on track for the completion of my study.

Sally Lykke Høgsted has prepared many of the program input data files, computer plots, hand illustrations, front and title pages. She manages the incredible and I thank her for all her help. This document was typed by Kirsten Weishaupt whom I thank for the professional way in which she carried out her job with a balance of great patience and attention to a tight schedule. I also thank Birthe Friis for her expedient computer service for the continuous updating of the reference list.

Last but not least, I thank Thit and Pia for their understanding and encouragement.

September 5, 1985 Ove C. Mørck*)
Thermal Insulation Laboratory
Technical University of Denmark

---

*) Last name changed from Jørgensen to Mørck on February 1, 1985.

CONTENTS

1. SUMMARY

Mathematical simulation models are introduced as indispensable and useful tools for the design of solar heating systems in buildings as well as for research and development purposes. The modelling process is described and is used as the underlying theme for the presentation in the document.

The first steps of the modelling process for solar heating systems, covering definition of system to be modelled, component break-down and boundary conditions, are described, and selected physical topics used for the foundation of the model construction are accounted for.

A summary of earlier work by the author, concerned with validation of simulation models for active solar systems, is given.

The development of a thermal network simulation program, to be used on micro-computers, is described with special attention to the solar radiation processor, solar radiation transmission and absorption in transparent covers and auxiliary heating control. The layout of the computer program is presented.

Following a brief introduction to the concept of validation, two empirical validation studies, which were undertaken for the developed simulation model, are described in detail. The predictions exhibit acceptable agreement with the measured data for both a direct gain test building and an attached sunspace.

The use of simulation models is illustrated by three separate examples: A parametric sensitivity study, a comparison of the performance of direct gain and solar wall passive systems, and an investigation of the impact of modifications to the attached sunspace used for the empirical validation work.

The future of solar heating systems design, using thermal simulation programs as part of integrated Computer Aided Design (CAD) software packages, is roughly sketched, and the attention is drawn to the critical importance of the interface between the CAD-systems and the thermal simulation programs.

2. INTRODUCTION

2.1 The Design Problem

Even the simplest mud-clad hut or snow igloo providing shelter from warm or cold weather creates complex physical systems in its thermal interactions with the environment. Complicated conductive, convective and radiative heat transfer mechanisms are taking place. A basic understanding of the practical implications of these mechanisms has been utilized successfully in vernacular architecture for centuries.

Just as the hut and igloo of older times were complicated structures, from a thermal physical viewpoint, modern buildings are even more so. An immense number of ways exists in which buildings can be composed utilizing the still-growing number of materials and construction methods. This complexity, in combination with a stronger community demand for thermal comfort at a reduced energy consumption level, has the implication that traditionally acquired knowledge no longer applies. Vernacular architecture may give guidance to todays designers, but the old principles cannot simply be considered valid. Also, since the oil crisis in 1973, a growing interest in the utilization of solar energy as a means of obtaining increased comfort at a reduced fuel consumption has made the design of buildings in balance with the local climatic conditions a matter of great complexity. The need for tools which can be used to provide a better understanding of the dynamic performance of buildings and solar heating systems has arisen. Mathematical modelling and simulation constitute the basis for the development of such tools.

2.2 Modelling and Simulation

A mathematicl model of a building or a solar heating system is a set of equations representing the physical reality.

The model is an imitation of the system. By stepwise calculations using known climatic conditions as boundaries, the model is brought through changing environmental conditions, typically over one year. In this process, the model behaves thermally like the system it imitates; thus the system is said to be simulated. What characterizes this simulation process is that detailed information about the thermal variables is available at each step of the calculation.

Mathematical modelling and simulation for the analysis of the thermal performance of buildings and thermal solar systems have received a considerable interest since the 1960's. A large number of computer models have been developed in different parts of the world. A recent survey of models for passive solar building performance analysis (Jørgensen, 1983) contains 31 different models for buildings alone. Other surveys include several other models developed for special purposes.

Mathematical simulation models should be used in parallel with, and as complementary to, the physical experiment. Compared to the physical experiment they offer substantial advantages:

- greater flexibility for system configuration, design and modification
- quickly obtainable results allowing for immediate evaluation and modification
- freedom from instrumentation and equipment performance problems (except for computer breakdowns) which can result in major delays
- ability to control input variables including system operation and climate conditions
- ability to evaluate the performance of innovative design concepts for which little or no hardware exist
- ability to identify optimal design parameters
- ability to evaluate seasonal performance without a year or more of testing.

In short, the use of simulation models makes it possible to achieve various results at a reduced cost, risk and use of time. The models can be used for design as well as research purposes.

But what is the reason for the existence of so many different models? Would one model not be sufficient? The large and still growing number of models is the combined effect of the following factors:

1. Models have been developed in different parts of the world and for use on different computers.
2. Modellers, persons who construct the models, have different viewpoints as to how a model should be constructed.
3. When a model is developed, it is impossible to foresee what new concepts it might be relevant to include in the model for future analysis. In particular, researchers often discover that existing models do not fulfil their requirements for the analysis of innovative design concepts.

Since these reasons will always be valid, new models or additions to existing models will always be developed.

2.3 The Modelling Process

Model development can be visualized as the cyclical process shown in fig. 2.1. To develop a certain model, the process often has to be repeated several times. Each stage of the process feeds or receives information about the problem in question, either to or from the total fund of knowledge, and the information gained during the validation of the model might, for example, add something new to the system analysis stage, which in turn changes the solution technique or computer program.

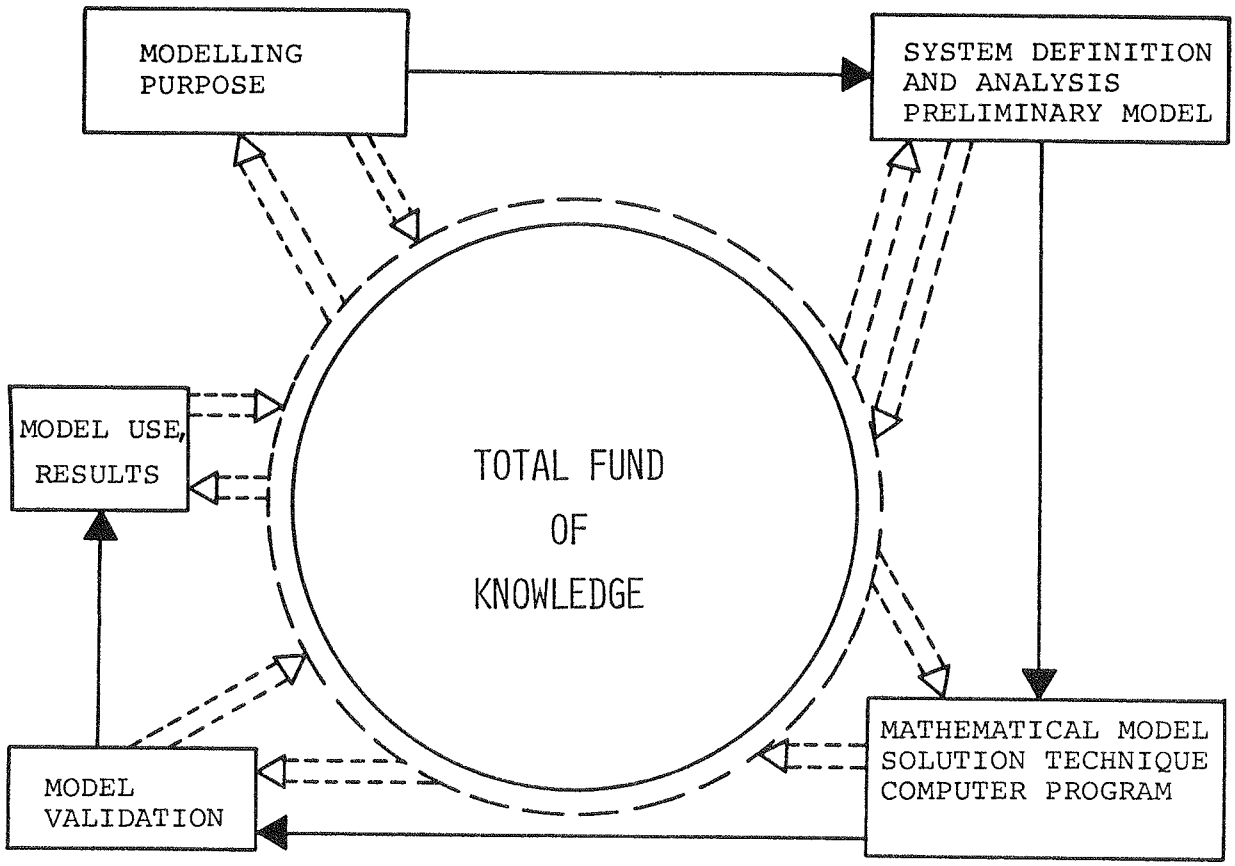

Fig. 2.1 Model development as a cyclical process.

Stage 1: Modelling purpose

The first stage of the modelling process is to resolve the purpose of the model. For example, is the model going to be used for investigation of innovative concepts or performance analysis in a design context?

Stage 2: System definition and analysis. Preliminary model

At this stage the system to be modelled is analysed. The analysis provides answers to questions such as: Which components form part of the system? What are the characteristics of these componenets? What are the boundary conditions? Which information is available? What is the level of detail needed? What are the primary variables to be considered?

On the basis of this analysis, a preliminary model can be generated. The preliminary model is a first rough sketch of how the actual system is going to be modelled, showing the level of detail, number of variables and chosen time scale. At the same time, a preliminary decision regarding a modelling strategy is taken, as this strongly influences the kind of information needed for the model as well as the possible output from the model.

Stage 3: Mathematical model, solution technique, computer program

In this stage the model is expressed in mathematical form by a set of equations. A solution technique for solving the equations and a computer program is generated. Choices to be made during this stage are:

- form and number of equations needed
- solution technique
- programming language
- method of providing input data to the model
- presentation of model results to fulfil stated purpose.

Stage 4: Model validation

When the computer program is generated, it has to be extensively tested before any confidence in the results can be achieved. In addition to what could be called external effects, such as user errors in interpretation of the actual building system or errors in weather data, the testing involves three aspects of the model:

- mathematical treatment
- programming errors
- model shortcomings

The mathematical treatment covers the form of the equations used to represent the model intensions and the solution techniques used. This can be tested by running several test cases and applying "sound engineering judgement" to the results. Also, special analytical test cases as described by Judkoff et al. (1983) are useful for this analysis.

Programming errors are difficult to handle. The simple ones show up at once, either by peculiar results or by runtime error messages from the compiler: "RUN TIME ERROR, DIVIDE CHECK OVERFLOW". Other programming errors or "bugs" in the program might not show up directly but affect the model predictions in a random way. These errors differ widely in nature, and no general method for testing and constructing programs to avoid "bugs" exists. Among programmers it is often heard that "the last bug is never found"; however, the validity of this expression is not very easy to check.

The search for shortcomings or model errors is concerned with how accurately the model resembles the physical reality. Comparisons between model predictions and measured data from real systems or buildings are the primary part of this test. As measured data do not exist for a large variety of systems, a useful complement to the model-to-data comparisons is model-to-model comparisons on a series of cases using systematic variations of parameters.

Stage 5: Model use, results

At this point the circle is closed. The model is used to produce the results intended from the outset. This might be anything from the detailed analysis of the thermal behaviour or a new salt-hydrate storage tank to parametric sensitivity analyses of the impact of window size and mass levels in direct gain multi-family dwellings.

2.4 Document Organization

The modelling process as outlined in the preceding section is the basis for the organization of the contents of this document. The modelling purpose has been dealt with in the two first paragraphs of this chapter. Chapter 3 deals with various aspects of system definition and analysis and also the setting up of preliminary models. Earlier work by the author on modelling and simulation of active solar heating systems has been summarized in chapter 4. This summary deals mainly with the three latter stages of the model development circle and it was believed appropriate to include it here before these stages are treated in detail for passive solar heating systems.

Chapter 5 describes the actual development of a computer model to simulate passive solar heating systems. Several aspects of this development is covered, ranging from choice of solar processing algorithms to overall organization of computer program.

The model developed was validated against two different sets of measured data. The first set originates from a Canadian two-zone direct gain test building. The second set of data stems from a dwelling built as part of the Danish activities within Task VIII, Passive and Hybrid Solar Low Energy Buildings of the IEA Solar Heating and Cooling Programme. These validation activities are described in chapter 6.

Chapter 7 provides examples of results obtained with different computer codes and discusses these briefly.

Overall conclusions are drawn in chapter 8, and chapter 1 provides a summary of the entire document.

3. SYSTEM DEFINITION AND ANALYSIS

3.1 Defining the Modelling Problem

Modelling the travel of a space vehicle does not follow the same strategy or employ the same solution techniques as the modelling of a district heating system. It is therefore necessary to carefully define and analyse the problem in question prior to the actucal model construction. This analysis provides and systematizes information needed for setting up a model and at the same time increases the understanding of the problem. In addition, this preliminary analysis often leads to significant simplifications and limitations of the problem.

In the following paragraphs, a preliminary analysis covering both active as well as passive solar heating systems will be presented. While attempting to be as general as possible (e.g. using the terms "solar heating systems"), the primary focus is on passive solar heating systems

3.2 The Environment

Solar heating systems strongly interact with their environment. Solar radiation, sky temperatures, ambient temperature, precipitation, humidity, and wind as well as ground temperature are the external conditions to which any solar system is exposed. Figure 3.1 is an illustration of this environment.

Solar radiation

Obviously, solar radiation is the dominating external variable for solar systems. The solar radiation reaching any surface on the earth is composed of a direct (beam) and diffuse component. Since the transmittance of the solar radiation through collector covers or windows is a function of the incidence angle, it is important to establish the correct relationship between direct and diffuse radiation.

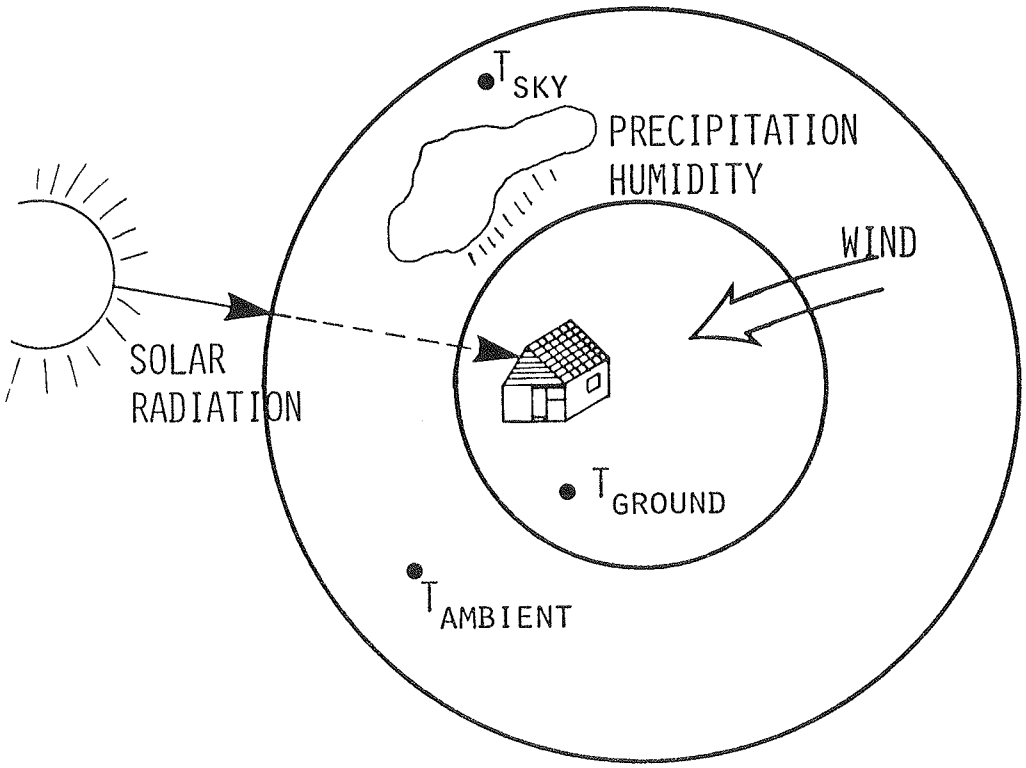

Fig. 3.1 Solar system environment.

As measurements of these quantities are not normally undertaken continuously over an extended period by the meteorological weather stations, they have to be calculated on the basis of global, horizontal radiation. Several approaches to this calculation have been suggested, some assuming that the diffuse radiation is isotropically distributed over the sky and some that it is anisotropically. An illustration of the impact on model predictions of using different solar radiation calculation procedures is found in Jørgensen (1979c).

Currently a task (Task IX) of the IEA Solar Heating and Cooling Programme (IEA, 1983) is carrying out a validation study of solar radiation models. Results and recommendations are expected at the beginning of 1986.

Ambient and sky temperatures

Any surface on the earth exchanges heat in the form of radiation with the sky. Information about sky temperatures are very seldom available and several expressions have been developed to calculate the sky temperature based on the ambient temperature (Duffie and Beckman, 1980). The presence of clouds and long wave radiation exchange with the ground complicate the picture, and a well-documented and tested procedure to calculate this radition exchange does not yet exist. For active solar systems it is usually of minor importance (Duffie and Beckman, 1980), and, for buildings, the heat loss coefficient from the roof is sometimes increased by 10-15% to take into account this additional heat loss.

Ambient temperature is measured at hourly intervals at many meteorological stations. It is the driving force for heat exchange by conduction and convection.

Precipitation and humidity

The impact of precipitation is considered to be of such an order of magnitude that it needs not be taken into account. Humidity, however, is important for latent load calculations in connection with the simulations of cooling systems. For heating systems alone, it need not be considered.

Wind speed and direction

The presence of wind increases the convection heat exchange at exterior surfaces. Several expressions (Duffie and Beckman, 1980) have been suggested to account for this effect, but the dependence on wind direction is still not clear. The wind speed also affects the air infiltration of a building. Different approaches have been suggested to account for this effect (see e.g. Palmiter and Wheeling), while the dependence of wind direction has yet to be clarified. Often a constant air exchange per hour is estimated instead.

Ground temperature

Again, measurements are scarce for ground temperature, but since ground coupling of passive systems is not an issue under Danish conditions, a simplified approach is often chosen by calculating heat losses to the ground, assuming the ground temperature to be 8^{o}C constantly over the year.

Test reference year

Meteorological conditions change from one year to another. To select a certain year for solar system simulations would therefore bias the results. As the dynamic nature will be smoothed out by simply averaging the climatic variables from several years, other methods have been developed to establish climatic data which are representative for a given site. For several CEC countries, such test reference years (TRY) have been constructed by selecting each month from several years of data using statistical methods (Lund, 1985). These TRY's contain hour-by-hour values of the climatic variables needed for solar system simulations. Other approaches to find or construct appropriate weather data exist outside the CEC countries, e.g. Test Meteorological Years (TMY) in the U.S.

Recently, several methods have been developed to construct short reference years which contain the same hour-by-hour data, but for selected periods of the year. The primary objectives of this development are to limit the time needed for simulation and the storage requirements. Typically, the simulation time on a micro-computer can be reduced from more than one hour to 10-15 minutes by using a short reference year. As the speed and capacity of micro-computers increase, short reference years will probably be of less importance in the future.

3.3 Solar System Components

A component-by-component breakdown of the solar system to be modelled is necessary to identify key variables for

which information from the simulations is wanted. This analysis is also useful for the actual programming of the computer model as it is often logical to organize the complete program in subprograms in accordance with the physical subdivision in components. The primary components of a solar heating system are: the collector, the heat transport mechanisms, the storage, the distribution system and the controls. Figure 3.2 presents in schematic form the components of typical active and passive systems.

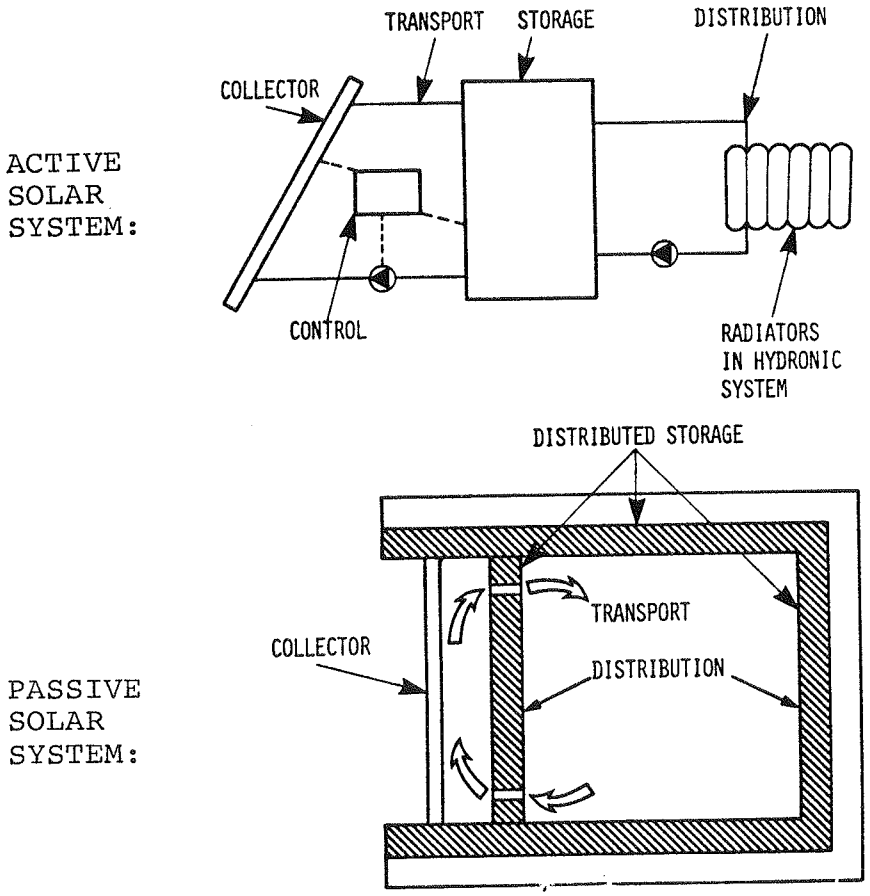

Figure 3.2 Active and passive solar system components.

The collector

As the designation indicates, the collector collects solar radiation. For active solar systems it is a clearly separate component. In passive systems it is often an integrated part of the structure. In both cases, however, the

collector encompasses a transparent cover and an absorber. The physical characteristics and dimensions of both are important parameters for the model. The temperature of the absorber is also an important variable as it is often used for control purposes.

Heat transport mechanisms

The way in which heat or energy is exchanged between collector and storage and from storage to load depletion is the basis for the designation of the system. In an active system, heat transport is carried out by mass transport forced by controlled fans or pumps. In a passive system, naturally occuring conduction, convection and radiation exchange the heat, and, in a hybrid system, a combination of these mechanisms take place. Naturally, the important parameters differ between the different systems. Mass flow rate, fluid densities and specific heat are the parameters to look for in active systems, and surface convection and radiation coefficients and thermal conductivity govern heat transfer in passive systems. Temperatures and mainly energy flows are the variables of interest.

Storage

The storage of heat is essential for the utilization of solar energy for heating. Both on a short term as well as on a long term basis, solar radiation generally arrives out of phase with the demand. In a way, the storage phase-shifts the collected energy to better suit the demand. The thermal capacity, heat loss coefficient and the resulting time-constant are parameters, and the temperatures plus the energy flows to and from the storage are the variables of primary interest.

The distribution system

The distribution system is probably the single component of

solar heating systems that physically exists in the largest variety; however, the thermal processes utilized in all cases are similar. In a hydronic system, heat is transported from the storage as mass transfer and dissipated by convection and radiation from the radiators. Heat storage walls or floors in passive systems also dissipates the heat by convection and radiation exchange. Again, thermal properties are the parameters, and temperature and especially energy flows the variables of interest.

The controls

Controles regulate the heat transport mechanisms. Primarily on/off controls are used but also controls working continuously from an off to a fully on position are used. The governing parameters are temperature set points, and the variable to be extracted from the simulation is the status of controls.

3.4 Physical Fundamentals

Physics is an old science. An abundance of information in the form of textbooks and articles can be found on basic physical principles relevant to the construction of solar thermal simulation models. An attempt is made here to put together the knowledge and information most relevant in this context.

General background

One textbook on active solar heating systems (Duffie and Beckman, 1980) is so well-known within the solar community that it almost seems superfluous to reference it. Acquaintance with this book is considered to be part of the necessary background of a solar system modeller. Also, relevant mathematical knowledge is implied.

The transient heat conduction equation

The transient heat conduction equation (Whitaker, 1983):

$$\frac{\partial T}{\partial t} = \alpha \nabla^2 T + \frac{\phi}{\rho C_p} \tag{3.1}$$

where α is the thermal diffusivity defined by:

$$\alpha = \frac{k}{\rho C_p} \tag{3.2}$$

is the basis for the numerical analysis of transient heat conduction processes on computers. By discretization of the space and time variables, an approximative equation can be obtained. For simplicity we look at the equation in one dimension and omit the heat flux term:

$$\frac{\partial T}{\partial t} = \alpha \left(\frac{\partial^2 T}{\partial x^2} \right) \tag{3.3}$$

Discretization yields:

$$\frac{T_{i,j+1} - T_{i,j}}{\Delta t} = \alpha \frac{(T_{i+1,j} - T_{i,j}) + (T_{i-1,j} - T_{i,j})}{\Delta x^2} \tag{3.4}$$

where the discrete time steps are designated by j, $j+1$ and discrete spatial steps by $i-1$, i and $i+1$.

In (3.4) the spatial derivative is evaluated at the time j, whereas the time derivative is evaluated at the time $j + \frac{\Delta t}{2}$.

It is seen that the temperature at the point i and at the new time $j+1$ is completely determined by the previous state of time j. This approach is called an explicit method or also referred to as simple Euler integration. Had the spatial derivative been evaluated at the time $j+1$ or any time between j and $j+1$, say $\frac{\Delta t}{2}$, the approach would be designated an implicit integration technique.

Implicit calculation is generally considered a more accurate method and the method is completely stable.

The explicit solution technique requires that:

$$\frac{\alpha}{\Delta x^2} < \frac{1}{2} \tag{3.5}$$

in order to obtain mathematical stability and to ensure that the second law of thermodynamics is not violated.

Another important aspect to consider when selecting one of these methods is that boundary conditions are imposed at once on the calculations using the implicit method, whereas their impact is always one step behind in the explicit method (Whitaker, 1983).

The Biot number

The size of the Biot number (3.6) calculated for a given wall surface of a building indicates the characteristics of the heat transfer process between the zone air and the wall surface.

$$N_{Bi} = \frac{hL}{k} \tag{3.6}$$

where L is an appropriate characteristic length, e.g. half the thickness of a slab or building material.

When $N_{Bi} << 1$ the film resistance dominates the process and the slab can be considered isothermal. In other words, the slab can be considered to have negligible resistance compared to the film coefficient. The total heat exchange over the surface during the time t is given by the expression (Whitaker, 1983):

$$Q = \rho C_p V(T_o - T_1)(1 - \exp(-t/\tau)) \tag{3.7}$$

where

$$\tau = \rho C_p V/\langle h \rangle A \tag{3.8}$$

is the time constant of the slab and $\langle h \rangle$ is the average

film coefficient over the area A. V is the volume of the slabs.

When $N_{Bi} >> 1$ the internal resistance in the slab dominates the heat transfer process and the situation is somewhat more complicated. The heat flux at the surface is shown by Whitaker (1983) to be:

$$Q = \frac{k}{\sqrt{\pi \alpha t}} (T_1 - T_o) \qquad (3.9)$$

This equation can be used to define a "new" film heat transfer coefficient:

$$h = \frac{k}{\sqrt{\pi \alpha t}} \qquad (3.10)$$

Building thermal network

Citing Muncey (1979): "The heat flow network in a building can generally be looked on as a set of slabs finite in the direction of heat flow and large in area of right angles thereto, connected in a series-parallel network". Each of these slabs has a thermal capacity and a resistance value. It is well known that dynamic heat transfer through buildings can be modelled using an analog electrical network, when capacitors resemble heat capacities and resistors resistances. Each capacity of the building can be modelled as a tee circuit, see fig. 3.3.

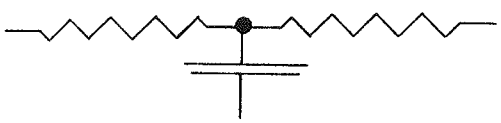

Fig. 3.3 Tee circuit model of building element.

The differential equations governing the network can be obtained by applying Kirchhoff's laws to the network: In short they say that all heat entering a node must leave it

again and that the temperature at each node is unambiguosuly determined by the temperatures of the surrounding nodes. The solution to the differential equations of the electrical network is identical to those of the heat transfer problem, provided that each capacity term of the latter is considered to be isothermal.

Active solar heating systems can also be approximated by analog electrical network models. The mass heat transfer process has only to be modelled as conductance through a very small resistance.

3.5 Required Level of Detail

From a researcher's point of view, a model is primarily intended to increase his/her understanding of the dynamic performance of the system modelled. All significant state variables (temperatures) must be available as model output. In active solar heating systems, the significant temperatures are the temperature of the absorber plate, temperatures within the piping, and at different heights of the storage tank; in short, temperatures throughout the system. Basically, the same is valid for passive systems. To really understand the dynamic response of a building, surface temperatures, temperatures inside walls and zone air temperatures, are all equally important. Also, the possibility to extract the main heat fluxes should exist at every instant of time.

3.6 Preliminary Model Selection

Three different approaches exist for the modelling of heat transfer problems within buildings. The response factor method is a powerful calculation procedure based on the linearity of the thermal systems described by the diffusion equation (3.1). This means that if f_1 and f_2 are two solutions both satisfying (3.1), then any combination $af_1 + bf_2$ (where a and b are constants) will satisfy the

equation. The harmonic methods build on the assumption of periodicity of events, an assumption which limits their use to design-day calculations.

In finite difference methods, building segments and system components are considered as nodes of a network, and differential equations for each of the nodes in the network are solved at successive time intervals. The primary advantage of this method is that the model network, in a direct logical way, represents the physical reality as an icon does. When constructing a model for a specific purpose, i.e. the modelling of a certain building to a certain level of detail, it is a straightforward process to identify nodes and to set up the governing differential equations. At the same time, the required level of detail automatically "pops out" of the calculations as all the node temperatures are calculated at each time step.

4. ACTIVE SOLAR HEATING SYSTEMS

4.1 Description of Activities

The author was involved [1] in international cooperation within the solar research and development programme of the CEC [2] and the IEA [3] on the subjects of development and evaluation of simulation models for active solar heating systems during the period 1978-1982. This involvement was completed with two activities documented in reports entitled: "Common Solar Simulation and Validation in Europe" and "Simulation Program Validation using Domestic Hot Water System Data", (Jørgensen, 1982a and 1982b). A brief overview of these activities, including the main objectives and findings, will be presented in this chapter.

Background

Both within the IEA and the CEC programmes, model-to-model comparisons were used in the initial model evaluation phase. Hypothetical systems were defined and simulated for different sets of weather data. The model predictions were compared on hourly, monthly and yearly bases. These comparisons of temperature profiles and energy flows resulted in the detection of programming errors and in the identification of model weaknesses (e.g. solar radiation processors). The underlying philosophy of this approach was: "If they all agree, they must be right, since they cannot all be wrong!" The reasoning behind this argument was that the many models used in these exercises were very different in the level of detail as well as in the chosen assumptions. The experience gained through this work is documented in (Jørgensen, 1979a, 1979b, 1979c).

[1] as the project leader and as a participant. As a project leader he was responsible for the planning of work and the summarizing of results.

[2] Commission of the European Communities.

[3] International Energy Agency.

Objectives

At the completion of the model-to-model exercises, detailed performance data from well-instrumented solar systems had become available. It was a natural follow-up to the previous work to test and evaluate the models by comparing the model predictions to measured data (model validation, see chapters 3 and 6).

The primary objective of both activities was therefore to validate the computer codes of the participants. A secondary objective was to use the models to perform sensitivity analyses, the latter also being considered as a test of the applicability of the models to the parameter variations.

The systems

The reader is referred to the original documents for a complete description of the systems providing the data. In brief, the systems used in the IEA work were four different domestic hot water systems located at the same place in the U.S. The CEC systems comprised a total of eight systems of the same design, a solar heating system for a single-family house with a collector area of 47 m^2 and a storage tank of 3 m^3. One system was erected in each of eight different countries of the CEC. These heavily instrumented and well-controlled systems were designated "Solar Pilot Test Facilities" (SPTF).

The IEA activities

One month of 10-minute data for the DHW-systems were used to validate the models. At a later date, one week of data for one of the systems were used for a second round of validation. A parameter sensitivity analysis for one of the systems was also repeated.

The CEC activities

The validation activities within the CEC were undertaken both as local activities using the data from the national SPTF and by data exchanged from two SPTFs to all the other participants. Furthermore, the validation work was subdivided into component validation and system validation work. In addition to the validation work, three parameter sensitivity analyses were performed.

4.2 Brief Model Survey

A total of 14 different simulation models were used in the two studies representing a wide range of approaches from a simple, lumped circuit model with one significant capacity, forwards Euler integration and constant collector parameters (U_L, $\tau\alpha$) to detailed thermal network models using 10-15 nodes for which the differential equations were solved simultaneously using an implicit method. Table 4.1 provides an overview of one of the main characteristics of the models: the integration method.

TABLE 4.1 DISTRIBUTION OF MODELS BY INTEGRATION METHOD USED.

Explicit,	(simple, forwards Euler) :	8
Explicit,	analytical :	2
Implicit,	(backwards Euler) :	3
Implicit,	trapez :	1
	Total :	14

Various ways of modelling the solar collector were possible in several of the programs. Simple straight-line efficiency curves with constant $\tau\alpha$ and U_L values could be exchanged with detailed subroutines. This large variety of models had two significant advantages. First, it was relatively easy to compare the predictions of different models on the same test cases to learn what the impact was of different approaches and

assumptions. Second, the feeling was that if models this different agreed in model-to-model comparison studies, increasing confidence could be gained in each of the models.

4.3 Results

CEC activity

The results of the national and common validation work were very similar. By comparing measured and predicted states of the system and dynamic behaviour on comparison plots, the agreement seemed satisfactory. A detailed comparison of integrated energy flows revealed, however, in some cases unacceptable differences on the order of 10-15%. The reasons for these differences are difficult to identify, the more obvious ones are:

- wrong input data
- inaccurate operation of the building load interface of the SPTF-system
- malfunctioning of components
- model shortcomings

A set of three parameter sensitivity analyses were undertaken. The conclusion drawn on the basis of the first analysis, which was simulation of the national SPTF, was that the SPTFs in the different countries differed more than expected.

When the same SPTF (the Danish) was modelled in the second study, a reasonably close agreement was obtained on collector area, storage volume and pump starting and stopping differential set points. All the models were used to analyse the same parameter changes, thus allowing for a model-to-model comparison evaluation of the models. The actual results were as expected and differences had simple explanations.

In the third analysis, where the sensitivity to pump energy, heat exchanger effectiveness and number of thermal layers in the storage were investigated, a reasonably close agreement was again obtained among the three models capable of analysing these changes (DK, GB2 and NL). Of interest here is to mention that 5-7 layers seemed sufficient for an adequate simulation of temperature stratification in the storage tank of this system.

Figure 4.1 presents the results of this analysis. It should be mentioned that the SPTFs were not particularly designed for a strongly stratified storage tank.

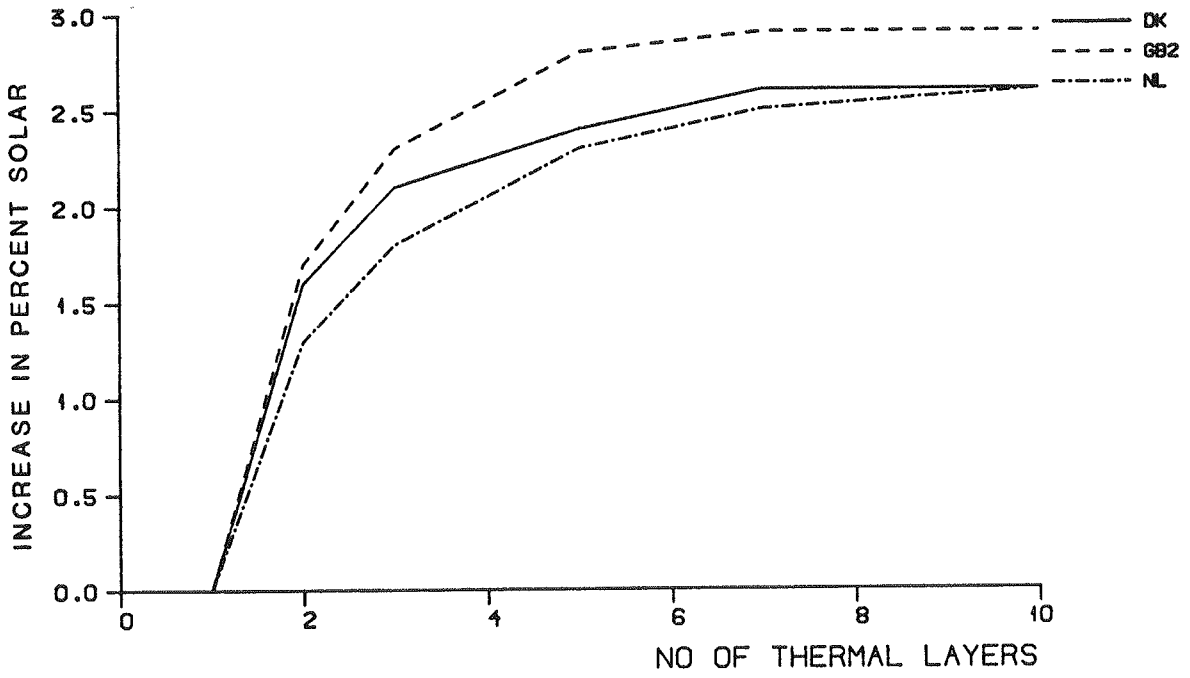

Fig. 4.1 Results of CEC parameter sensitivity analysis III. (Jørgensen, 1982a).

IEA activity

Two rounds of computer simulation model evaluation work were undertaken. Both consisted of model-to-measured data validation and model-to-model comparisons in a parameter sensitivity analysis. The second round showed drastically improved results for both activities.

The main reason for this improvement lies in the fact that each modeller participating in this work interpreted the system description and the other specifications according to his/her own background. When the results were presented and discussed at experts' meetings, the differences in interpretation became apparent and could be coordinated to achieve a more uniform approach by all the participants. This led to the more satisfactory results in the second round. The improvement obtained in the second round is clearly illustrated in table 4.2.

TABLE 4.2 MEASURED AND PREDICTED SOLAR FRACTIONS.

(Jørgensen 1982b)

	Measured	Predicted						
		B & D	H	I	J	K	L.F.	T & K C & N
round 1	66	67	82	74	68	75	70	90
round 2	60.5	58.1	59.9	59.1	61.5	60.9	60.5	60.3

B & D: Boussemaere & Delire,B
H : Hedstrom, USA
I : Inooka, J
J : Jørgensen, DK
K : Kennish, USA
L.F. : La Fontaine, U.K.
T & K: Therre & Kuijk, Sch.
C & N: Calatayud & Nilsson, Sch.

The exceptionally fine agreement obtained between model predictions and measured data is also illustrated by fig. 4.2, showing hourly values of a highly dynamic variable, the solar collector output. The predictions shown here stem from a thermal network code utilizing matrix inversion techniques for a simultaneous solution of the 13 differential equations. This code, developed by the author (Jørgensen and Mørkeberg, 1980), is based on the same principles and thus very similar to the network program described for passive solar buildings in chapter 5.

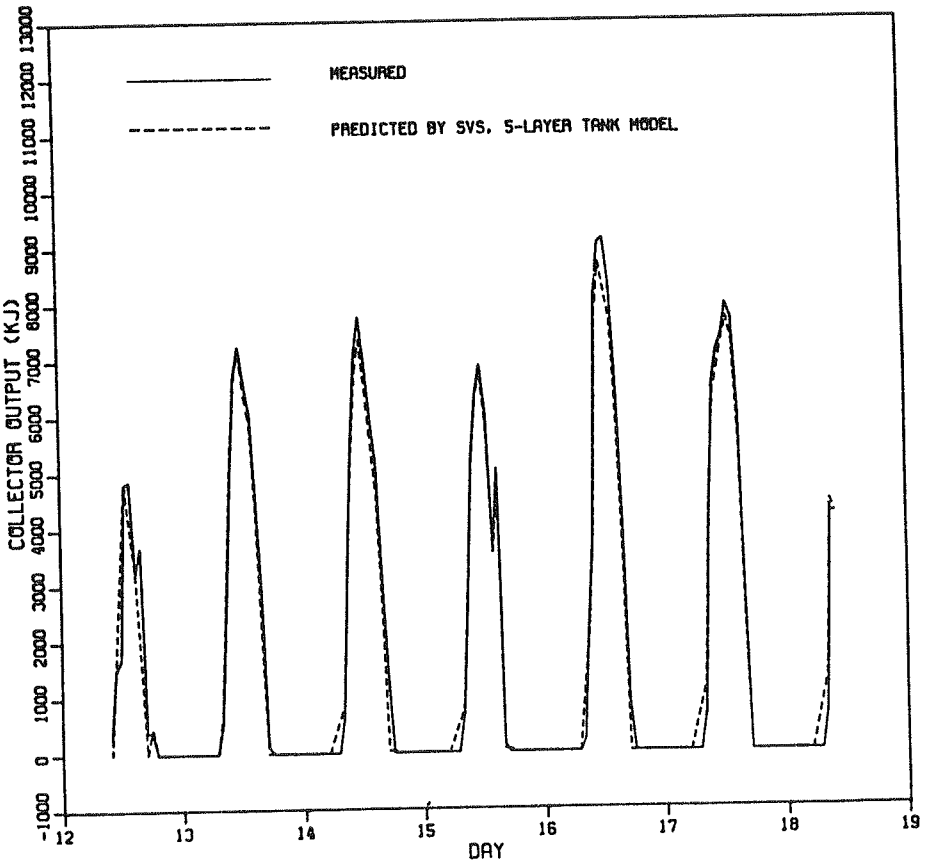

Fig. 4.2 Measured and predicted collector output for DHW-system.

The parameter sensitivity study revealed that not all the models were applicable for investigation of the impact of collector flow rate and control strategy variations.

4.4 Derived Investigations

In the course of the period when the cooperative research activities were active, several key issues were addressed by the participants. Of these, the author dealt with the following three areas:

- The collector capacity impact on the performance of the solar system.
- Modelling of collector pump control.
- The reduction in solar gain caused by the increase of storage temperature during a time-step.

Collector capacity effect on solar system performance

It has been shown by Klein (1973) that the main impact of the solar collector heat capacity on system performance is due to the storage effect. Duffie and Beckman (1980) suggest accounting for the early morning part of this effect by subtracting the energy stored in the collector from the actual gain in the first time-step of operation. When this gain, as suggested, is calculated by the simple non-capacity HWB equation:

$$Q_u = F_R \left[S - U_L(T_p - T_a)\right] \Delta t \qquad (4.1)$$

the gain calculated during the period of non-operation will be too small since, in reality, it will not have been reduced by the collector heat removal factor F_R, and since the plate temperature T_p has not reached the operating temperature, the losses will be smaller.

Another approach is to find when the absorber plate reaches the set-point temperature designated for the controller to switch on the pump. This can be done by using the following equation:

$$\tau = \tau_c \ln\left[(T_s - T_{p,initial})/(T_s - T_p)\right] \qquad (4.2)$$

where

$$T_s = (S + U_L T_a)/U_L \qquad (4.3)$$

is the plate stagnation temperature, T_p is the setpoint temperature desired and τ_c is the overall collector time constant.

The reduction in solar gain can then be calculated as:

$$Q_u \cdot \tau/\Delta t \qquad (4.4)$$

where Q_u is calculated by (4.1) as before.

A technical note on this subject is included as an Appendix.

Modelling of collector pump control

The immediate simulation results obtained by varying the collector flow rate of the IEA domestic hot water system were in contradiction to the expectations. Increasing flow rates made the collector output decrease. Changing the time step of the simulation from one hour to ten minutes reversed the situation. Also, the overall system performance increased by introducing the 10-minute time step for the base case, where the collector pump flow rate had not been increased. A closer look at the collector output, hour by hour (see figs. 4.3 and 4.4), revealed the reason for this discrepancy. Using an hourly time step means that collection is either on or off for the entire hour in question. Whereas the 10-minute time step allows the collector pump to be on for part of the hour resulting in a net positive gain during this hour. The increased flow rate elucidated this problem inasmuch as it meant a reduced collector output temperature and therefore more hours of absolutely no collection.

On the basis of the above analysis of collector heat capacity effects, a more advanced control strategy was implemented in the model. When a control shift was going to happen during a time step, this particular time step was

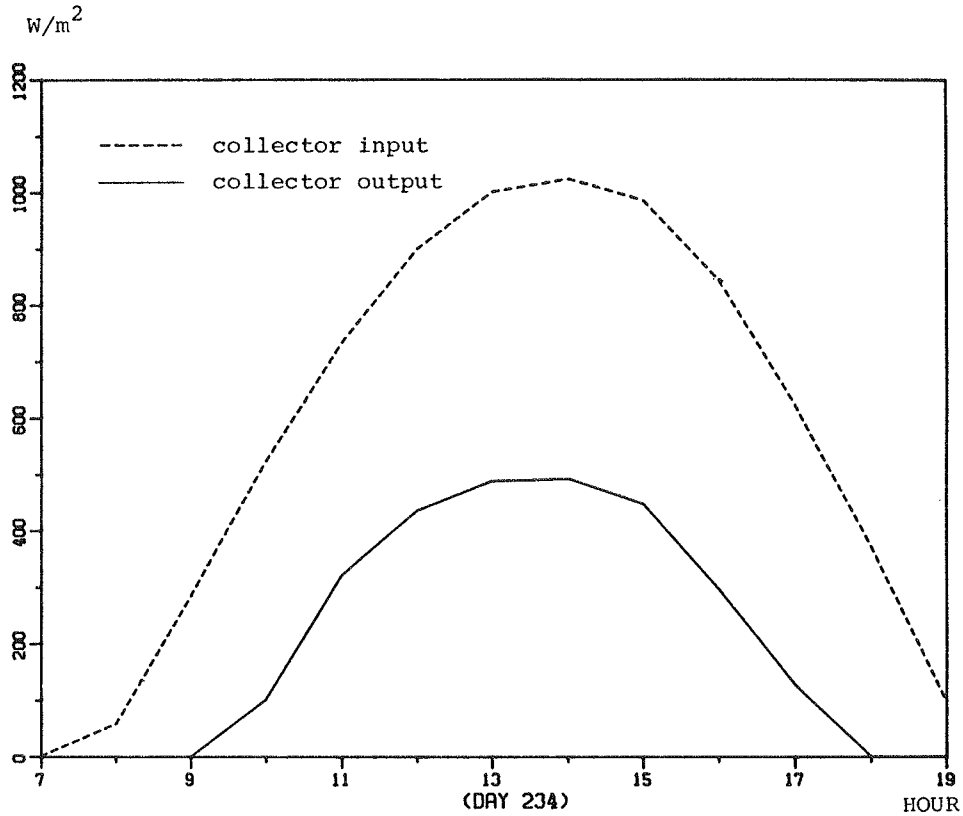

Fig. 4.3 Predicted collector output using 10-minute time steps.

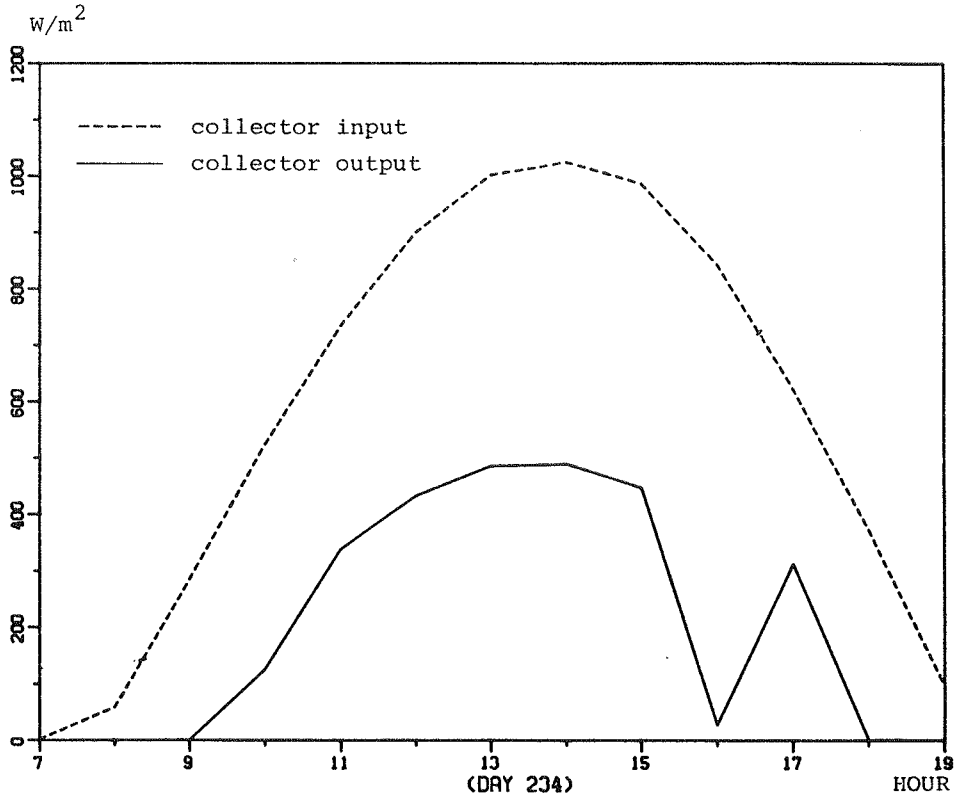

Fig. 4.4 Predicted collector output using hourly time steps.

split into two allowing the collection to be on for part of the time step and off for the rest. The length of each portion of the step was calculated using the above equation (4.2). When the model was rerun using an hourly time step with this improvement, the results resembled those obtained using the 10-minute time step (see fig. 4.3).

A similar analysis was performed as part of the CEC activity. Here the sensitivity to change in time step from one hour to 300 seconds was investigated. A significant increase in solar contribution of about 10% (relatively) was found to be due to two separate effects:

- Control shift during a time step
- Integration error accumulation

Again, a partition of the hourly time step in on/off situations showed that the main reason for the observed difference was inaccurate modelling of control shifts, and only a minor part (about 2%) could be ascribed to the accumulation of integration errors.

Increase_of_storage_temperature_during_a_time-step

In many simple, lumped circuit simulation models an explicit, simple forwards Euler solution is used to solve the differential equation for the storage temperature:

$$C \frac{dT}{dt} = Q_u = AF_R' [S - U_L(T_i - T_a)] \qquad (4.5)$$

where

Q_u is the useful solar gain based on the initial storage temperature T_i, W.

F_R' is a correction factor for collector fin efficiency, collector flow rate and heat exchanger effectiveness. Storage losses are ignored for simplification.

This implies that the useful solar gain is calculated on the basis of the storage temperature at the beginning of the time step. In reality this temperature increases during the time step, thus reducing the useful solar gain.

However, a correction factor which reduces the useful gain in the simulation can easily be introduced.

The exact analytical solution to equation (4.5) is:

$$T_f = T_s + (T_i - T_s)\exp(-AF'_R\ U_L\ \Delta t/C) \qquad (4.6)$$

where

Δt is the time step, s

T_s is the stagnation temperature:

$$T_s = (S + U_L \cdot T_a)/U_L, \quad ^oC \qquad (4.7)$$

and

T_f, T_i are the final and initial storage temperature of the time step in consideration, ^oC

Re-arranging (4.6) yields:

$$\frac{Q'_u}{C} = \frac{(T_f - T_i)}{\Delta t} = \frac{\tau(1-\exp(-\Delta t/\tau))(T_s - T_i)}{\Delta t \cdot \tau} \qquad (4.8)$$

where

$\tau = C/U_L \cdot AF'_R)$ is the time constant of the system, s

$\frac{Q'_u}{C}$ = the correct useful solar gain in the time step, W

Continuing:

$$\frac{T_s - T_i}{\tau} = \frac{AF'_R U_L}{C}\left(\frac{S+U_L \cdot T_a}{U_L} - T_i\right) = \frac{AF'_R(S+U_L(T_a - T_i))}{C} \qquad (4.9)$$

which is the storage temperature differential quotient calculated at the beginning of the time step. Therefore:

$$\frac{T_s - T_i}{\tau} = \frac{Q_u}{C} \qquad (4.10)$$

From (4.8) and (4.10) it then follows that:

$$\frac{Q'_u}{C} = \frac{Q_u}{C} \cdot \frac{\tau(1 - \exp(-\Delta t/\tau))}{\Delta t} \qquad (4.11)$$

which means that the corrected useful solar gain can be calculated as follows:

$$Q'_u = AF''_R [S - U_L(T_i - T_a)] \qquad (4.12)$$

where

$$F''_R = F_s \cdot F'_R \qquad \text{and}$$

$$F_s = \tau(1 - \exp(-\Delta t/\tau))/\Delta t \qquad (4.13)$$

Another worker (Lawaetz, 1980) has suggested using a different correction term assuming a linear temperature rise over the time step and evaluating the differential quotient at the middle of this time step:

$$F_s = \left(1 + \frac{AF'_R \Delta t\ U_L}{2C}\right)^{-1} = \left(1 + \frac{\Delta t}{2\tau}\right)^{-1} \qquad (4.14)$$

That this, however, is an approximation to equation (4.13) can be seen by taking the first three terms of the series expression of the exponential function of equation (4.13):

$$F_s \approx \tau\left(1 - \left(1 - \Delta t/\tau + \frac{(\Delta t/\tau)^2}{2}\right)\right)/\Delta t \qquad (4.15)$$

$$= \left(1 - \frac{\Delta t}{2\tau}\right) \approx (1 + \Delta t/2\tau)^{-1} \quad \text{(q.e.d.)}$$

4.5 Conclusions

During the course of the activities, briefly described above, many different subjects were touched upon and many lessons learned. The lessons learned and the conclusions drawn can roughly be categorized as either of a general or of a more specific nature.

General findings and conclusions

The user's interpretation of the system specifications, also known as the user-effect, unfortunately plays a dominating role in the use of simulation models. To overcome this problem in a cooperative model evaluation effort, the experience showed that meaningful results can be achieved in a two-round process. The first round of analysis provides a basis for discussion and identification of specific problems; the second round often results in more accurate predictions and increased comparability of data.

Validation work is generally complicated by the fact that control decisions in the real systems are made by non-ideal devices whose switching points drift significantly with time in an unpredictable manner. A temperature sensor drift of only a fraction of a degree may advance or delay the switching of a pump or valve by hours, causing large instantaneous differences between measured and predicted results throughout the system. Because of the negative feed-back mechanism of thermal solar systems, these differences might not cause significant disagreement when comparing model predictions and measurement of long term performance. Obviously it is important to take their effect into consideration when deciding on necessary time-periods for validation work.

The main conclusion was that all types of models worked well within their limits of applicability. In many cases these limits could easily be expanded by simple means, e.g. introducing a correction factor for storage temperature increase during a time step and splitting a time step into two when a control shift occurs. Even then, the real issue seems to be to establish the limits of applicability of the models.

Parameter sensitivity studies with model-to-model comparisons proved to be an effective complement to the validation spot checks to establish these limits.

Specific findings and conclusions

. Klein's formula (Duffie, Beckmann, 1980) for the calculation of the collector top loss coefficient showed close agreement with more detailed calculations. Also, a linear dependency of plate and ambient temperature difference seemed to be a reasonable assumption. Even the use of a constant loss coefficient can be justified from the results obtained during this work, provided that a detailed analysis goes into finding the right parameter to use.

. It is more important to calculate the $\tau\alpha$- product than the collector loss coefficient at each time step.

. Using a time step of one hour does not always lead to correct results. The size of time step necessary is influenced by these factors:

    . type of model, explicit or implicit

    . system time constant

    . system control strategy

. As a general rule, implicit methods are much less sensitive to the choice of time step than explicit methods.

5. MODEL DEVELOPMENT

5.1 Modelling Purpose

The development of a specific model is described in this chapter. The model was developed to be used as part of the performance evaluation of a Danish passive solar house. The house is one of 55 single-family dwellings built in connection with the Danish participation in Task VIII of the IEA Solar Heating and Cooling Programme.

Within Task VIII, Passive and Hybrid Solar Low Energy Dwellings, common performance evaluation procedures have been established (Mørck et al., 1985). The performance evaluation methodology outlined in these procedures calls for a comparison between the monitored house and a reference house built according to average standards. The model was developed to be used for this comparison. When close agreement between the model-predicted data and the data from the monitored house has been obtained, the same model is used with the reference house parameters and, by using the same weather data, predictions of the thermal performance of the reference house can be compared to the performance of the test house.

The model can also be used to increase the understanding of the dynamic performance of the monitored house and to ease the calculation of the different terms of the heat balance equation of the house.

A photograph of the monitored house is shown in fig. 5.1. Besides 45 measurements of temperatures and other variables within the house, solar radiation data, ambient temperature, wind velocity and outdoor humidity are recorded. The measurements will be further described in chapter 6.

It appears from the above that the model to be developed should possess the ability to closely resemble a specific house. Another objective, however, was that this model

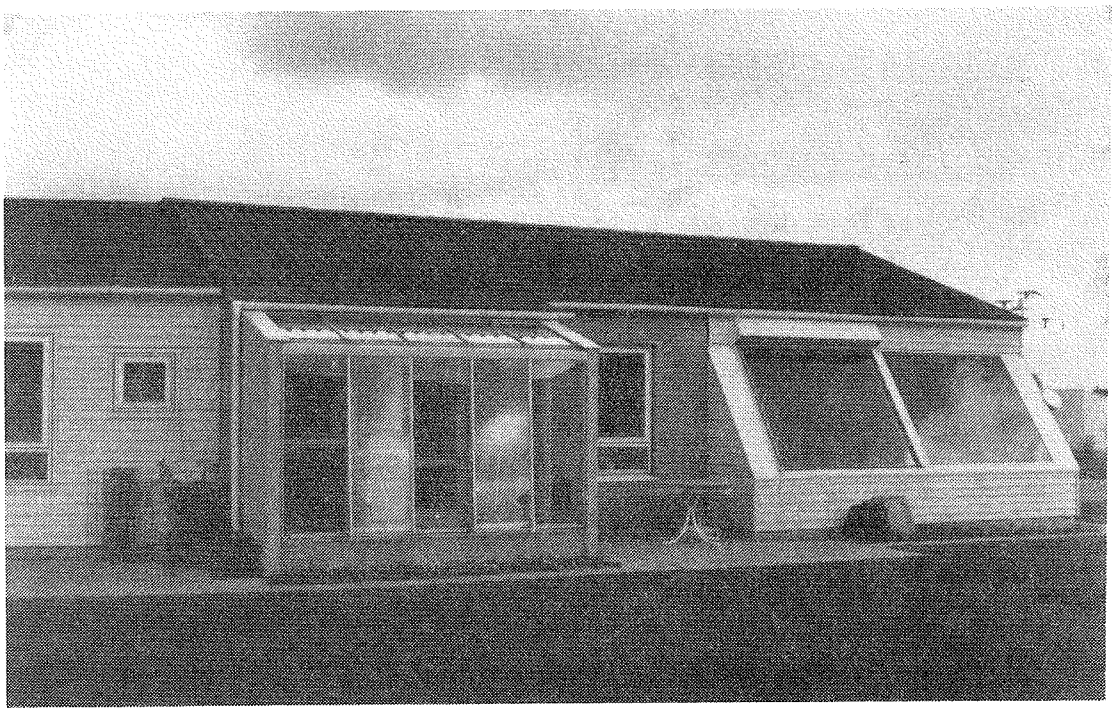

Fig. 5.1 Photograph of monitored dwelling.

(after extensive validation) could be used both as a research tool as well as a design tool.

5.2 Modelling Strategy

The stated objectives directed the development towards a general thermal network model, which in a logical straightforward way could be used to simulate a large variety of solar systems by creating input data files with the thermal characteristics of the nodes.

To achieve any significant dissemination, a design tool today has to be developed on a micro-computer. Very few architectural or engineering firms have access to a main-frame- or mini-computer, whereas a micro-computer is within their reach.

The use of micro-computers has another advantage - the large number of advanced software packages which can be used to edit and create input data files, and present

model out-put in various ways. Therefore, the attention of the programming can be directed towards the thermal model itself.

Even though the micro-computers have become extremely powerful, an essential draw-back in using them for larger simulation tasks is that the run-times are relatively long compared to mini- and mainframe computers. Run-time should be reduced as much as possible, specially when several runs have to be performed to investigate a certain parameter. As the processing of solar radiation data involves many hourly calculations of trigonometrical functions to calculate the correct amount of beam radiation on different surfaces, pre-processing of the weather data using a separate program, allows for considerable run-time reductions. For each design problem, this has to be done only once, creating an intermediate weather data file containing hourly values of incidence angles, direct and diffuse components of solar radiation for the various surfaces to be considered. After that, the parametric sensitivity studies can be carried out using this intermediate weather data file.

Based on the above considerations, the model was structured as shown in fig. 5.2.

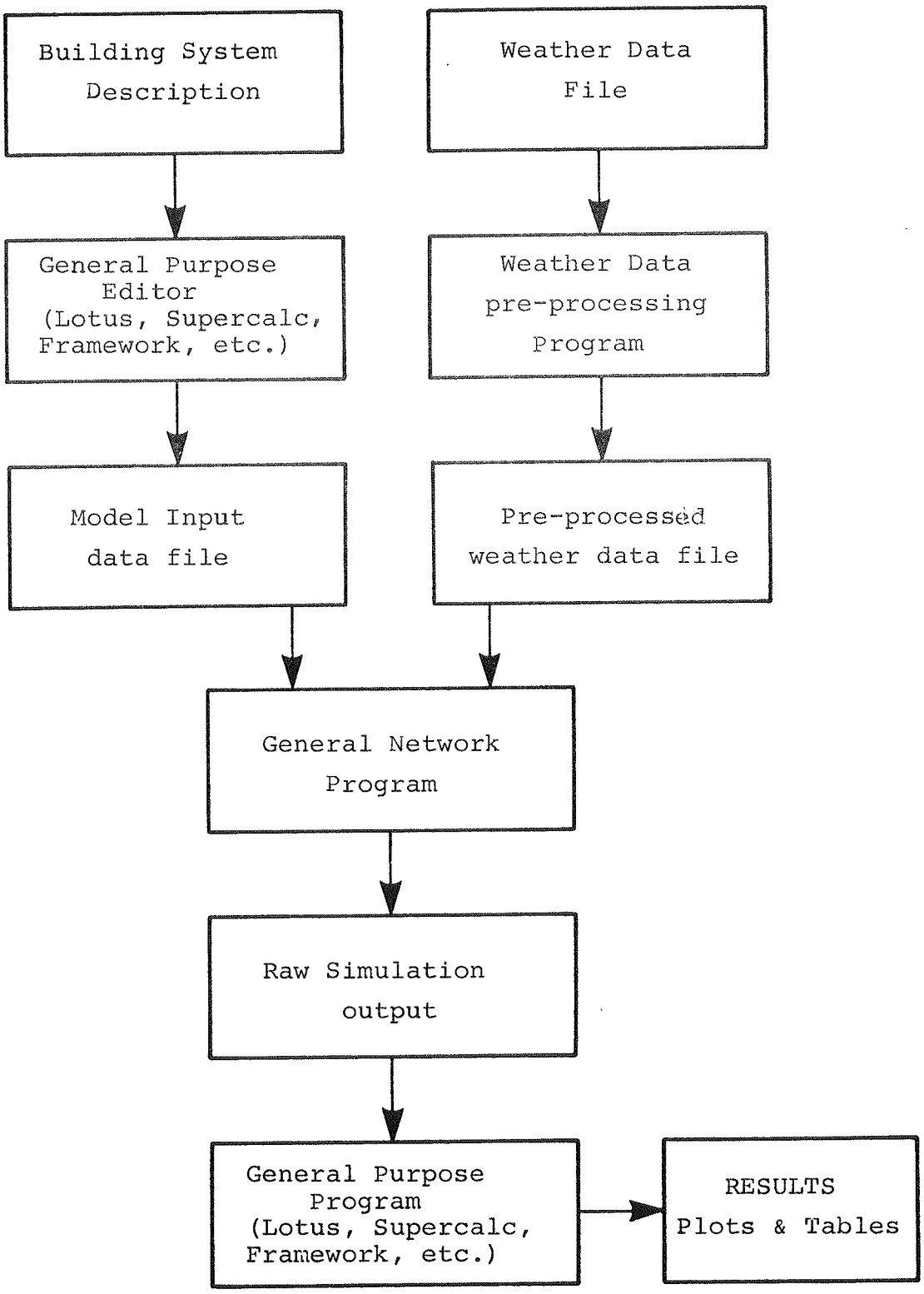

Fig. 5.2 Computer program structure.

5.3 Solar Radiation Processor

Most test reference years and other hourly weather data sets to be used for solar system simulations contain at least two of the following data: Global horizontal, diffuse horizontal or direct normal solar radiation. On this basis the direct, diffuse and reflected components of the radiation for any surface orientation and tilt can be calculated using standard methods; see, for example, Duffie and Beckman (1980).

The solar radiation measurements undertaken at the building to be modelled include global radiation at three different tilts, one being horizontal. This approach was chosen instead of the traditional measurements of global horizontal and diffuse horizontal radiation for two reasons:

1. At high latitudes, such as those of Denmark, the solar altitude is very low during winter months, introducing relatively large errors in horizontal solar radiation measurements.

2. The use of a shadow-ring to measure diffuse radiation requires frequent adjustments of the shadow-ring to yield accurate measurements. Frequent adjustments are not needed for global radiation measurements.

Based on the global radiation measured at the two different slopes β_1 and β_2 and at horizontal H, the direct and diffuse components of the incoming solar radiation can be deduced by solving three equations for three unknowns G_b, G_d and ρ (ground reflection):

$$G_1 = \cos\Theta_1 G_b + ((1 + \cos\beta_1)/2)G_d + ((1 - \cos\beta_1)/2)\rho G_H \quad (5.1)$$

$$G_2 = \cos\Theta_2 G_b + ((1 + \cos\beta_2)/2)G_d + ((1 - \cos\beta_2)/2)\rho G_H \quad (5.2)$$

$$G_H = \cos\Theta_H G_b + G_d \quad (5.3)$$

assuming isotropical distribution of diffuse and reflected radiation. Since the above expressions are valid only for solar irradiance (momentary values) an integration of the time period between recordings should be performed to obtain irradiation values. The error in omitting the integration is neglible, however, for one-hour time periods (Steinmüller).

5.4 Solar Radiation Transmission and Absorption

The total solar gain through glazing is the sum of transmitted solar radiation and the inward flowing fraction of absorbed radiation.

Not all the solar radiation impinging on the glazings is transmitted; it is reduced by reflection and absorption effects. At each surface of the glazings a fraction of the radiation is reflected; within the glazings, an endless number of reflections are taking place. Well known (Duffie and Beckman, 1980) laws of Snell and Fresnel are applied to calculate the resulting transmittance as a function of incidence angle, glazing properties and dimensions plus number of layers. It is important to notice that the transmittance of perpendicular and parallel polarization components differ.

The radiation absorbed in the glazings is calculated according to the law of Bougert based on the angle of refraction, the thickness and number of layers and the extinction coefficient.

The transmitted solar radiation is calculated as:

$$\tau = \tau_\rho \cdot \tau_\alpha \qquad (5.4)$$

where τ_ρ is the transmittance calculated, neglecting absorption losses, and τ_α is the transmittance calculated, neglecting reflection losses.

The absorbed radiation increases the temperature of the

glazings and thus affects the heat exchange with the room and the environment. The reduction in losses from the room behind the glazings can be considered as an inward flowing fraction of the absorbed radiation. Thus, the absorbed radiation must be distributed between inward and outward flowing fractions. A simple way of doing this, adopted here, is based on surface heat transfer coefficients and heat resistance of the air-gap between the layers. The absorbed radiation for each layer is divided inversely proportional to the resistances in either direction. So, the relationship between inward α_i and outward α_o flowing fractions are given as:

$$\frac{\alpha_i}{\alpha_o} = \frac{m_o}{m_i} \tag{5.5}$$

where

m_o = total resistance towards ambient

m_i = total resistance towards room

Typically, the inward flowing fraction for a double pane window corresponds to about 5% of the incoming radiation.

5.5 Thermal Network Model

Following the analysis within chapter 3, a series-parallel nodal network can be constructed to represent the building.

The governing differential equation for each node is of the form:

$$C_j \frac{d}{dt} T_j = \sum_{k+j} U_{jk}(T_k - T_j) + U_{jG}(T_j - T_G) + U_{ja}(T_j - T_a) + S_j + Q_j + F_j \tag{5.6}$$

where

C = capacitance

T = temperature

U_{jk} = overall heat transfer coefficient

S = net solar gain

Q = auxiliary heating supply

F = free heat gain

and subscripts

j,k = node numbers

G = ground

a = ambient

Numerical integration of the set of equations (5.6), applying the implicit integration method, results in a set of simultaneous algebraic equations for each time step which can be brought on matrix form:

$$\underline{\underline{A}} \cdot \underline{\underline{T}}_{|}^{i+1} = \underline{\underline{B}}_{|} \qquad (5.7)$$

where

$\underline{\underline{T}}_{|}^{i+1}$ = temperatures of nodes at the end of (i+1)'th time step

$\underline{\underline{A}}$ is a matrix composed of all capacitances and overall heat transfer coefficients

$\underline{\underline{B}}_{|}$ contains stored energy in each capacity, ground and ambient loss terms, auxiliary heating, free heat and solar gain for (i+1)'th time step.

Multiplying on both sides by the inverse matrix A^{-1} yields:

$$\underline{\underline{A}}^{-1} \underline{\underline{A}} \underline{\underline{T}}_{|}^{i+1} = \underline{\underline{T}}_{|}^{i+1} = \underline{\underline{A}}^{-1} \underline{\underline{B}}_{|} \qquad (5.8)$$

The matrix $\underline{\underline{A}}$ does not contain any node temperatures or external variables. Therefore, the inverse matrix $\underline{\underline{A}}^{-1}$ needs to be calculated only once at the outset of the simulation, and the computation at each time step is reduced to a simple matrix multiplication. The presumption of this

strategy, however, is that all overall heat transfer terms remain constant throughout the simulation - which they don't. Some of the terms change as a consequence of configuration changes of the building: Opening or closing of windows, shutters or doors between zones, operation of fans between zones, etc. A limited number of combinations of these building configurations exists, and it is advantageous to invert matrices for each configuration and apply the stored inverted matrices when appropriate.

Often changes in the matrix elements occur because of non-linearities of material properties or surface film coefficients. These non-linearities are relatively small, and the simplification introduced by not considering these effects is justifiable.

However, natural convection heat flows are often very significant for the heat transfer between zones, and they are highly non-linear. A stepwise linear approximation to the non-linear function limits the number of combinations to handle, so that the pre-calculation of inverted matrices can still be an efficient procedure.

5.6 Auxiliary Heating Control

The amount of auxiliary heating needed to maintain a specified set point temperature in a given zone can be calculated in a number of different ways. The calculation is complicated by the fact that energy supplied to a zone in a time step dissipates via the overall heat transfer mechanisms to the other nodes of the network. Two different approaches were investigated.

When auxiliary heating is supplied to one or more zones during a time step and the heating power is adequate, the temperature of these zones will be the corresponding set point temperatures at the end of the time step. In other words, these temperatures are no longer unknowns in the

set of equations. The unknowns are now the auxiliary heating energy to be supplied to each zone. Separating the auxiliary heating terms from the $\underline{\underline{B}}$ matrix, equation (5.8), becomes:

$$\underline{\underline{T}}_1^{i+1} = \underline{\underline{A}}^{-1} \underline{\underline{B}}_1 + \underline{\underline{A}}^{-1} \underline{Q}_1 \qquad (5.9)$$

where $\underline{Q}_1$ is the column matrix of auxiliary heating supply. Now:

$$\underline{\underline{T}}_1^{i+1} - \underline{\underline{A}}^{-1} \underline{Q}_1 = \underline{\underline{A}}^{-1} \underline{\underline{B}}_1 = \underline{\underline{T}}_1' \qquad (5.10)$$

where $\underline{\underline{T}}_1'$ is the node temperatures reached at the end of the time step if no auxiliary heating is supplied.

For each heated zone, (5.10) results in an equation. If, for example, nodes 1 and 2 are the zones to be heated, two equations can be solved for the two unknowns Q_1 and Q_2.

$$T_1^{i+1} - A_{11}^{-1} Q_1 - A_{12}^{-1} Q_2 = T_1' \qquad (5.11)$$

$$T_2^{i+1} - A_{21}^{-1} Q_1 - A_{22}^{-1} Q_2 = T_2' \qquad (5.12)$$

At each simulation time step $\underline{\underline{T}}_1'$ is calculated first, and if auxiliary heating is required the equations (5.11) and (5.12) are solved to find $\underline{Q}_1$. Thereafter, (5.9) is applied to find $\underline{\underline{T}}^{i+1}$.

The second approach is based on the Biot-number analysis for overall surface heat transfer described in chapter 3. Again, the intermediate temperature $\underline{\underline{T}}_1'$ has to be calculated according to (5.10). The differences between the zone air temperature set points and the intermediate temperatures of the zones give rise to an additional heat transfer to the surfaces surrounding the zone air. This additional heat transfer is calculated based on the Biot-number analysis, equations (3.7) and (3.9).

The total amount of auxiliary heating needed in each zone is then calculated as the sum of this additional heat transfer and the energy needed to heat the capacity of the zone (air, furniture, etc.) to the set point temperature.

The obtained values for $\underline{\underline{Q}}_i$ is used in equation (5.9) to calculate $\underline{\underline{T}}_i^{i+1}$.

During the testing of the model, both approaches worked satisfactorily and identical results were obtained.

5.7 Computer Program Layout

The overall modelling strategy is described in paragraph 5.2. This paragraph describes network model input data generation, the network structure and the model output handling.

Generation of network input data

A general network model requires data in the form of nodal capacitances, overall loss coefficients to the ambient and the ground and inter-nodal overall heat transfer coefficients. Besides, window areas and directions as to distribution of solar gain among the nodes have to be given.

This network model reads these data from a file which can be prepared either by a text-editor or a spreadsheet program. The workload in preparing the input data file is greatly reduced by using the latter. A library of the basic thermal physical properties of building materials can be stored in a separate part of the work sheet. At another part of the sheet, building descriptive data can be entered. Formulas combining information from the different parts of the work sheet then automatically generate the input data file. In principle, a number of different configurations, covering typical solar systems, may be constructed on different spreadsheets. To analyse a

specific case, a designer only has to load the appropriate worksheet and enter the building descriptive data; he/she does not need to know anything about the other part of the worksheet. For the advanced user, this approach gives the opportunity to utilize the possibilities of a general network to analyse completely new concepts.

Figure 5.3 shows the input data file as produced by the spreadsheet program.

```
Network Model Input, Canadian Test cell
Number of nodes
   13
Node  capacity  loss    groundlwn sfr  wn sfr  wn sfr  wn sfr  wn sfrac
   1   448.49   14.29    1.76  1 1.00  2 0.00  3 0.00  4 0.00  5 0.00
   2   466.18    8.04    1.76  1 0.00  2 0.00  3 0.00  4 0.00  5 0.00
   3   357.99    0.00    0.00  1 1.00  2 0.00  3 0.00  4 0.00  5 0.00
   4   357.99    0.00    0.00  1 0.00  2 0.00  3 0.00  4 0.00  5 0.00
   5   357.99    0.00    0.00  1 0.00  2 0.00  3 0.00  4 0.00  5 0.00
   6   837.01    0.00    0.00  1 0.00  2 0.00  3 0.00  4 0.00  5 0.00
   7   930.01    0.00    5.00  1 0.00  2 0.00  3 0.00  4 0.00  5 0.00
   8   837.01    0.00    0.00  1 0.00  2 0.00  3 0.00  4 0.00  5 0.00
   9   930.01    0.00    5.00  1 0.00  2 0.00  3 0.00  4 0.00  5 0.00
  10  1103.27    0.00    0.00  1 0.00  2 0.00  3 0.00  4 0.00  5 0.00
  11  1225.85    6.95    0.00  1 0.00  2 0.00  3 0.00  4 0.00  5 0.00
  12  1262.52    0.00    0.00  1 0.00  2 0.00  3 0.00  4 0.00  5 0.00
  13  1402.79    7.45    0.00  1 0.00  2 0.00  3 0.00  4 0.00  5 0.00
Node to node conductances (node i,node j,cond[i,j)
   1         2   56.28
   1         3  470.51
   1         6  595.02
   1        10  784.30
   2         5  470.51
   2         8  595.02
   2        12  897.51
   3         4  216.53
   4         5  216.53
   6         7  331.96
   8         9  331.96
  10        11  437.56
  12        13  500.72
1000         0    0.00
Window nr.,net area[sqm],orientation;
   1     2.60    0.00
   2     1.00  180.00
1000        0    0.00
weatherdatafile
b:cansim
```

Fig. 5.3 Network model input data file.

Network model structure

One of the new powerful compilers developed for micro-computers, taking advantage of the numerical capabilities of the Intel 8087 coprocessor, Turbo Pascal 87, was used for the actual programming of the model. Like many other modern compilers, Pascal allows for the development of a highly structured computer program based on the use of procedures and functions. The structure of the developed network model SOLMAT appears from fig. 5.4. Each step of the calculations is described in the parentheses.

```
program Solmat;(Version 1.0%July, 1985%Ove Merck)
begin                                (Program execution starts)
Inputdata;                           (Reads building description file)
Initialize;                          (Initializes variables)
Matset;                              (Sets up matrices of equations)
Invert(mat1);                        (Invert the matrices for implicit calc.)
for daycounter:=1 to 14 do           (Simulation for a 14 day period starts)
begin
   Readdata;                         (Reads preprocessed weatherdata )
   Marching;                         (Performs hourly simulation)
   Plottemp;                         (Production of temperature plot)
   Plotpower;                        (Production of auxiliary heating power plot)
end;                                 (Simulation ends)
end.                                 (Program execution terminates)
```

Fig. 5.4 Structure of network model SOLMAT.

Model output data handling

The network model produces only raw output data in the form of specified nodal temperatures, node-to-node energy flows and auxiliary heating requirements. These data are stored in a file, either on an hourly or on a daily basis. The file is read by the spreadsheet program. The calculation power and ease of use of the spreadsheet program can be used to produce tables or plots needed for the presentation of results.

The following chapters contain examples of plots produced by a spreadsheet program based on the network model output data.

6. VALIDATION

6.1 The Validation Process

Before using a computer simulation program as a design or a research tool it has to be verified that reliable results may be obtained. This verification of the validity of a program is commonly referred to as validation.

Validation is often perceived as synonymous with empirical validation which means comparisons of simulation model predictions to measured data. Empirical validation, however, is very time-consuming and expensive; therefore, this ultimate check of the model validity can be carried out only at a limited number of positions within the total parameter space for which a given model is intended to be used. Comparisons of different computer code simulation results for a parametric sensitivity study is a method to extrapolate the empirical validation results to a larger parameter space. This may also be considered as validation, and in general, all activities undertaken to test and verify the simulation programs should be considered as validation activities. Perceived this way, it is clear that validation is an integrated part of the simulation program development process.

It is important to stress that a simulation program never can be said to be validated. It is not possible to prove that there are no errors in a given program. It is only possible to show that for certain systems, parameter values, climatic conditions, etc. reliable results may be obtained. The validation process may thus be seen as an extension of the range of applicability of the program.

Ron Judkoff et al. (1983) have systematized the validation techniques to be applied for solar system simulation programs. Table 6.1 presents an overview of their characterization of each of these techniques.

TABLE 6.1 VALIDATION TECHNIQUES (Judkoff et al., 1983).

Technique	Advantages	Disadvantages
Comparative Relative test of model and solution process	No input uncertainty Any level of complexity Inexpensive Quick: Many comparisons possible	No truth standard
Analytical Test of numerical solution	No input uncertainty Exact truth standard given the simplicity of the model Inexpensive	No test of model Limited to cases for which analytical solutions can be derived
Empirical Test of model and solution process	Approximate truth standard with accuracy of data acquisition system Any level of complexity	Measurement involves some degree of input uncertainty Detailed measurements of high quality are expensive and time-consuming A limited number of data sites are economically practical

Two different empirical validation studies have been performed to verify the new simulation program, the development of which is described in chapter 5.

In the first study, the model predictions have been compared to measured data from a Canadian direct gain test building. The second study was concerned with the attached sunspace of the Danish IEA Task VIII building for which the model was developed, see paragraph 5.1.

6.2 Description of Direct Gain Test Case

The Canadian gain test building had previously been used for an extensive validation study of 11 different simulation programs conducted within Task VIII of the IEA Solar Heating and Cooling Programme (Mørck, 1985). The test was selected because of it's well-documented, simple construction, and high quality data, suitable for validation purposes were available from this facility.

By participating in this work (Jørgensen, 1983b) the author became well-acquainted with the test building and the data available. The results obtained by the IEA participants confirmed the building description and the reliability of the data. Therefore, this case seemed to be an obvious choice for the first empirical validation study of a newly developed model.

The building

The test building, documented in details by Barakat (1982), consists of a south and north oriented room with a connecting door. Each end wall has a window. Towards south

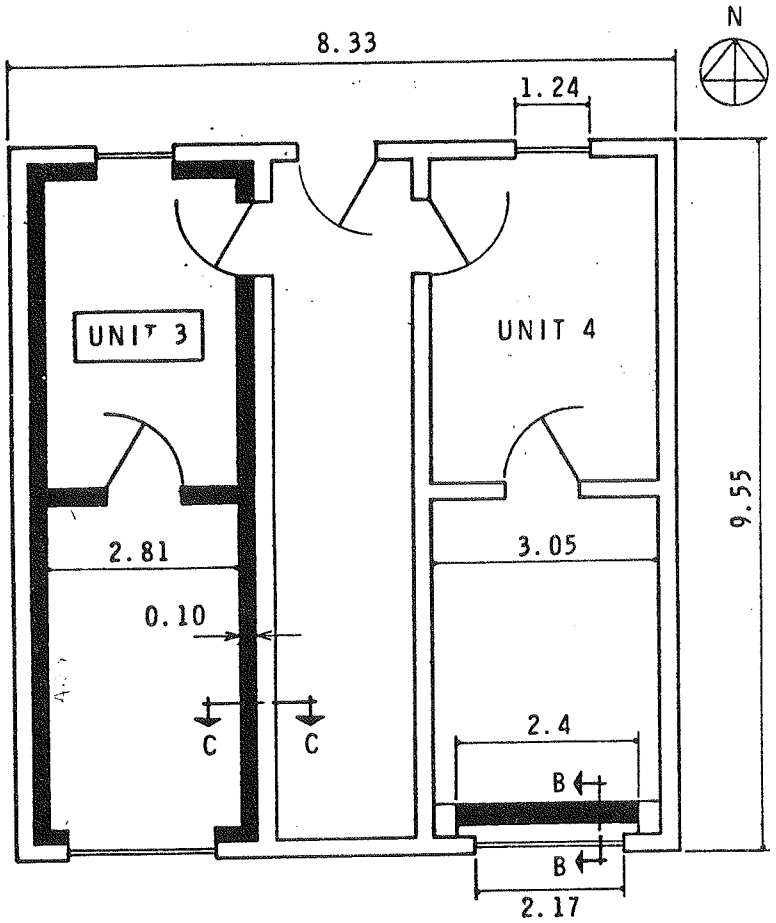

Fig. 6.1 Plan of Canadian direct gain test building. (Barakat, 1982).

it has a net glass area of 2.6 m^2 and towards north of 1 m^2. The building is a one-storey, insulated wood-frame construction over a heated basement. The side wall towards east in both rooms is separating the rooms from a heated corridor. All the other walls are exposed to the ambient. The ceiling is connected to a well ventilated attic.

Figure 6.1 shows a plan of the test building and table 6.2 presents the main characteristics of the test cell.

TABLE 6.2 CHARACTERISTICS OF TEST BUILDING. (Mørck, 1985).

Room length	4.38	m
Room width	2.81	m
Room height	2.4	m
Floor area per room	12.3	m^2
Overall wall* thermal resistance	2.1	$m^2 \cdot K/W$
Overall ceiling thermal resistance	3.5	$m^2 \cdot K/W$
Overall floor thermal resistance	7.0	$m^2 \cdot K/W$
Gross south window area	3.4	m^2
Net south window glass area	2.6	m^2
Gross north window area	1.4	m^2
Net north window glass area	1.0	m^2
Window glazing thermal resistance	0.35	$m^2 \cdot K/W$
Window frame thermal resistance	0.37	$m^2 \cdot K/W$
Partition door area	1.65	m^2
Partition thermal resistance	0.44	$m^2 \cdot K/W$
Corridor door area	1.9	m^2
Corridor door thermal resistance	1.25	$m^2 \cdot K/W$
Circulation fan power	21	Watts
Heating set point	20	^oC
Heating controller deadband	0.1	^oC
Ventilation set point	27	^oC
Basement temperature	21	^oC
Corridor set point temperature	20	^oC
Thermal storage mass	13,565	kg
Heat capacity	11.55	MJ/K

* All walls are of wood-frame construction, 38 x 89 mm studs at 0.6 m centres.

The data

Hourly data for the 14-day period December 29, 1980 to January 11, 1981 were provided. The weather data consisted of:

- average outdoor air temperature, ^{o}C
- total global horizontal radiation, W/m^2
- total vertical south solar radiation, W/m^2
- total vertical north solar radiation, W/m^2
- direct normal solar radiation, W/m^2
- average wind speed, km/h
- wind direction, degree

The following monitored data were supplied:

- average south room air temperature, ^{o}C
- average north room air temperature, ^{o}C
- average corridor air temperature, ^{o}C
- average attic air temperature, ^{o}C

6.3 Weather Data Pre-Processing

The supplied solar radiation data allowed for several ways of obtaining the split between direct and diffuse solar radiation at the windows.

One approach is based on the assumptions of isotropical distributed diffuse solar radiation from the sky and reflected radiation from the the ground. At this time of the year the solar azimuth never exceeds 90^{o} from south, so the north surface is not exposed to direct sunlight. The direct radiation at the south surface is therefore obtained simply by subtracting the global north solar radiation from the global south solar radiation.

The alternative methods for obtaining direct and diffuse radiation at the surfaces were briefly investigated. Using

direct normal and global horizontal radiation or direct normal and global south radiation both resulted in significantly larger fractions of diffuse radiation than could be deduced from the total north radiation. The use of both these methods implies an assumption of the albedo of the ground which can only be made to a large degree of uncertainty. Also, the anisotropic distribution of the diffuse solar radiation cannot easily be accounted for by these methods.

The former, simple and straightforward method, however, accounts implicitly for both ground albedo and the anisotropic distribution of the diffuse radiation. By using this method, the relatively large fraction of diffuse radiation, originating from a sky area close to the position of the sun, is treated as direct radiation, which it should be. After applying this method to the measured data, the incidence angle of the direct solar radiation at the south facing window was calculated for each hour and added to the data.

Wind speed and wind direction were omitted from the data as it was decided not to use this information since the test buildings were of a very well-insulated, airtight construction.

A data file containing ambient temperature, direct and diffuse solar radiation at the south facing window, incidence angle of direct solar radiation also at the south facing window and diffuse radiation at the north facing window, were created to be used for the simulations.

6.4 Nodal Model Construction

A 13 capacity node network configuration was set up to model the test building. The massive concrete partition wall between the south and north zone, directly hit by solar radiation, was assumed to be the most dynamically active part of the construction, and was consequently

modelled by 3 nodes. All other walls were modelled with 2 capacity nodes. The side and end walls towards the ambient were lumped into one wall for each zone. Finally, one node was used for each zone, covering the zone air capacity and the capacity of the surfaces of floor and ceiling. Table 6.3 presents an overview of the 13 nodes.

TABLE 6.3 CAPACITY NODES OF DIRECT GAIN TEST BUILDING NETWORK MODEL.

Node 1	:	South zone
Node 2	:	North zone
Node 3	:	Partition wall, south side
Node 4	:	Partition wall, middle section
Node 5	:	Partition wall, north side
Node 6,7	:	South room concrete brick wall lining towards corridor, inner and outer sections
Node 8,9	:	North room concrete brick wall lining towards corridor, inner and outer sections
Node 10,11	:	South room concrete brick wall lining towards ambient, inner and outer sections
Node 12,13	:	North room concrete brick wall lining towards ambient, inner and outer sections

The capacities of each node were calculated using the geometrical configuration of the test cell, see fig. 6.1, and the physical properties of the material as provided by Barakat (1982). Likewise, overall heat loss coefficients for the walls, floor and ceiling were provided and used as such.

Inter-nodal, overall heat transfer coefficients were calculated based on the k-value and the thicknesses of the materials and a lumped radiative and convective film coefficient of 9 W/m^2K. For the inter-zone heat exchange, the fan coupling was modelled as a corresponding overall heat transfer coefficient.

To investigate the impact on simulation results of the number of wall nodes, an eight node network was also set up. In this network the partition wall was modelled with two nodes and all other walls with one node.

6.5 Alternative Modelling Strategy

The construction of the nodal network model described in the previous paragraph can be considered as a traditional building star network model. Using this approach implies a difficult problem for the modeller. The incoming solar radiation has to be correctly distributed among the surfaces and the zone air of each room. If this is not done adequately, the dynamic behaviour of the zone will not be simulated satisfactorily, which again means that an evaluation of thermal comfort, based on the predictions, will be misleading. In a few larger models (Pasole, Derob), methods to track the incoming radiation to actually calculate this distribution, are included. However, this is very time-consuming procedures and not well-suited for micro-computer programs.

An approach to avoid this problem was investigated. The idea is to lump the zone air with a thin layer of each of the surrounding walls, floor and ceiling surfaces. All the incoming solar radiation may then be delivered to this lumped zone node and, further, heat transfer of this energy to the neighbouring nodes will be calculated automatically based on the material properties and the thicknesses and areas of layers.

The thickness of the surface layer to be lumped with the zone air node was estimated, based on a Biot number analysis. The criteria:

$$N_{Bi} = hL/k << 1 \qquad (6.1)$$

where

L = an appropriate length, m

h = the surface film coefficient, W/m^2K

k = conductance of the material, W/m K

must be fulfilled for each layer.

For a surface layer thickness of 0.005 m of the concrete bricks, the Biot number is of the order of 0.01, and it was decided to use this thickness.

The crude philosophy behind this approach is that, because of the relatively strong convective and radiative coupling between zone surfaces and zone air, they are "most of the time" at temperature levels which are very close. The zone temperature resulting from simulations using this approach will be an internal temperature which may be perceived as a mixture of zone air temperature and zone radiant temperature.

6.6 Results of Direct Gain Validation Simulations

The various configurations of the model were investigated by comparing the simulation program predictions with the measured data. In addition to those already mentioned, a single zone model, set up by increasing the inter-zone heat exchange to a very large number, was also tested. The results are presented below.

Figures 6.2 and 6.3 present the first and very encouraging results obtained. It is seen that the model tracks the dynamic performance of the test building very well.

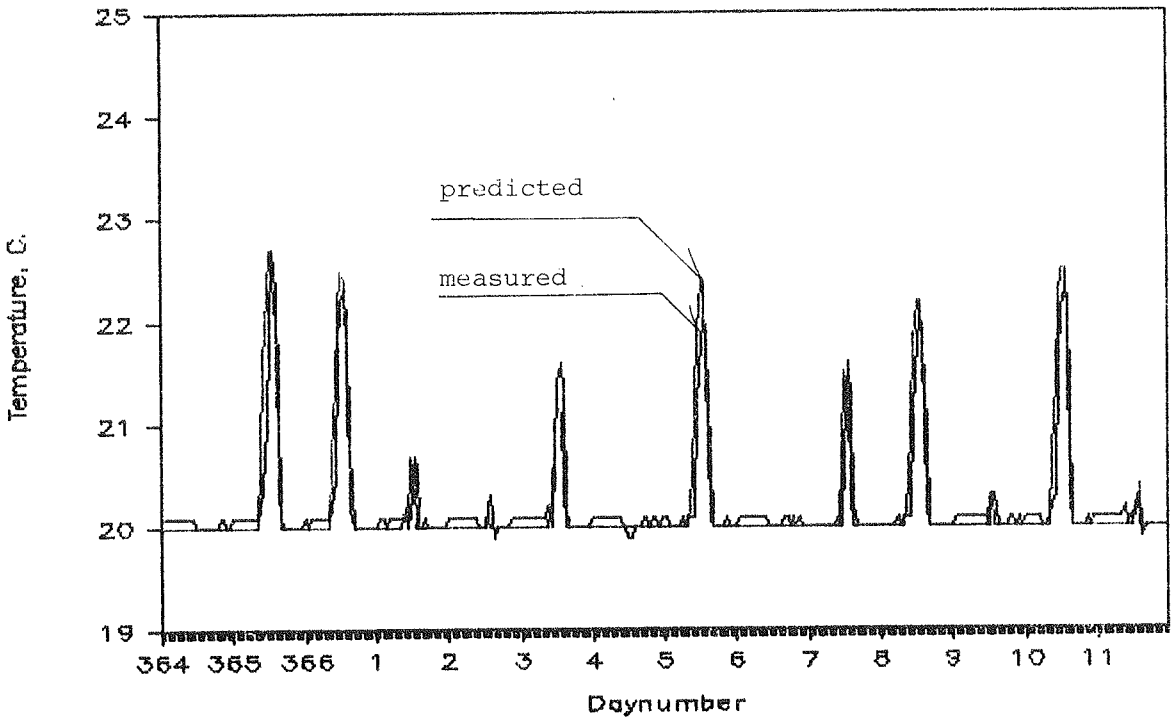

Fig. 6.2 Direct gain validation results.
Measured and predicted temperatures of south room,
zone air fraction of solar gain = 0.3.

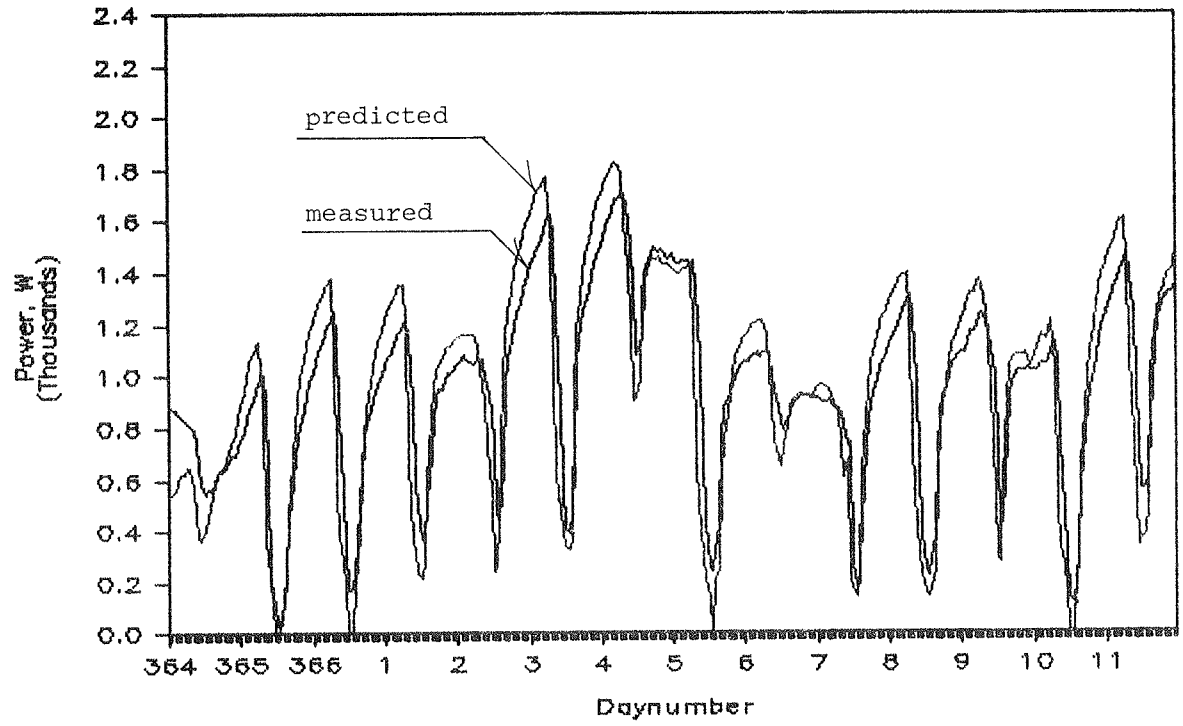

Fig. 6.3 Direct gain validation results.
Measured and predicted auxiliary power,
zone air fraction of solar gain = 0.3.

For the predictions presented in figs. 6.2 and 6.3, the fraction of total solar gain, directly supplied to the zone air node, was assumed to be 0.3. That this assumption highly impacts the results is shown in fig. 6.4 for which this fraction was raised to 0.42, a figure based on relative areas of the lightweight and massive parts of the construction. It is clearly seen that the use of this number makes the simulation program significantly overpredict the zone air temperature during solar gain periods. An even more distinct illustration of the impact of this parameter is provided by fig. 6.5, which shows predicted south zone temperatures calculated for a case where all the incoming solar radiation is absorbed by the zone node. Obviously, the solar distribution has to be estimated with great care.

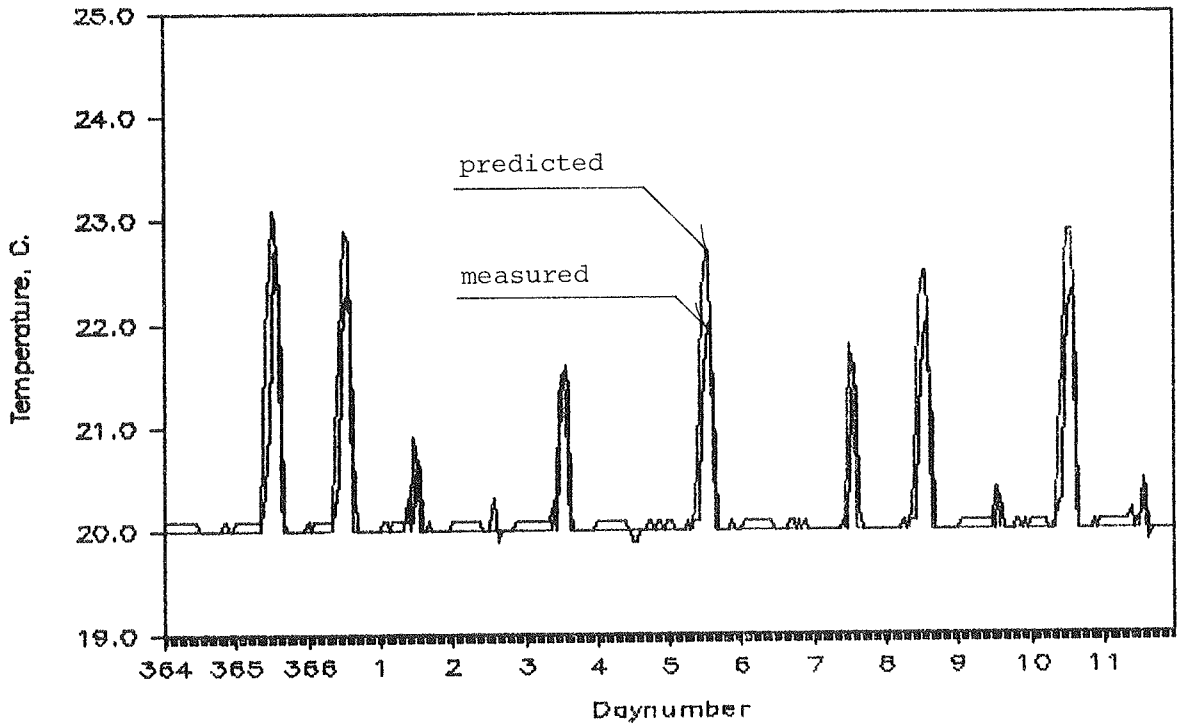

Fig. 6.4 Direct gain validation results.
Measured and predicted temperatures of south room, zone air fraction of solar gain = 0.42.

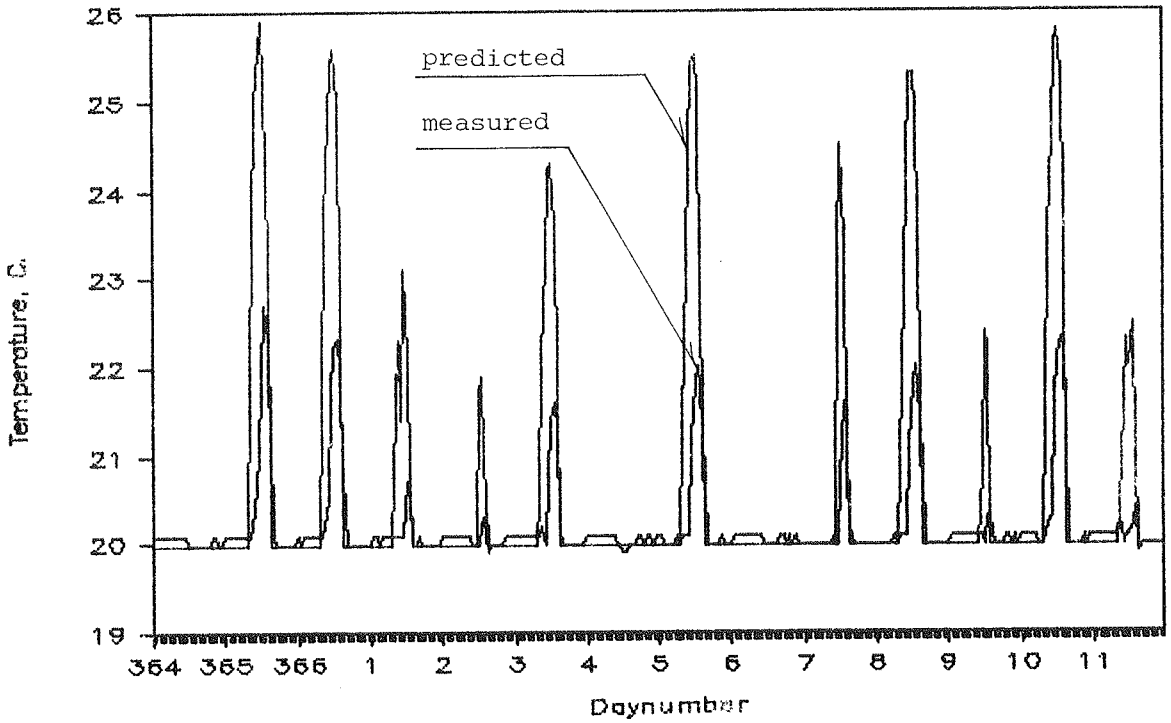

Fig. 6.5 Direct gain validation results.
Measured and predicted temperatures of south room,
zone air fraction of solar gain = 1.0.

The predictions shown in fig. 6.6, however, are also based on a zone node solar fraction of 1. In this case, the zone is lumped with the surface layers of the mass walls as described above. A comparison of this plot with the plot in fig. 6.2 shows that the predicted temperatures are almost identical. That this is also the case for the predicted auxiliary heating power is seen by comparing fig. 6.3 and fig. 6.7. Both predictions also agree very closely on the predicted energy consumption for heating during the period.

A summary of predicted and measured quantities is provided in table 6.4.

Based on these results, it can be concluded that the method of lumping massive wall surfaces to the zone nodes, in this case, was a viable approach. Further investigations will show how well it will apply in other cases.

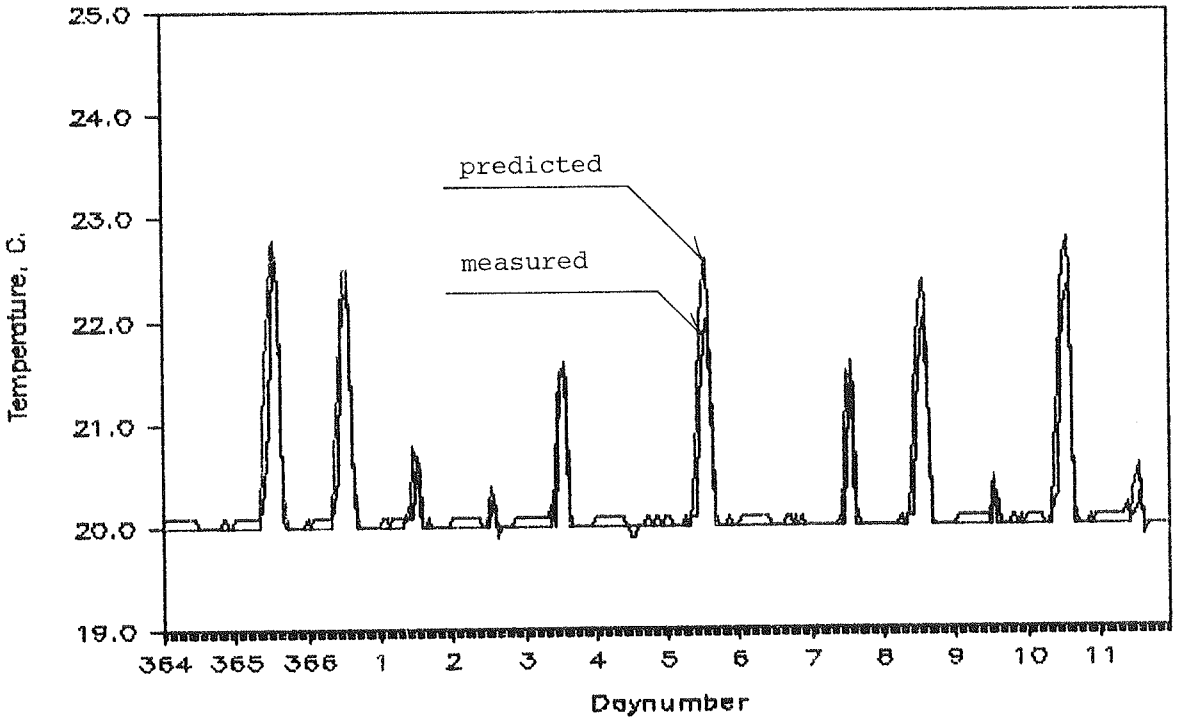

Fig. 6.6 Direct gain validation results.
Measured and predicted temperature of south room, lumped model.

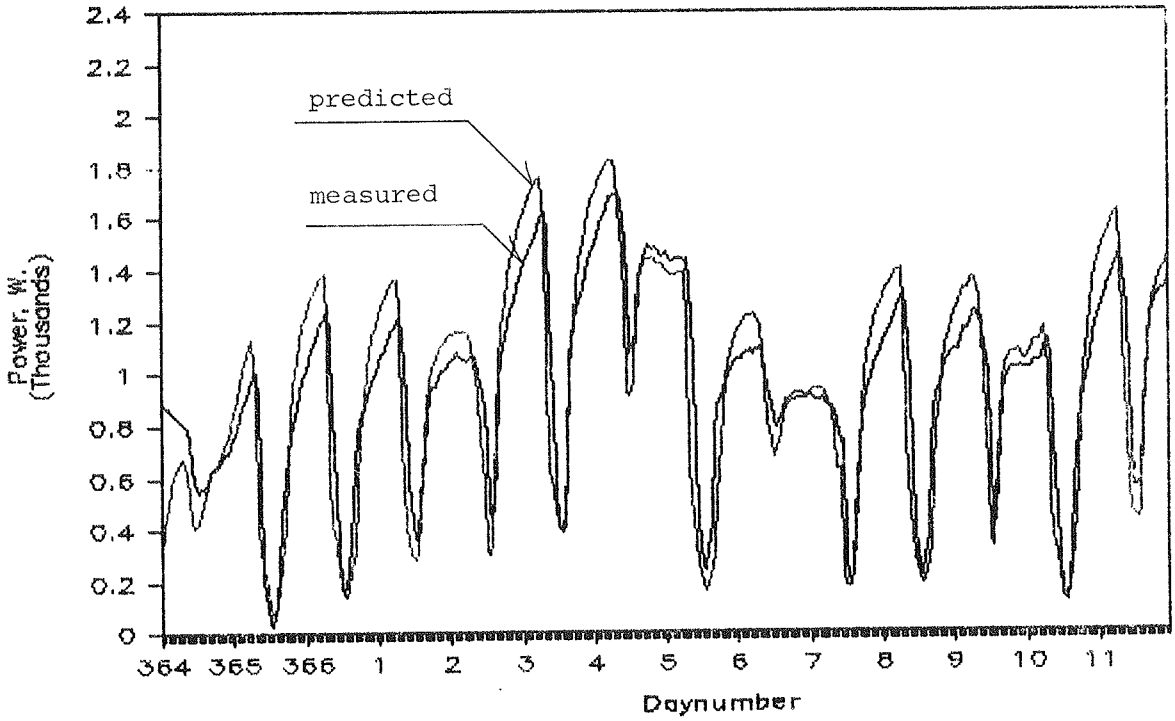

Fig. 6.7 Direct gain validation results.
Measured and predicted auxiliary power, lumped model.

TABLE 6.4 PREDICTED AND MEASURED QUANTITIES.

Results Identification	Auxiliary Heating Energy, kWh	South Room Mean Temp. ^{o}C	North Room Mean Temp. ^{o}C
MEASURED	323	20.2	19.9
PREDICTED			
Traditional Model	323	20.2	19.9
Lumped Model	318	20.2	19.9
Lumped Model with 8 nodes	327	20.2	19.9
1 zone Model	316	20.1	20.1

Table 6.4 also presents gross results of two other investigations performed. First, the sensitivity of the simulation results to the number of nodes in the concrete mass walls was investigated by changing this number from two to one for all the walls. From table 6.4 it appears that the results obtained agree very well with the results obtained with two wall nodes. On the temperature and auxiliary heating plots, not shown here, no difference could be observed. The prediction of the dynamic behaviour of the building did not change at all. This finding, that one capacity node is sufficient for the modelling of a 10 cm massive wall, agrees with what is usually recommended for network models (see e.g. Palmiter and Wheeling).

The bottom line of the table shows the results of the final investigation using the Canadian data. Instead of modelling south and north zones separately, the building was modelled as one zone. It appears from the table that if the purpose of the simulation is to find the auxiliary heating energy consumption, the one-zone model provides satisfactory results. This is in close agreement with an earlier investigation with a one-zone model (Jørgensen, 1983b). The dynamic behaviour of each individual zone is, of course, completely smoothed out, and this model cannot be used for

investigations of heating power requirements of the individual rooms or of comfort conditions.

To conclude this paragraph, it can be stated that the developed model proved to be valid for this case, and the results showed that the lumping of surface layers to the zone air node seemed to be a viable approach.

6.7 Description of Sunspace Validation Case

The simulation program described in chapter 5 was primarily developed for use in the analysis of measured data from a Danish solar house. The house is one of 55 dwellings built in connection with the Danish participation in the IEA, Task VIII programme. All the houses are built according to the same energy saving concept and at a common site. The photograph in fig. 5.1 shows the monitored house.

The concept utilized to reduce the energy consumption for heating consists of the following improvements or additions to a traditionally designed house:

- orientation of primary window areas towards south
- heavy construction
- increased insulation levels in walls, floor and ceiling
- outside insulating and reflecting shutters on primary window area
- heat recovery system for ventilation
- solar domestic hot water system integrated in the south facade
- attached sunspace at south facade

The monitoring programme developed for the project includes detailed continuous monitoring of one house for one and a half year, and weekly gross heating energy consumption measurements of all the houses for the same period. The

detailed monitoring of one house includes measurement of ambient temperature, relative humidity and global radiation at three different slopes. All data are stored as half-hour values. Figure 6.8 below shows a plan of the monitored house with indication of sensor placements.

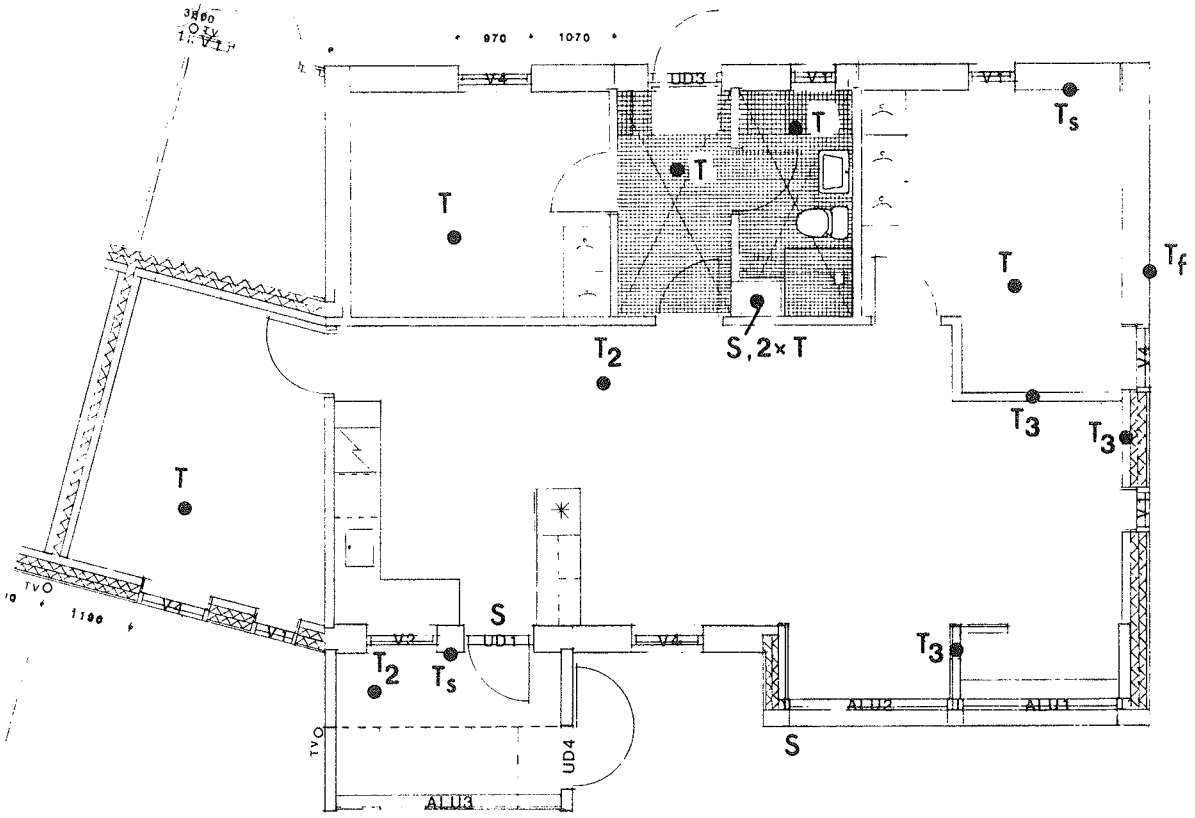

Fig. 6.8 Indication of sensor placements in monitored house.

Symbols: T = temperature, T_2 = both dry bulb and globe temperature, T_3 = temperature measured in three different depths of wall element, T_f = temperature measurements of foundation, S = switches for open or closed operation, T_s = surface temperature. (Jørgensen, 1984).

The installation of the sensors and the data acquisition equipment began in February 1985, and the monitoring and data recording commenced on April 1. However, the monitoring of the status of the mechanical ventilation system and the floor heating created some problems during the first months of operation. Also, two solarimeters were not mounted correctly at the beginning. Therefore, solar radiation data suitable for validation purposes were not produced until the first part of July.

During the summer months, the main building kept an almost constant temperature of around 25^{o}C, whereas the sunspace exhibited temperature swings of about 20 K. Since attached sunspaces have become very popular in Denmark, in spite of their, in many cases, very poor design from a thermal viewpoint, a virtue was made of necessity, and the sunspace was chosen for a validation excercise. After the validation, the model could be used for the analysis of a few alternative design strategies. The results of these studies are presented in the following chapter.

The occupants of the house were away on vacation for one week in July. The data taken during this week were chosen for the validation. In the sunspace, the windows and doors towards the ambient and towards the parent house were closed during this period. Thus, the configuration of the sunspace was unchanged, and nobody entered the sunspace during the week in question.

The sunspace is attached to the south facade of the main dwelling at the most westerly end, as shown in fig. 6.8. The wall separating the house and the sunspace is an insulated cavity wall with a double-pane window and a glass door. The end walls of the sunspace are made of heavy concrete, and the east wall has a glass door. The entire south facade and the outer half of the roof are glazed with

double-pane glazing. The inner half of the roof consists of a leca-concrete *) element covered with asbestos cement roof tiles. Figure 6.9 shows a photograph of the sunspace taken from south-east.

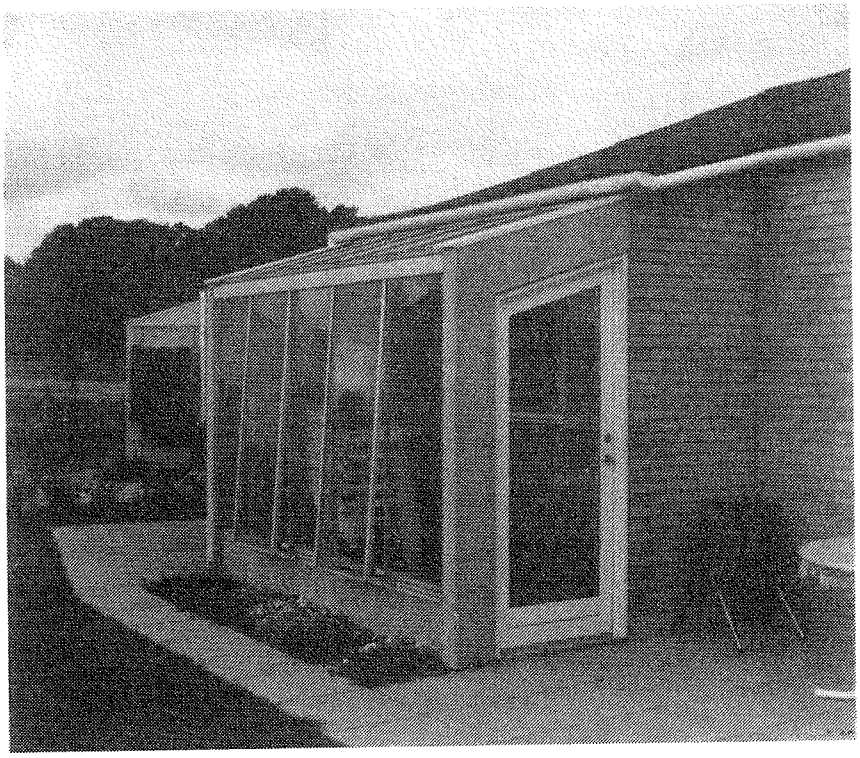

Fig. 6.9 The attached sunspace seen from south-east.

Tables 6.5 and 6.6 provide a summary of the sunspace geometry and the building element characteristics.

*) leca = expanded clay

TABLE 6.5 MAIN CHARACTERISTICS OF SUNSPACE.

Length	2.95 m
Width	2.05 m
Height	2.72 - 2.05 m
Floor area	6.05 m^2
Gross south vertical glazed area	4.72 m^2
Net south vertical glazed area	4.49 m^2
Gross south sloped glazed area	2.95 m^2
Net south sloped glazed area	2.47 m^2
Door, net glazed area	0.8 m^2
Net glazed area towards kitchen	1.6 m^2
Roof slope	30 degree
Sunspace orientation	15 degrees towards east

TABLE 6.6 DETAILS OF BUILDING ELEMENTS.

BUILDING ELEMENTS	MATERIAL	DENSITY (kg/m^3)	THERMAL CONDUCTIVITY (W/m·K)	THICKNESS (m)
Walls	Concrete	2300	1.6	0.11
Floor, tiles	Concrete	2300	1.6	0.07
Floor, gravel	Gravel	1700	1.2	0.10
Roof	Leca-concrete	1100	0.42	0.10

6.8 Weather Data Pre-Processing

For the simulation of the sunspace, hourly data of direct and diffuse radiation at each surface plus house and ambient temperatures are required. The instrumentation at the site included three solarimeters, but because of incorrect installation of one of them, only the global horizontal radiation and the global radiation at one sloped surface were available. The three equations (5.1), (5.2) and (5.3) are therefore reduced to two:

$$G_t = \cos\theta_t \, G_b + ((1 + \cos t)/2)G_d + \rho((1 - \cos t)/2)G_H \qquad (6.1)$$

$$G_H = \cos\theta_H \, G_b + G_d \qquad (6.2)$$

which must be solved for G_b and G_d for each hour

From (6.2) it follows that:

$$G_d = G_H - \cos\theta_H \, G_b \qquad (6.3)$$

substituting in (6.1) and rearranging yields:

$$G_b = \frac{G_t - (x + y)G_H}{\cos\theta_t - x \cos\theta_H} \qquad (6.4)$$

where t is the tilt of the sloped surface, 57 degrees, and

$$x = (1 + \cos t)/2 \qquad (6.5)$$

$$y = \rho(1 - \cos t)/2 \qquad (6.6)$$

As this set of equations has three unknowns, one has to be estimated. The reflection of ground seemed to be an obvious choice and ρ was tentatively fixed at 0.2. For small and negative values of $\cos\theta_H$ and $\cos\theta_t$, a simplified set of equations were used:

$$G_d = G_H \qquad (6.7)$$

$$G_b = 0 \qquad (6.8)$$

Using these conditions, a calculation of beam and diffuse radiation was attempted for the period. However, erroneous results were obtained as the beam radiation component often exceeded the solar constant, and the diffuse component became negative.

The erroneous results are probably due to a combination of uncertainties and non-valid assumptions implied in the set of equations (6.3) and (6.4). The dominating sources of errors are:

- Solarimeter errors which at low solar angles (for relatively small values of $\cos\Theta_t$ and $\cos\Theta_H$) are amplified.
- Assumption of isotropic distribution of diffuse sky radiation.
- Reflection of solar radiation from ground. The equation (6.6) is developed on the basis of isotropic diffuse reflection of both diffuse and beam reflection hitting the ground. For the beam component, the ground to some extent acts as a mirror, and the reflected beam radiation cannot be calculated by (6.6).

To be able to produce the data needed for the simulation another approach was used. Based on the global, horizontal radiation, the hourly clearness index k_T was calculated, and using the correlations of Orgill and Hollands (1977) the ratio of diffuse radiation could be calculated.

Then the beam radiation, using both equation (6.1) and (6.2), was calculated and the average of these two values was accepted as the best value obtainable on the basis of the current data.

The diffuse and beam radiation obtained this way were used to calculate direct and diffuse solar radiation at each surface of the sunspace. These data were, together with cosinus of the incidence angles, ambient and parent house temperatures, stored in a file to be read by the simulation program.

6.9 Nodal Model Construction

A network model consisting of ten capacity nodes was set up to model the sunspace. The location of the ten nodes is shown on the plan and section of the sunspace in figs. 6.10 and 6.11.

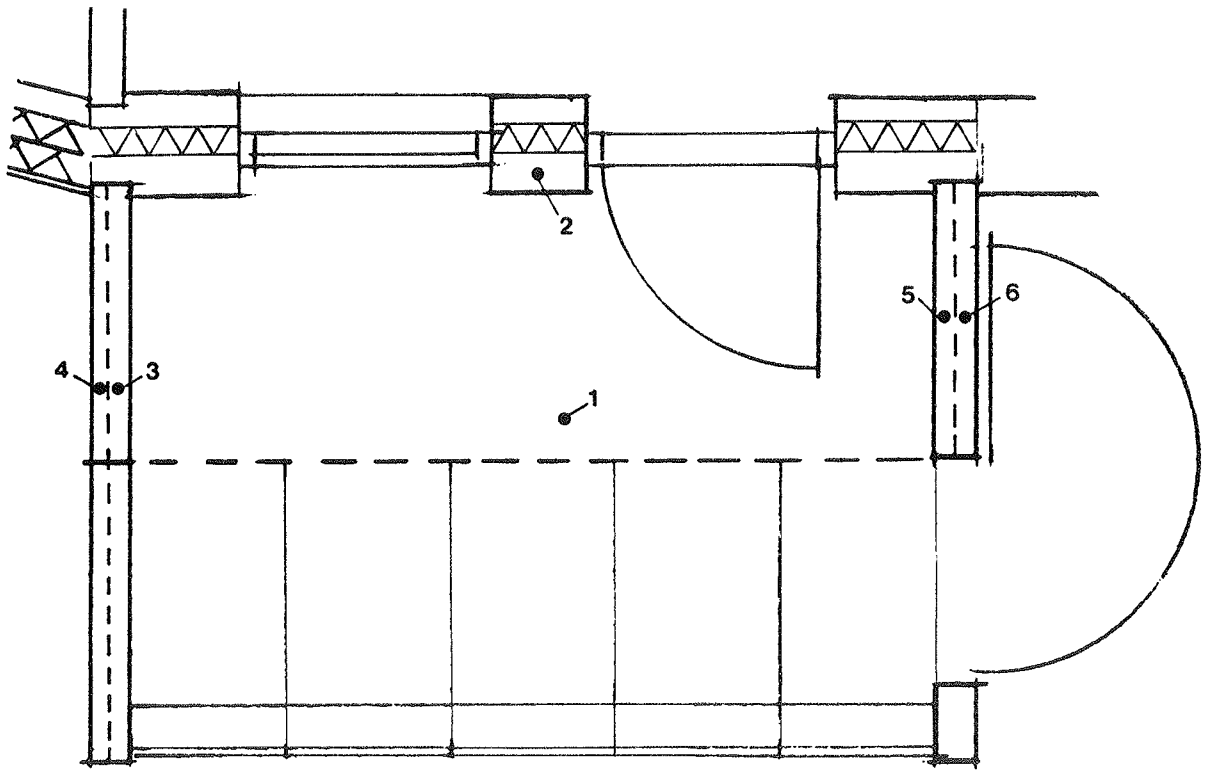

Fig. 6.10 Plan of sunspace. Location of thermal network nodes indicated by numbers.

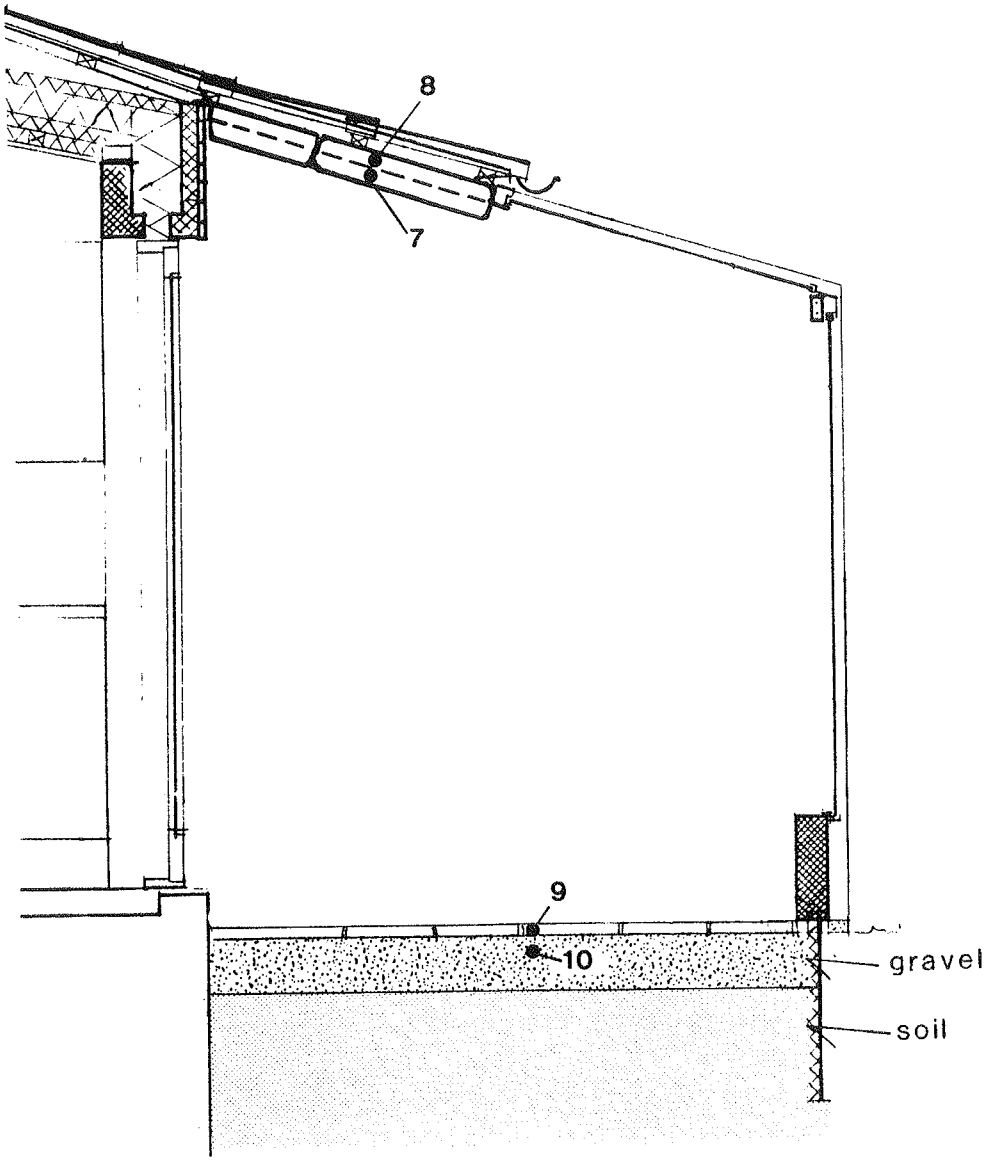

Fig. 6.11 Section of sunspace. Location of thermal network nodes indicated by numbers.

The use of two nodes for each end wall of the sunspace instead of only one was chosen, because these walls are directly exposed to the ambient temperature as well as to solar radiation gain. They will therefore be subject to large temperature swings and heat transfer in both directions. This reasoning also applies for the opaque part of the roof.

The method of lumping a thin surface layer of each mass element, as described in paragraph 6.5, was also adopted here.

6.10 Sunspace Validation Results

The monitoring of the house includes three temperature measurements in the sunspace. They are: air and globe temperatures plus a surface temperature of the wall separating the sunspace and the house. None of the three temperature sensors were directly exposed to sunlight during the period chosen. Figure 6.12 is a photograph showing the air and globe temperature sensors.

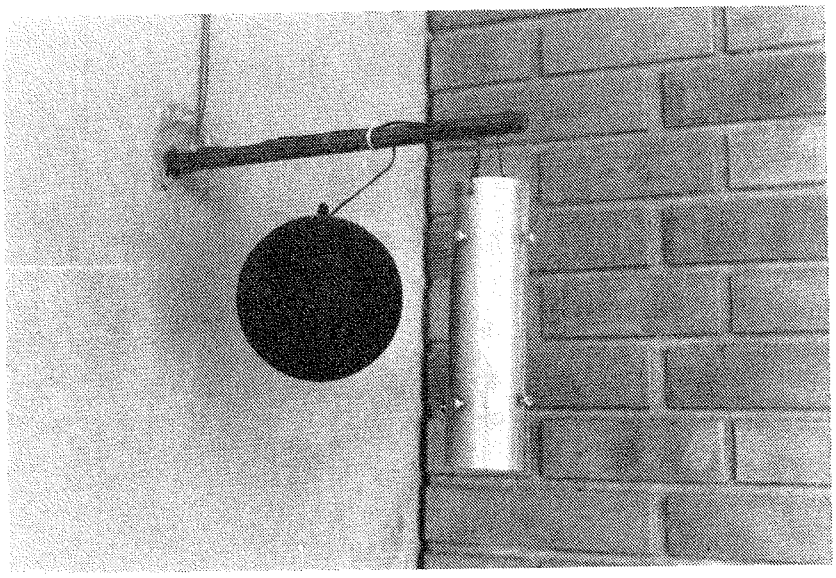

Fig. 6.12 The air and globe temperature sensors.

The air, globe and wall temperatures are plotted in fig. 6.13 along with the ambient temperature.

In fig. 6.13 it is seen that the sunspace air and globe temperatures are very close during the whole week. It may also be observed from fig. 6.13 how the mass wall seeks to stabilize the temperatures within the sunspace. Because

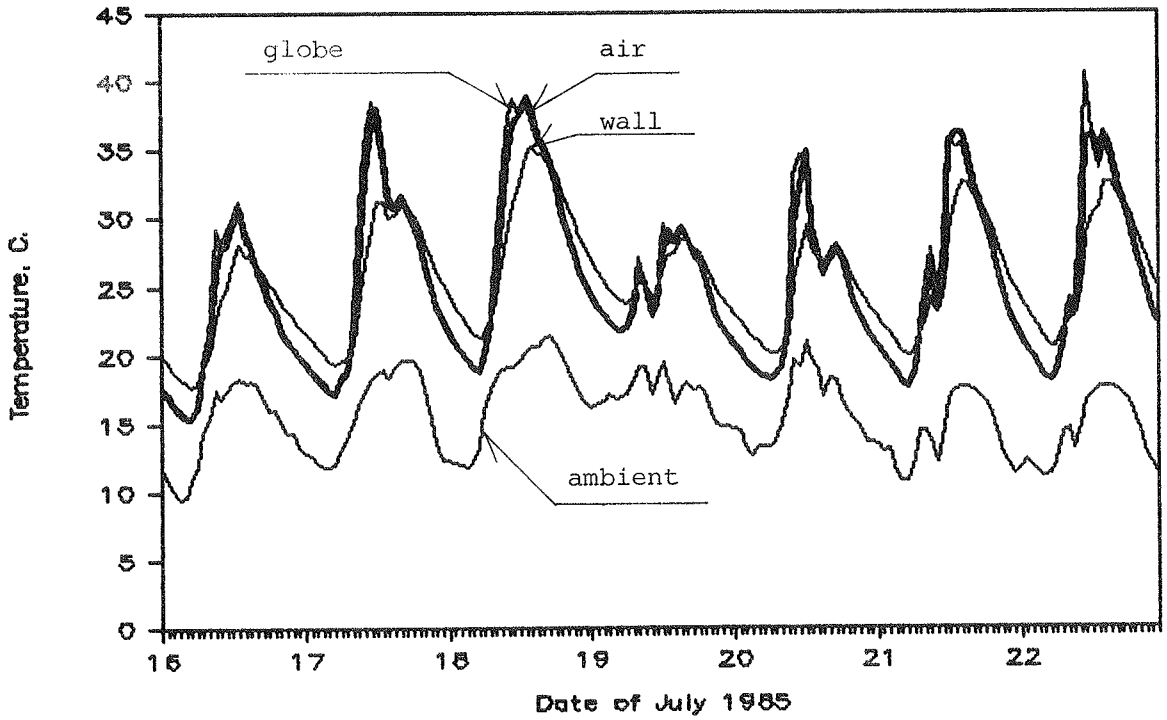

Fig. 6.13 Sunspace validation case.
Measured globe, air, wall and ambient temperatures.

the air and globe temperatures are so close, there is no point in establishing a weighted average for the comparison to the model prediction of a "mixed" internal temperature. The air temperature was chosen for the comparison, which is shown in fig. 6.14.

From fig. 6.14 it can be seen that the simulation model tracks the measured thermal dynamic behaviour of the sunspace very closely. The predicted temperature curve is shifted a little upwards compared to the measured. A fact which also shows up when comparing the average measured and predicted temperatures during the period, respectively 25.4 ^{o}C and 26.2 ^{o}C.

Figure 6.15 shows a comparison of measured and predicted wall temperatures. Again, the dynamic behaviour is tracked rather well, with the predicted curve shifted a little more upwards relative to the measured. The average measured wall temperature for the period is 25.5 ^{o}C and the predicted is 26.7 ^{o}C.

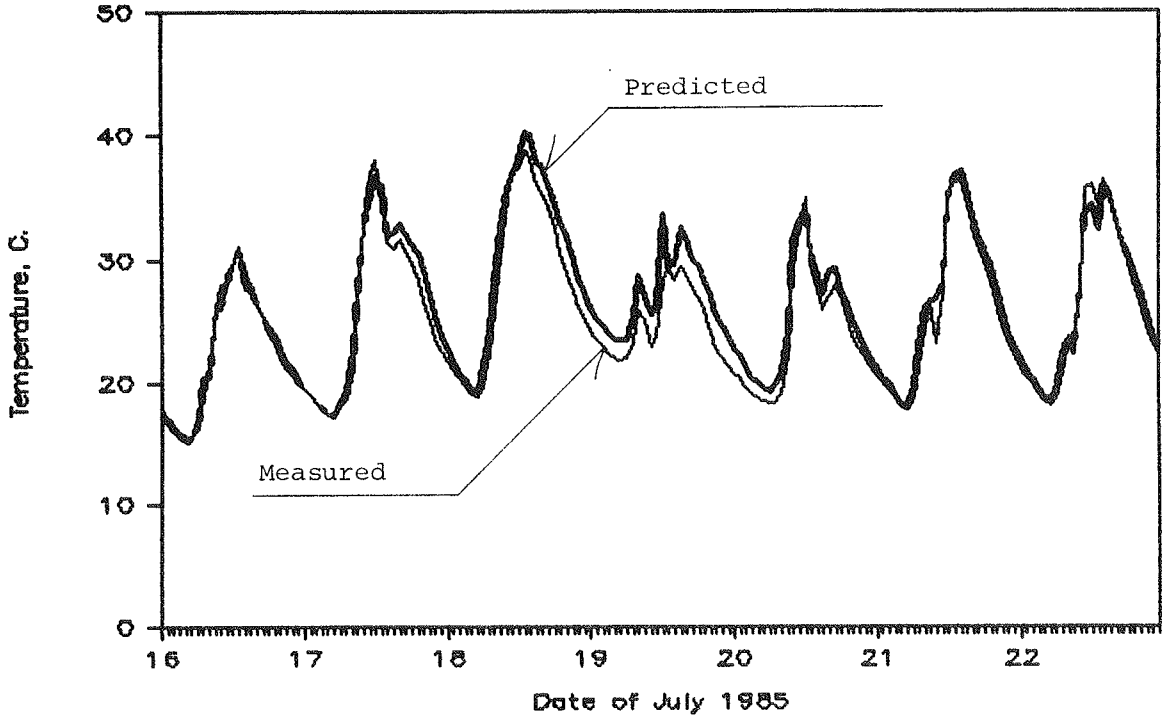

Fig. 6.14 Sunspace validation case.
Measured and predicted internal sunspace temperatures.

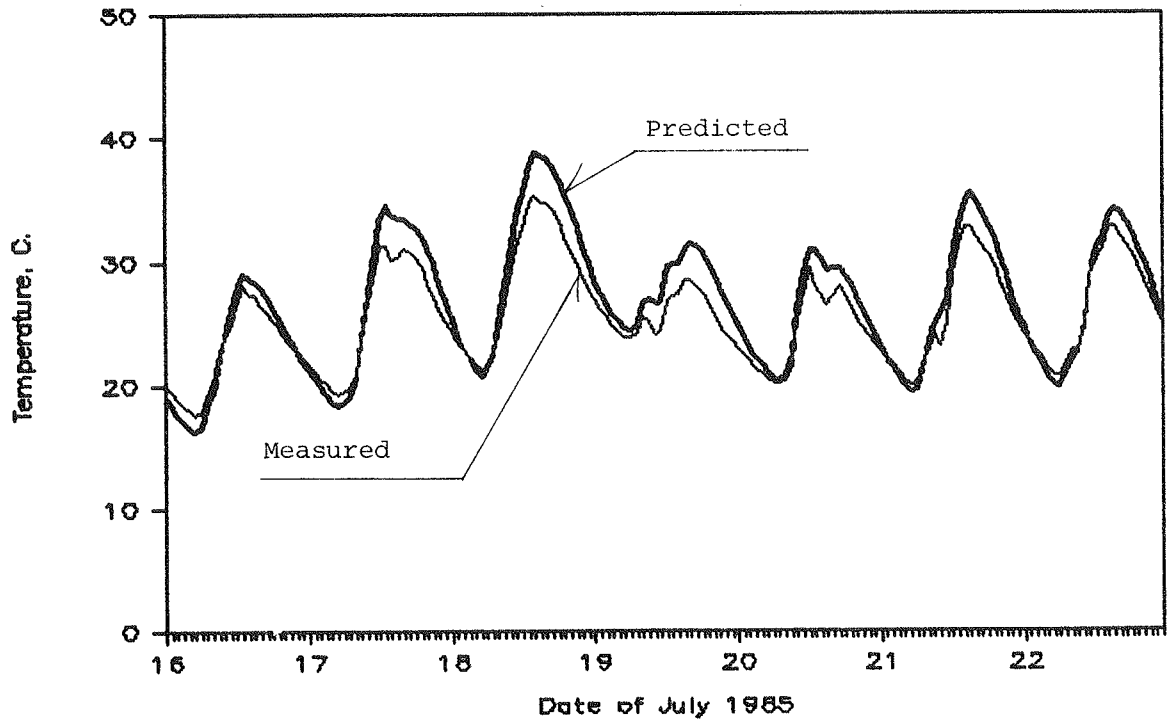

Fig. 6.15 Sunspace validation case.
Measured and predicted sunspace wall temperatures.

The overprediction of wall temperature may be a consequence of the lumped model approach. A correct distribution of the solar radiation within the sunspace, in a traditional model, might have resulted in a closer agreement for this variable. However, the close agreement on the internal temperature of the sunspace, which by far is the most interesting of the two, is a satisfactory validation result. On this basis further validation work, including the rest of the house in a stepwise procedure, can be pursued. Also, this agreement justifies the use of the developed model and simulation program for investigations of the thermal consequences of alterations of the design of the sunspace. A few examples of such investigations are presented in chapter 7.

7. MODEL USE

7.1 Design or Research

Results generated by simulation models can be used in a number of different ways. A researcher may use the results to gain new insight in the thermal behaviour of a construction designed according to a new concept, or use the results to generate design guidelines for designers. For larger projects simulation models may be used directly in the design process. In this chapter a few examples of results obtained by simulation models are presented as an illustration of the use of simulation models for different purposes and the kind of results which can be achieved.

7.2 Parametric Sensitivity Study

Usually the time and money available for the design of small scale projects, i.e. one or a few single-family houses, do not allow for a thorough thermal design analysis using a simulation program. For projects like these, the existence of quantitative guidelines is essential in order to obtain a satisfactory thermal performance of the buildings. Quantitative design guidelines may be developed by performing numerous simulations for different building types and configurations and for different parameters. A series of simulations with varying parameters is referred to as a parametric sensitivity study.

Within the IEA Task VIII research programme, the results of parametric sensitivity studies will be used to generate quantitative design guidelines, which will become a substantial part of a design handbook. These guidelines will be developed for each country or each climatic region. The guidelines developed for Denmark will be based on parametric sensitivity studies performed with the American simulation program, SERI-RES (Palmiter and Wheeling) using the Danish Test Reference Year (Lund, 1985) as climate input data.

SERI-RES is a simulation program based on a thermal network representation of the building, and is therefore in many ways similar to the program described in chapter 5. SERI-RES was also validated against the Canadian direct gain test building (see chapter 6) with satisfactory results.

The base building defined for the outset of the parametric sensitivity study was the same for all the IEA participating countries. It is a middle unit, two-storey rowhouse with a total floor area of 96 m^2. The east and west walls are common with the next houses in the row, and the glazing is equally distributed on the north and south facades. The heating set point was 20^{o}C. For the Danish conditions, a few modifications were made to obtain a base building in accordance with the Danish building regulations. It is worth mentioning that all the participants simulated the base case first and compared their results to results produced with SERI-RES by the U.S. participant (Holtz and Teller, 1984). In this way, a starting point was established from which the individual researcher could step away to a country-specific base building.

The conduction of a parametric sensitivity study takes careful planning to limit the number of simulation runs needed to generate the desired results. It is necessary to decide in which form the results should be presented and to guess what the results are likely to be. By doing that, it is possible to plan the simulation runs in a way which allows for optimum use of the generated results.

The following six figures present the results of the parametric sensitivity study simulation runs performed so far. The simulation runs were planned in such a way that the results of as many as possible of the simulations could be used as points on different sensitivity lines. The six figures represent the results of 48 simulations.

The first four figures show the sensitivity of a direct gain passive solar house to different parameter variations, and the latter two are made for attached sunspace designs.

The six figures are all constructed according to the same concept. Each curve is a so-called Load-curve, which means that for each point on the x-axis, the curve shows the corresponding heating load of the house in question to be read at the y-axis. The x-axis on the first four figures reflects south facing window area, and on the two latter figures the sunspace area measured at the south facade of the house.

The impact of moving north facing windows to the south facade is shown in fig. 7.1. The not surprising design guideline, which can be derived from this figure, is that as much of the window area as possible should be oriented towards south. What, perhaps, is surprising to some, is the relatively large impact of moving a 5 m^2 window area from north to south.

A light house is defined as a house built as a light timber-frame wall construction, typical of U.S. construction. The heavy house is a masonry wall construction, like a typical Danish masonry house.

The four curves in fig. 7.2 very clearly illustrate how the optimum window area dramatically changes with the type of glazing. The definition of super-glazings used here is a window with the same transmissivity as a double pane window, and a U-value being half of the U-value of a traditional double pane window (1.5 W/m^2K). The flatness of the lower curves is worth noticing. For the heating bill, the size of the south facing window does not mean a lot.

The importance of mass for the utilizability of the solar gain is illustrated in fig. 7.3. When additional mass has been added in a Danish masonry construction type building, especially for solar energy utilization, the lower curve

should be used to find the optimum window area. It is seen that the addition of mass is essential if the south facing window area exceeds 10% of the floor area.

The utilization of solar energy in a direct gain passive house is highly dependent on the temperature swings accepted. The energy is stored as sensible heat, which means that the storage capacity is directly proportional to the difference between heating and venting set points. This effect is illustrated by fig. 7.4. It is seen that the larger storage capacity obtained between 18^{o}C and 26^{o}C more than doubles the optimum window area.

Just as for houses, finding the optimum balance between glazing and insulation, is also a discussion point with regard to attached sunspaces. Should the end walls of a south facing sunspace be glazed or insulated? Figure 7.3 shows that the performance, from an energy point of view, is somewhat better for a sunspace with insulated end walls than for a sunspace with glazed end walls.

Also, for the common wall between the house and the sunspace, the optimum size of the glazed area may be found. This is, of course, very dependent on other passive solar gains to the house influencing how much of the solar gain entering through the sunspace can be utilized. For the case shown in fig. 7.6, the only other passive gain is a direct gain window of 2.4 m^2. It is seen that, even though the losses to the sunspace are smaller than to the ambient, the optimum area of double pane windows in the common wall is rather low. This is a somewhat surprising result, and the case needs further analysis before design guidelines can be deducted.

The results presented in this paragraph are showing only the sensitivity of heating energy to the parameter changes. Design can also be based on another important aspect, namely the temperature. The following two paragraphs illustrate how this may be done.

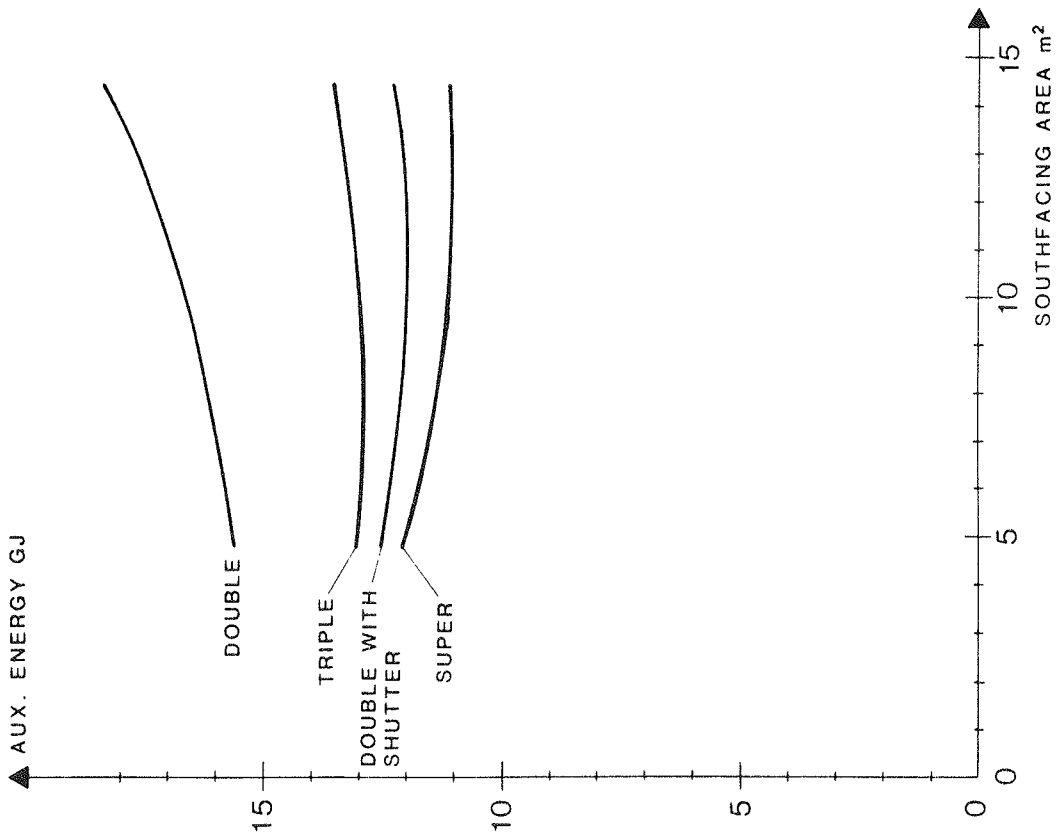

Fig. 7.2 Impact of increasing the window area for different glazing types.

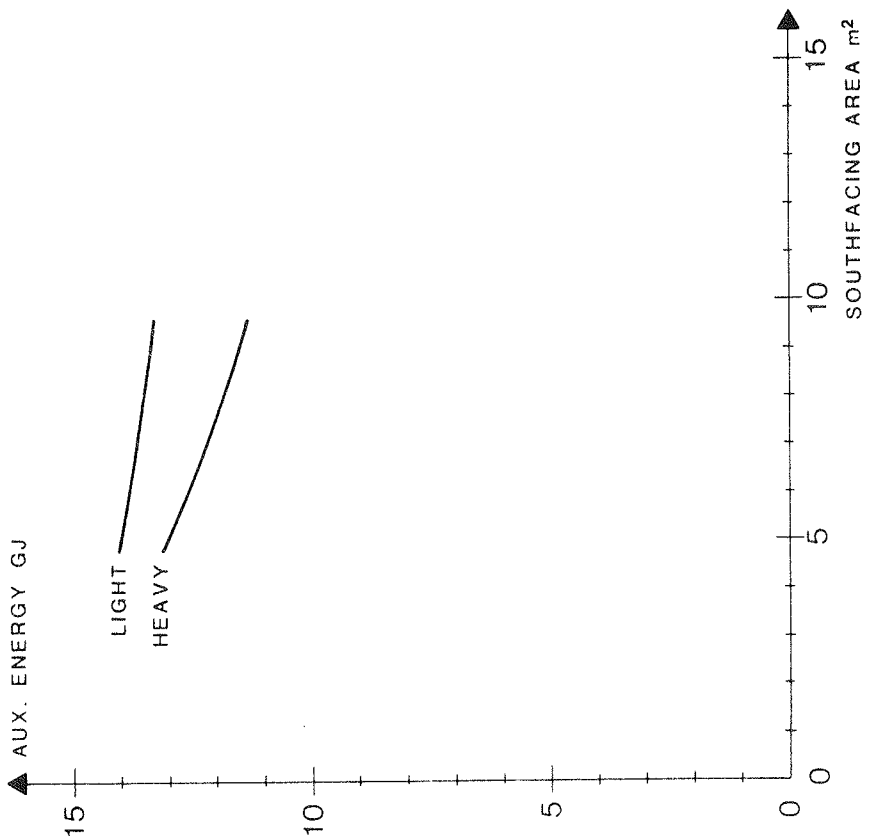

Fig. 7.1 Impact of moving windows from the north facade to the south.

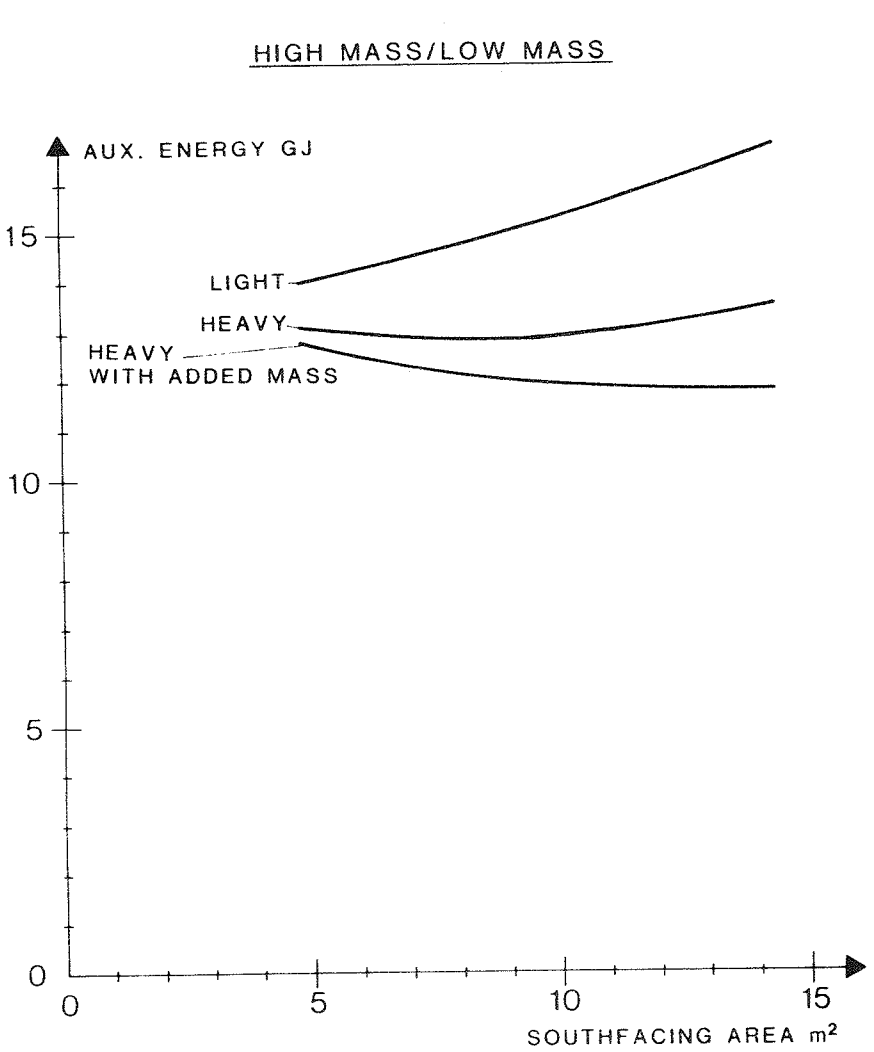

Fig. 7.3 Impact of mass level on optimum window area.

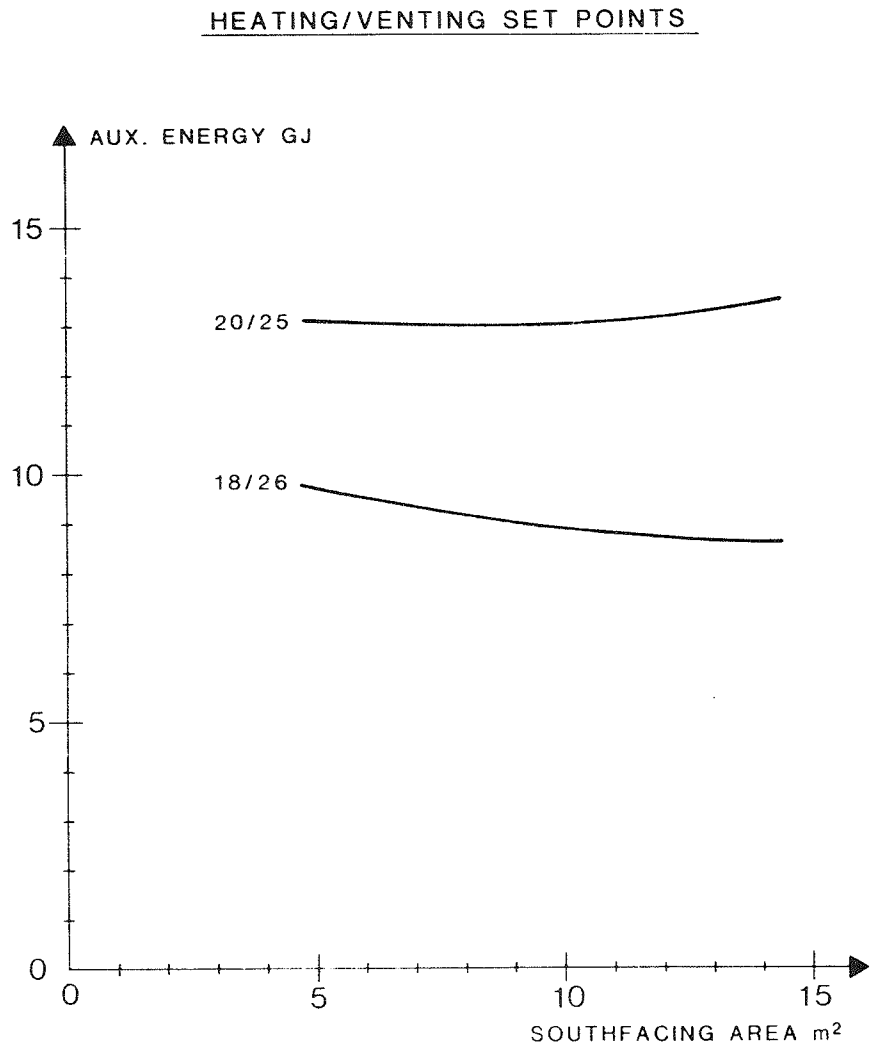

Fig. 7.4 Impact of heating and venting set points on optimum window area.

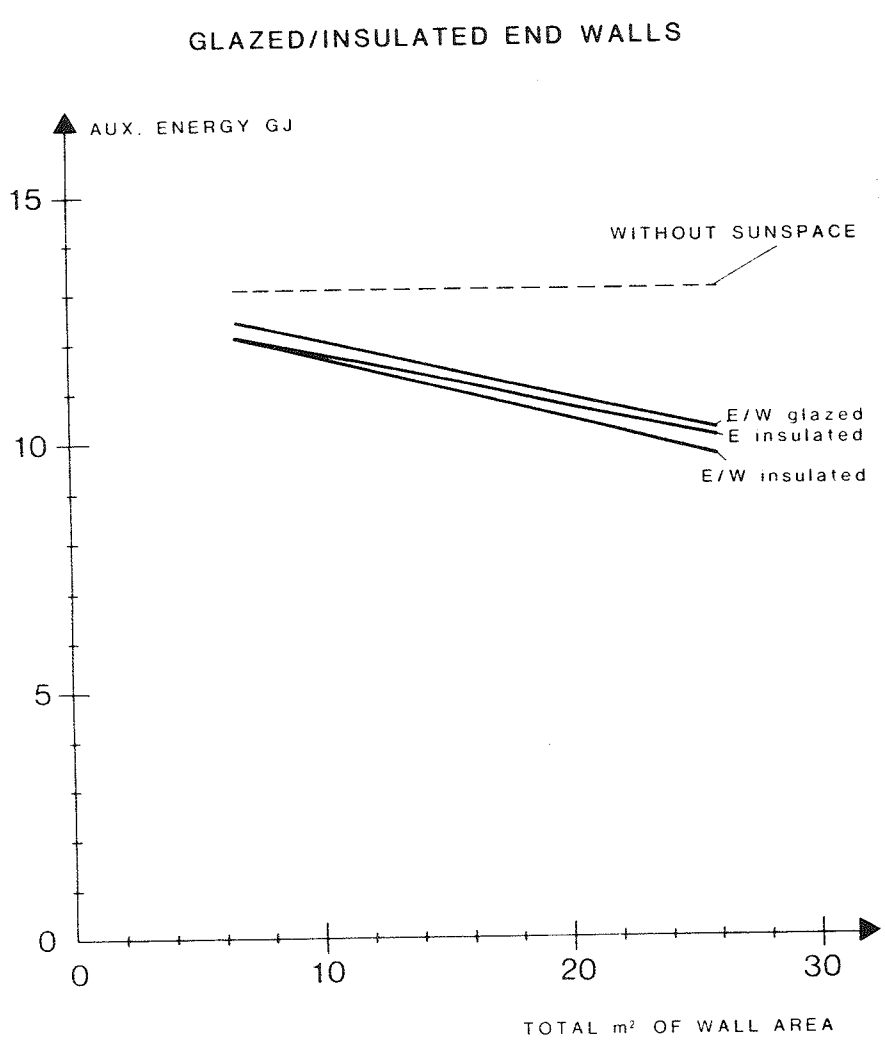

Fig. 7.5 Impact of glazed or insulated end walls on sunspace performance.

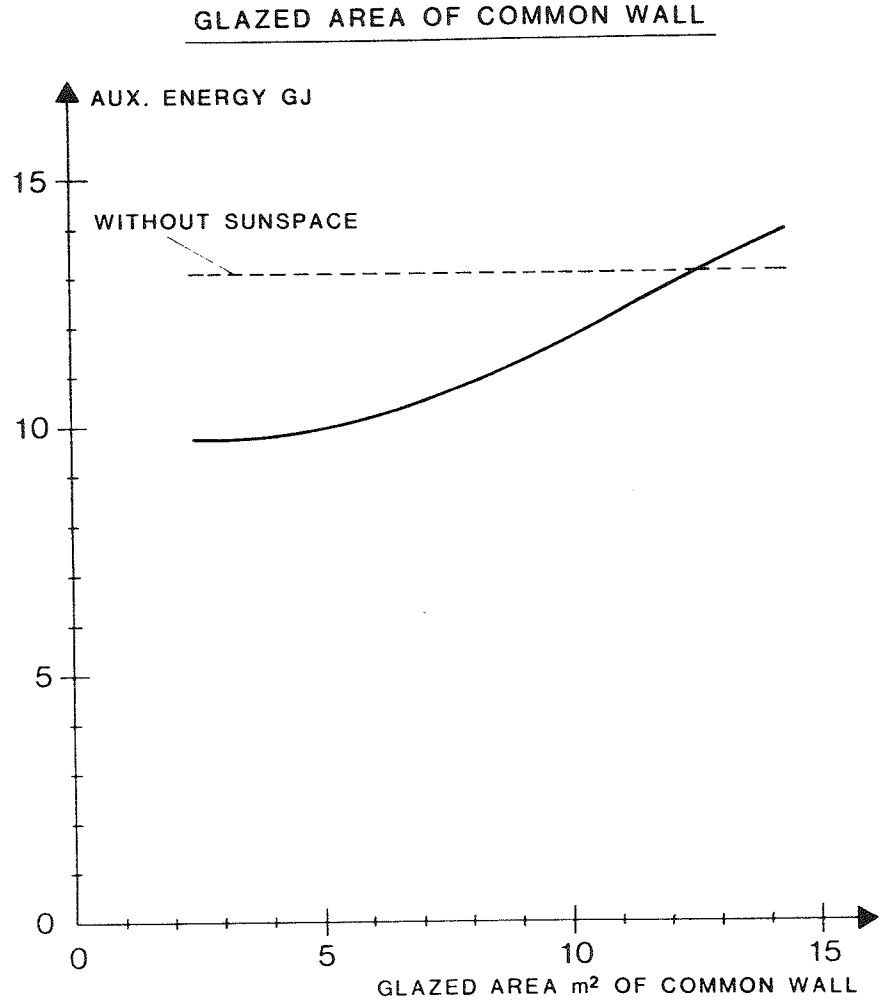

Fig. 7.6 Impact of the area of glass in the common wall.

7.3 Design by Temperature

The temperature within building zones and construction elements are the thermal state variables of the building system. As such, temperatures explicitly indicate what the states of the building are at each instant of time, and the change of temperatures with time gives insight in the performance of the building.

The temperature may be looked at as the pulse of the building. Temperature is something we all know about by personal experience. It is not as abstract as energy consumption, on the contrary, it is immediately understandable. Temperature is something which can be sensed by the body.

Because of the facts stated in the above paragraphs, temperature is the single most important variable from a pedagogical point of view. The understanding of the basic thermal physical principles, underlying any solar heating system design, is increased by seeing how the temperatures of different systems or building elements develop as a consequence of the climatic conditions. In this paragraph the use of temperature plots, as a pedagogical means for an introduction to passive solar design, is illustrated. As part of an introductory course on passive solar heating design, given by the author to a class of architect students at the Royal Academy of Fine Arts in Copenhagen, a network simulation program, in principle identical to the program described in chapter 5, was developed. The program was used to model some of the students' designs in order to show how the different designs performed.

The results presented here are for a well-insulated, middle unit, two-storey rowhouse with an unheated buffer zone towards the north. The house was designed both as a direct gain solar house and equipped with a solar wall in the south facade.

The students had designed an outside movable insulating shutter, and the impact of this shutter on the performance was part of the investigation. A section of the building modelled is presented in fig. 7.7.

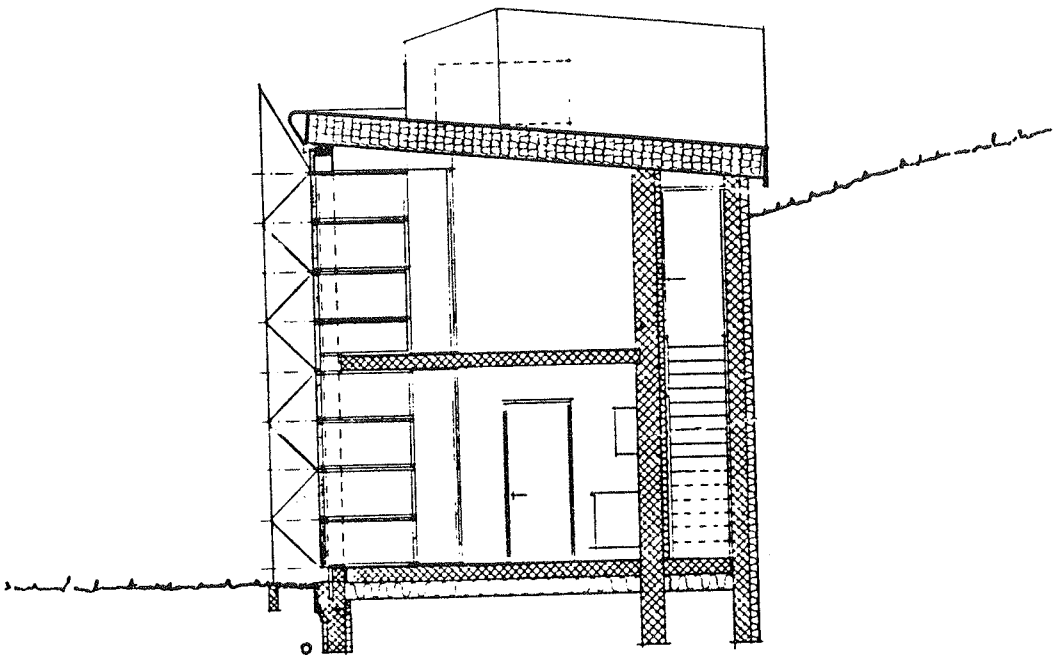

Fig. 7.7 Section of the students' test house.

The house is insulated to a U-value of 0.2 $W/m^2 \cdot K$ in the walls and 0.15 $W/m^2 \cdot K$ in the roof. The mass is placed in the floor, the storey partition, and in the wall towards the buffer zone. Two different direct gain cases were modelled; a moderate mass case in which each of the above elements consisted of 10 cm thick concrete, and a very heavy mass case in which the thicknesses of the concrete elements were increased to 20, 25 and 30 cm, respectively. In the solar wall case, the floor and wall are made of 10 cm concrete, the storey partition is massless, and the solar wall is a 20 cm concrete element. In all cases, a 10 cm mineral wool insulation layer is placed on the outside of the wall, towards the buffer zone. During the

simulations, the bathroom was heated to 21°C, while the rest of the house was neither heated nor cooled. The shutters were opened between 8 a.m. and 4 p.m. and closed for the rest of the day.

The houses were modelled by a 15 node network using three nodes for each of the main capacity elements. The placement of the nodes is shown in fig. 7.8. The heated bathroom is node 15.

A five-day period of January of the Danish Test Reference Year was simulated for each house design. The plots presented here cover three days at the end of the period from January 7 to January 9. The 5th and 6th of January are very cold days with literally no sunshine, well-suited for an initiation period for the simulation. Plots of ambient temperature and solar radiation for January 7 to 9 can be seen in the next paragraph.

In principle, a temperature plot can be obtained for each of the nodes in the network. Four of these have been selected to illustrate how the three different designs performed during the cold and sunny period of January. Figures 7.9, 7.10 and 7.11 show how the indoor temperature of the lower zone (node 2) changes during the period. Fig. 7.12 shows the development of the temperature in the inner and outer surface layers of the solar wall.

It is interesting to compare how the solar gain affects the indoor temperature in the three different designs (figs. 7.9, 7.10 and 7.11). In both direct gain cases, the increase in temperature is rather steep and occurs at the same time. The additional mass of the heavier of the two results in a maximum temperature within comfortable limits, whereas the temperature in the lighter case reaches 27°C. The solar wall has the expected effect, as it both delays the solar gain to the room for 6-7 hours and prevents overheating. Especially on January 8 and 9 it is impressive how stable

the temperatures are in the solar wall design.

Figure 7.12 illustrates the temperature delay and the dampening effect on the solar wall. The temperature of the outer surface layer rises very quickly as it absorbs the solar radiation. The thermal resistance of the wall causes a delay of 4-5 hours before the inner surface temperature reaches its maximum. As the zone air is heated by the inner surface, another 1-2 hours delay occurs before the zone air reaches its maximum.

The conclusion reached on the basis of these simulations is that, from a comfort point of view, the solar wall passive design is superior, even to a very heavy direct gain design. It needs to be emphasized that this is on the presumption that identical outside, movable insulating shutters are applied to each design.

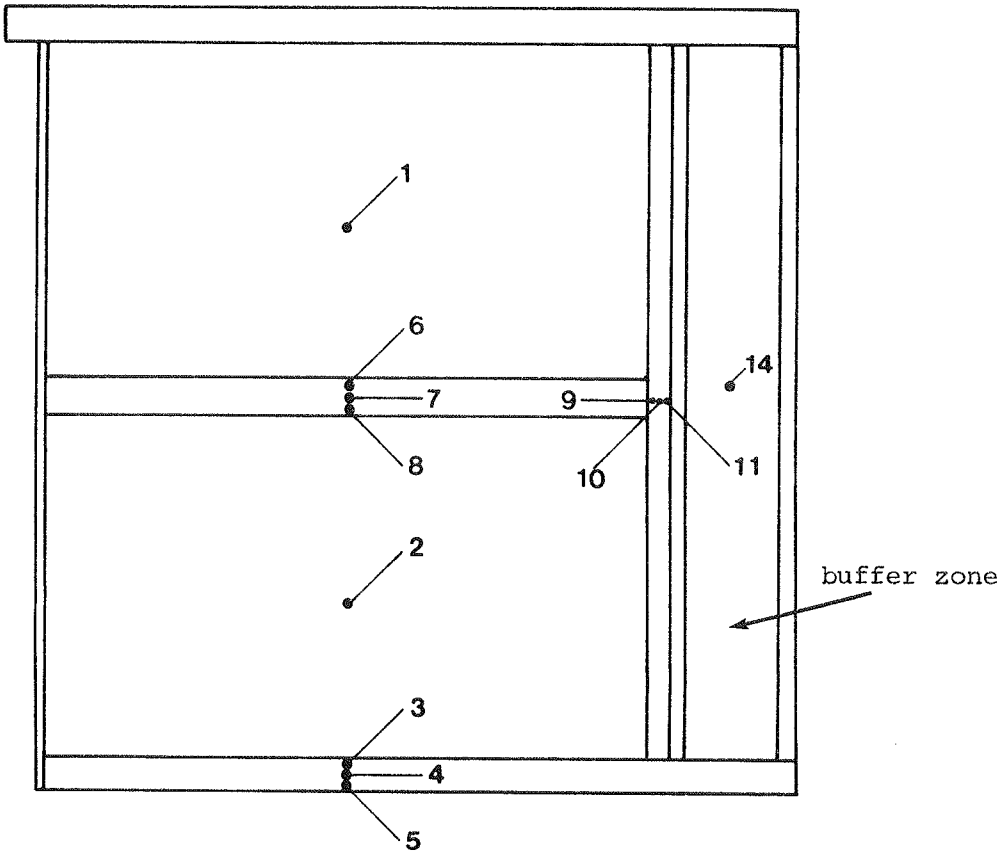

section, 1:50

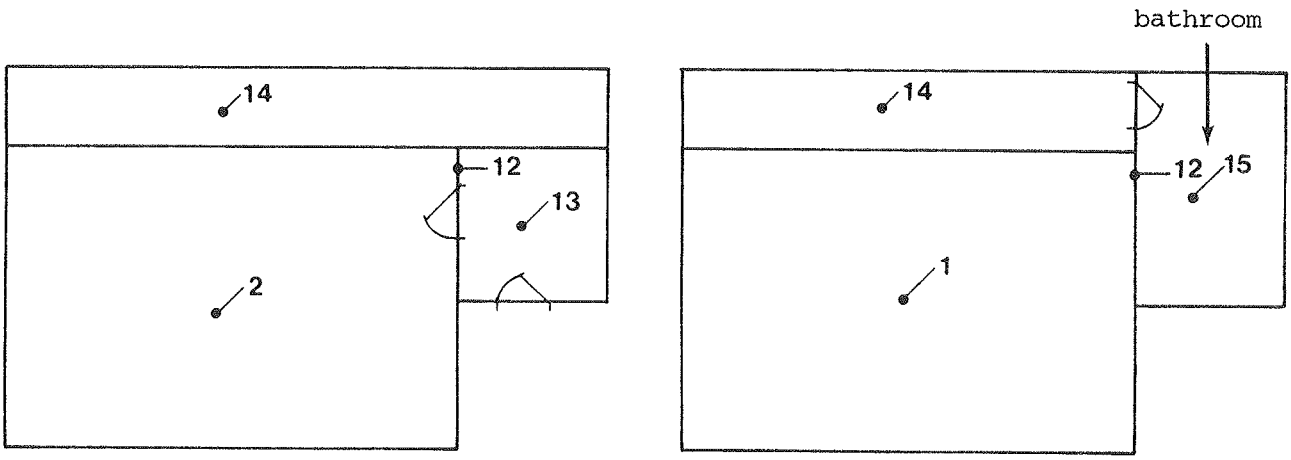

1st floor plan, 1:100

2nd floor plan, 1:100

Fig. 7.8 Location of network model nodes in students' test building.

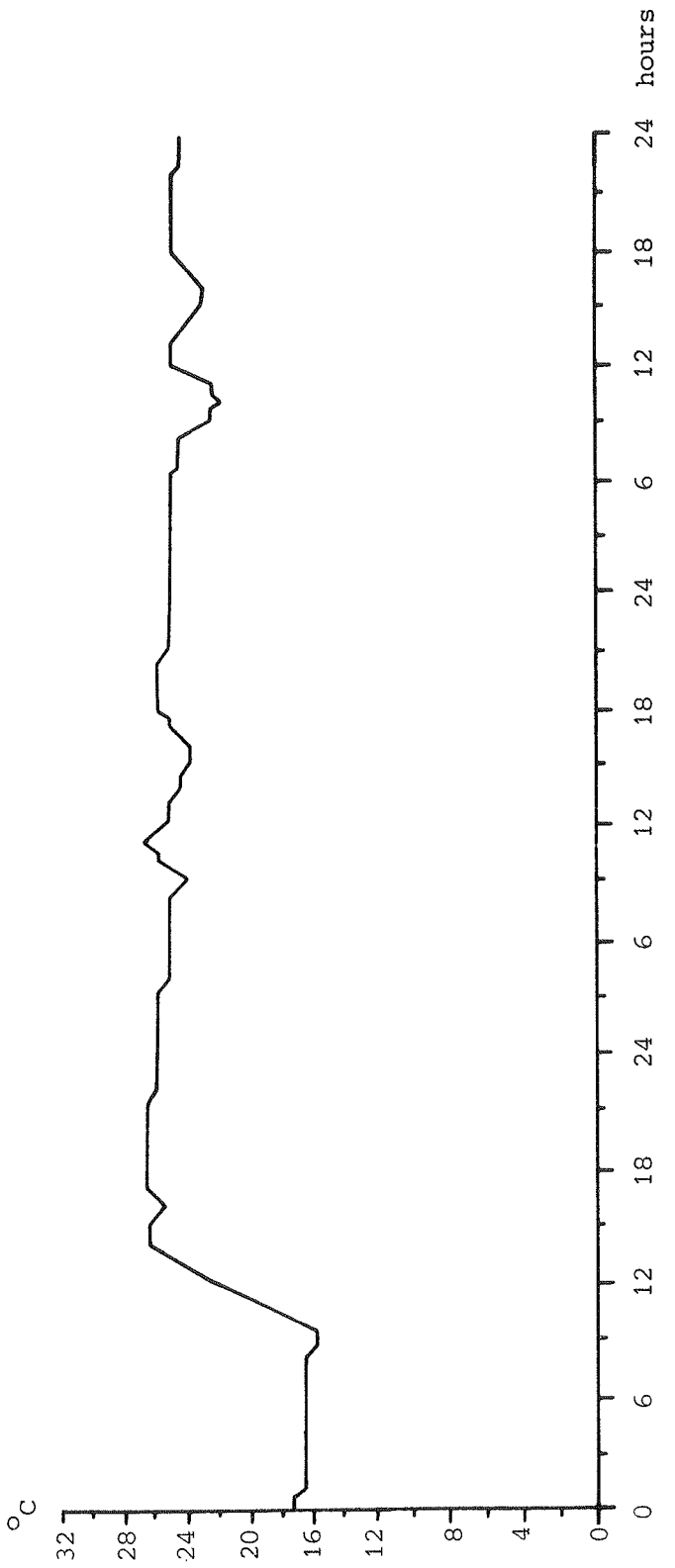

Fig. 7.9 Indoor temperature predicted for "light" direct gain building.

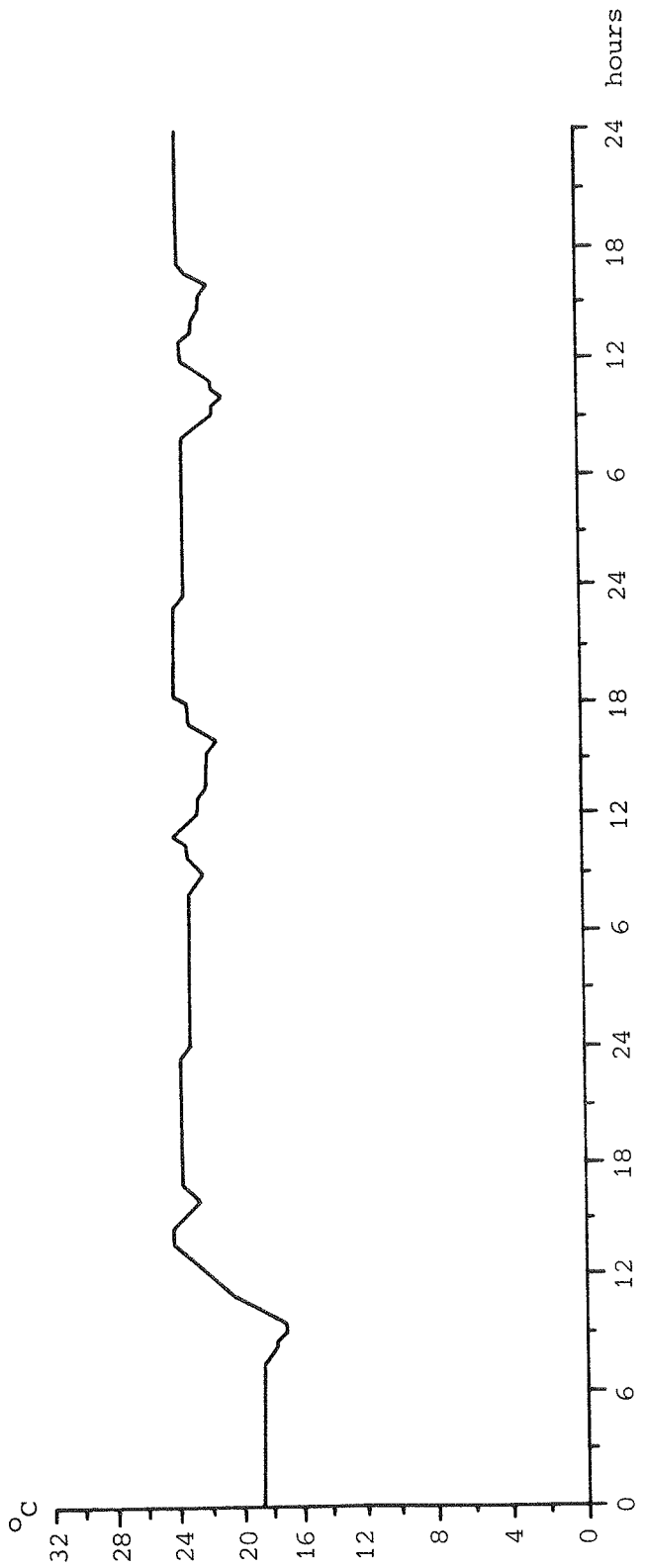

Fig. 7.10 Indoor temperature predicted for heavy direct gain building.

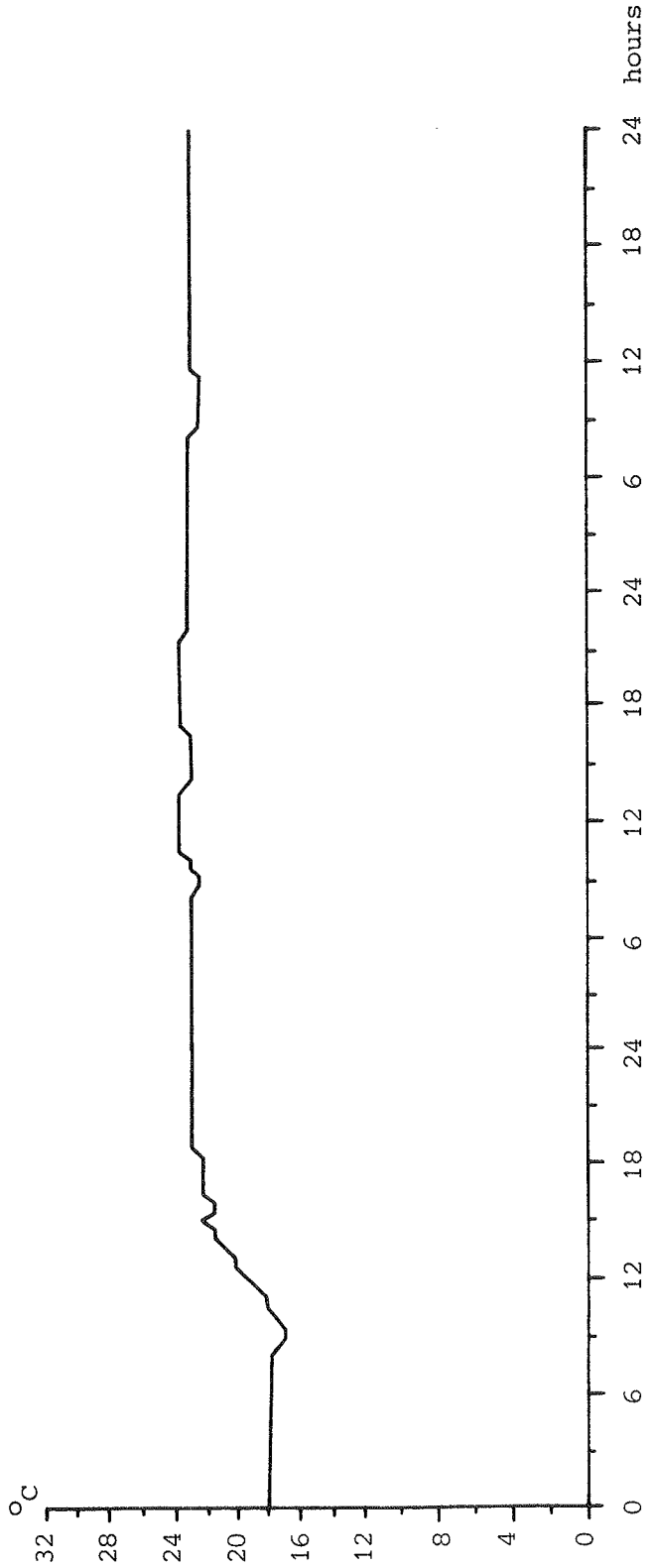

Fig. 7.11 Indoor temperature predicted for building with solar wall.

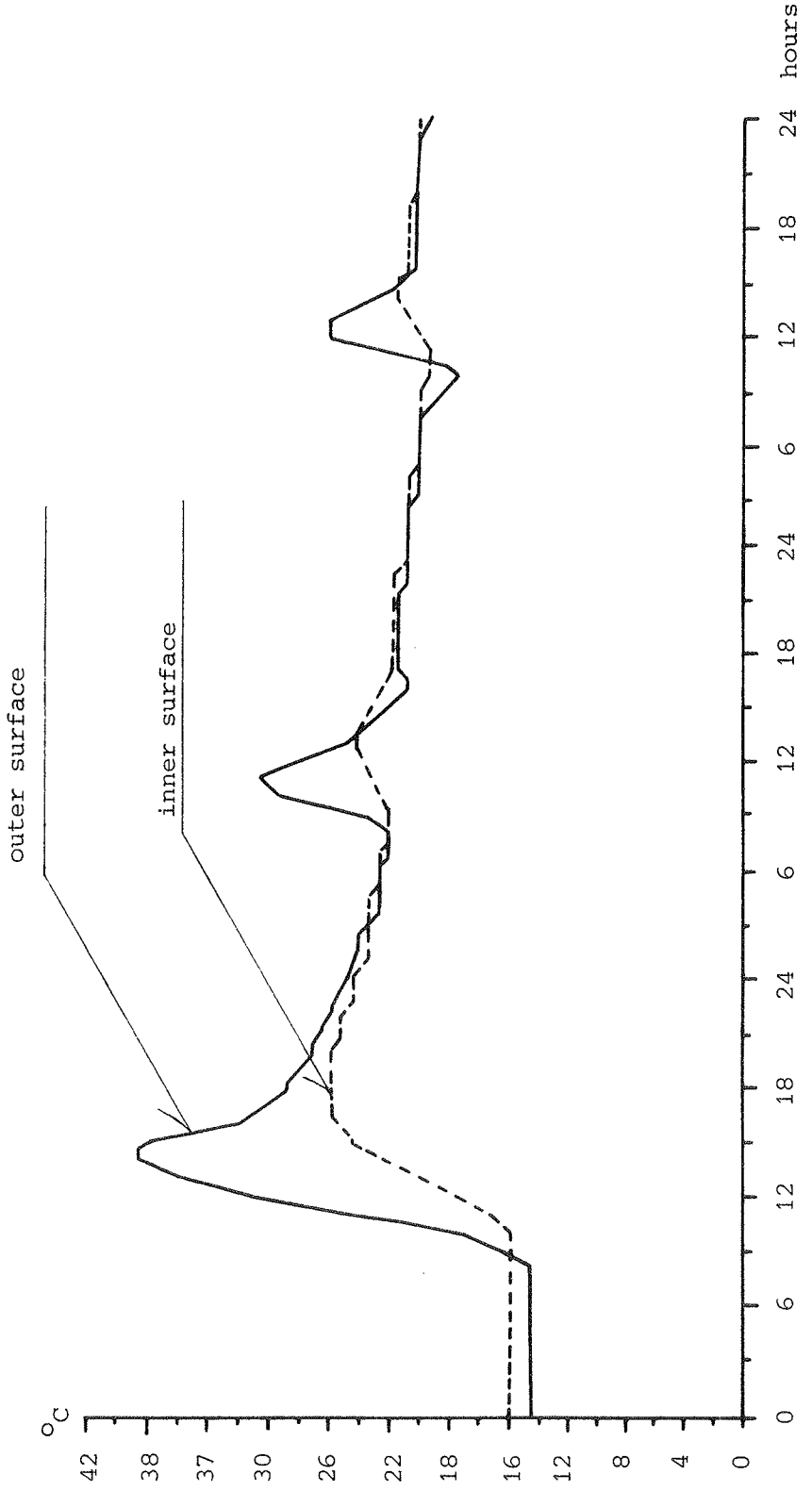

Fig. 7.12 Outer and inner solar wall temperatures.

7.4 Attached Sunspace Design Modifications

Attached sunspaces have become very popular in Denmark during the last five years. Many different designs have been developed with very little attention to the thermal performance of the sunspaces. They are often largely overglazed and have no internal mass. The result is that the temperature within the sunspace fluctuates a lot, and periods of comfortable temperature conditions are shorter than they need to be. It is therefore interesting to analyse attached sunspaces under Danish climate conditions in order to provide design guidelines for designers and house owners.

It is not the intention to undertake and present a full analysis of attached sunspaces in this context, but rather to show the relative impact of certain design modifications for a specific case. The results of this study may then be used as basis for a more extensive and complete analysis.

The results obtained in the empirical validation study on the attached sunspace, described in the previous chapter, justify the use of the network model constructed for this sunspace for an analysis of the impact of design modifications to this design. The following five modifications to the base case were made:

1. The number of layers of glazing was reduced from two to one.
2. Additional mass, corresponding to 250 litres of water, was added to the zone.
3. Additional mass, corresponding to 500 litres of water, was added to the zone.
4. The end walls and the unglazed part of the ceiling were insulated with 5 cm of mineral wool.
5. Modification 3 and 4 in combination.

The base design and the five modified designs were all simulated through one week of weather data from January and one

week of data from April. Both periods were selected from the Danish Test Reference Year. These weeks were selected to elucidate two main questions relevant for attached sunspaces under Danish climate conditions: How often will the sunspace reach temperatures below zero? What are the thermal comfort conditions provided by the sunspace during spring and autumn?

The Danish Test Reference Year includes hourly normal solar radiation and hourly diffuse solar radiation. Assuming an isotropical distribution of the diffuse radiation over the sky and of the reflected radiation, it is straightforward to calculate the direct and diffuse radiation impinging on each surface at the sunspace (Duffie and Beckman, 1980). Figures 7.13 and 7.15 show the calculated direct and diffuse radiation at the south, vertical surface. It is seen that the first three days of the week in January are extremely sunny, whereas the solar radiation level is more moderate in the week of April. Figures 7.14 and 7.16 show the ambient temperature and the temperature predicted for the base case design of the sunspace. The average ambient temperature during the week of January is $-2.4^{o}C$. The average temperature of the coldest month, being February, is $-1.1^{o}C$. The average ambient temperature for the week in April is $4.5^{o}C$.

The results of the temperature predictions for each of the modified designs are compared to the predictions of the base design in the figures (figs. 7.17 - 7.26).

Figures 7.17 and 7.18 show the impact of using one layer of glass in the sunspace instead of two. It is seen that the temperatures are constantly $1-2^{o}C$ lower than for the original design during both weeks.

The mass added to the sunspace, in order to stabilize the temperature swings, appears from figs. 7.19 - 7.22 to be very effective. In both cases (250 litres and 500 litres of

water added) it is seen that the temperature does not drop as drastically as for the base design in January. In April, the added mass reduces the peaks and makes the temperature drop at a lower slope during the afternoon and evening hours.

The impact of insulating the end walls and the unglazed part of the ceiling, which in the base design is made of uninsulated concrete, is shown in figs. 7.23 and 7.24. It appears that the temperatures reached at the peaks are close to those for the base case, whereas the temperature drops are very much reduced.

Finally, the impact of adding both mass and insulation to the base design can be seen in figs. 7.25 and 7.26. It is obvious that these design modifications very effectively smooth out the temperature swings in the sunspace. The temperature is below freezing point for only a very few hours in January, and in April temperatures are up to $3^{o}C$ higher in the evenings than for the base design.

In order to provide an overview of the results, the minimum temperatures reached during the week of January and the mean temperatures obtained in both weeks are compiled in table 7.1. As seen from the plots, it is obvious that the reduction from two to one layer of glass in the sunspace reduces the thermal performance of the sunspace, while it is increased by the other modifications. However, to produce more definite guidelines, this analysis has to be followed up by simulations using the complete Test Reference Year. Not to be overlooked is the question of economics which, inevitably, will have to be dealt with by the individual builder or house owner.

TABLE 7.1 PREDICTED MEAN AND MINIMUM TEMPERATURES FOR THE DIFFERENT SUNSPACE DESIGNS.

CASE	JANUARY		APRIL
	Minimum	Mean	Mean
Base	-5.8	2.6	12.7
1	-8.1	1.1	10.4
2	-3.7	2.4	12.8
3	-3.7	2.4	12.8
4	-3.0	2.7	13.2
5	-2.0	3.3	13.5
Ambient	-12.6	-2.4	4.5

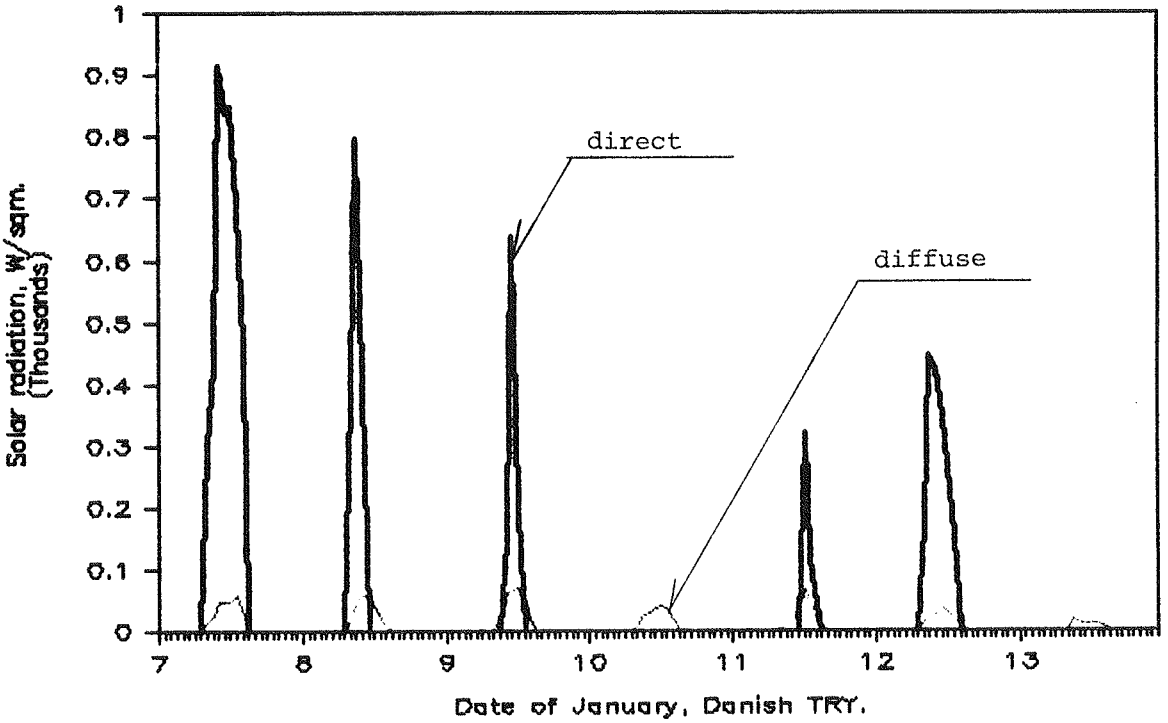

Fig. 7.13 Direct and diffuse radiation at a vertical south surface for selected week of January.

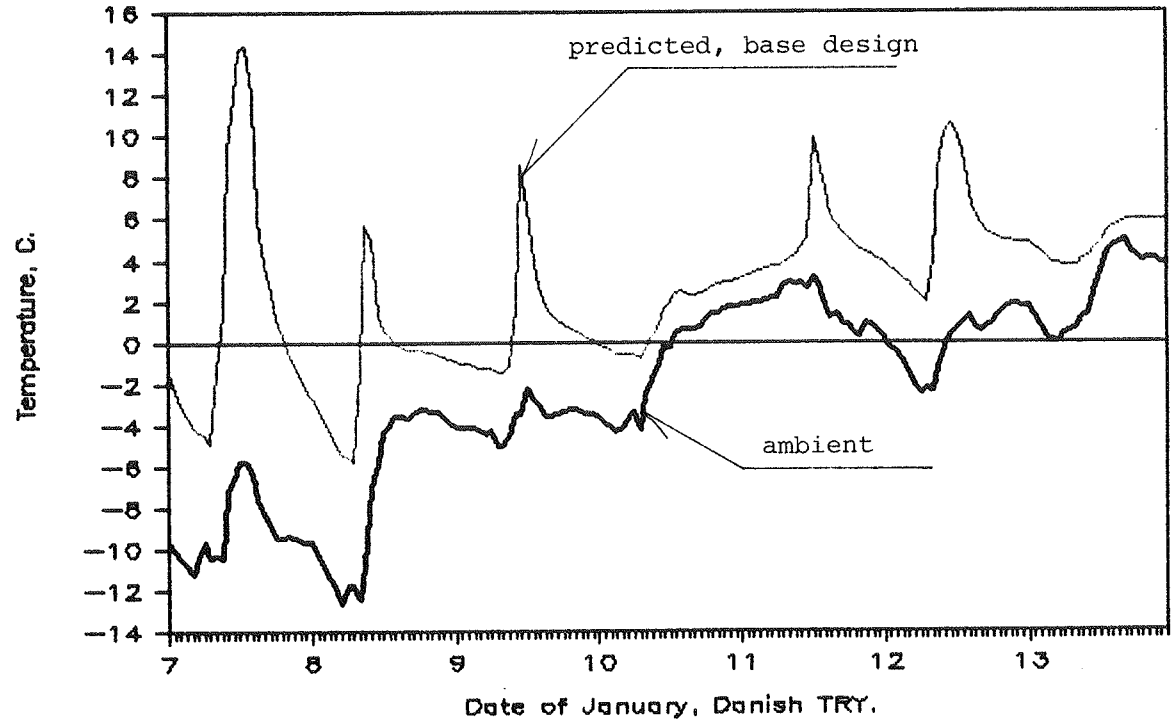

Fig. 7.14 Ambient and predicted temperatures for base design.

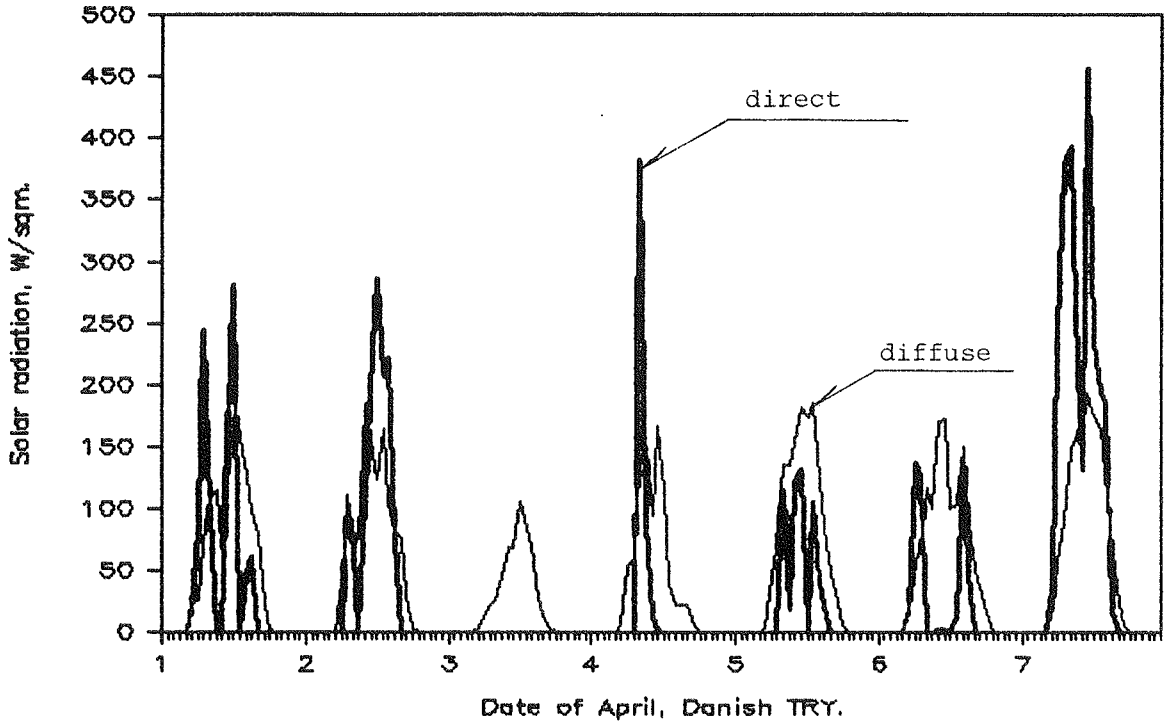

Fig. 7.15 Direct and diffuse radiation at a vertical south surface for selected week of April.

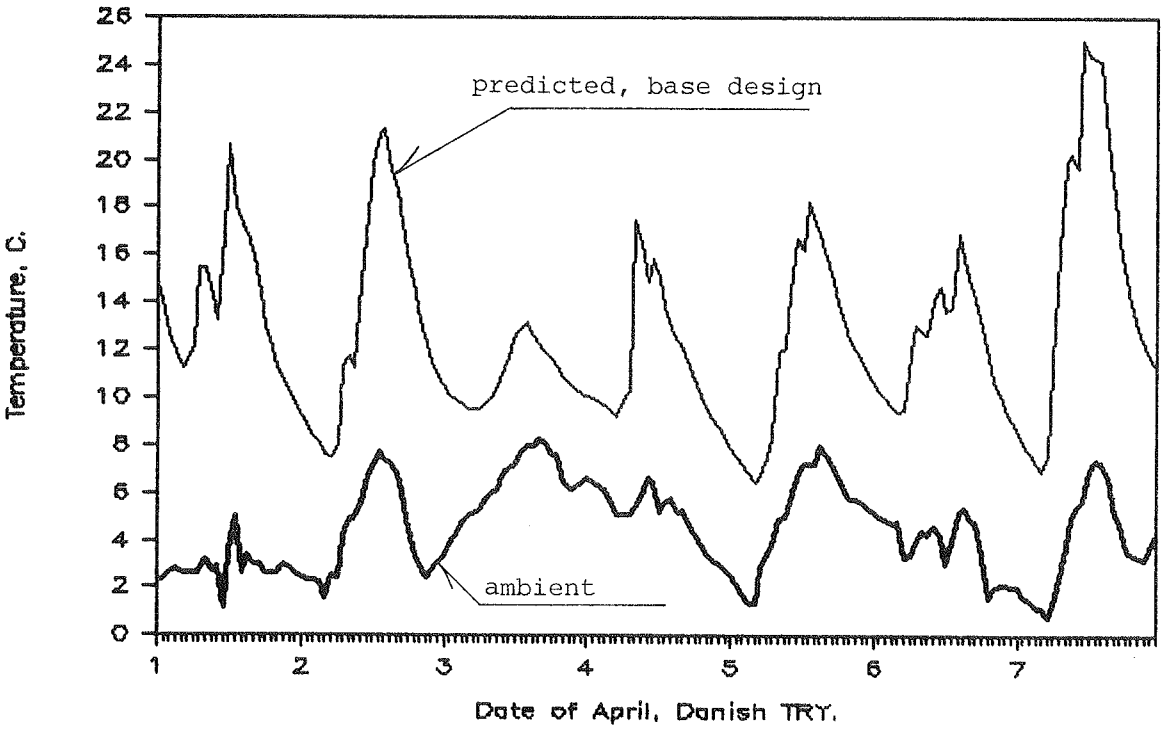

Fig. 7.16 Ambient and predicted temperatures for base design.

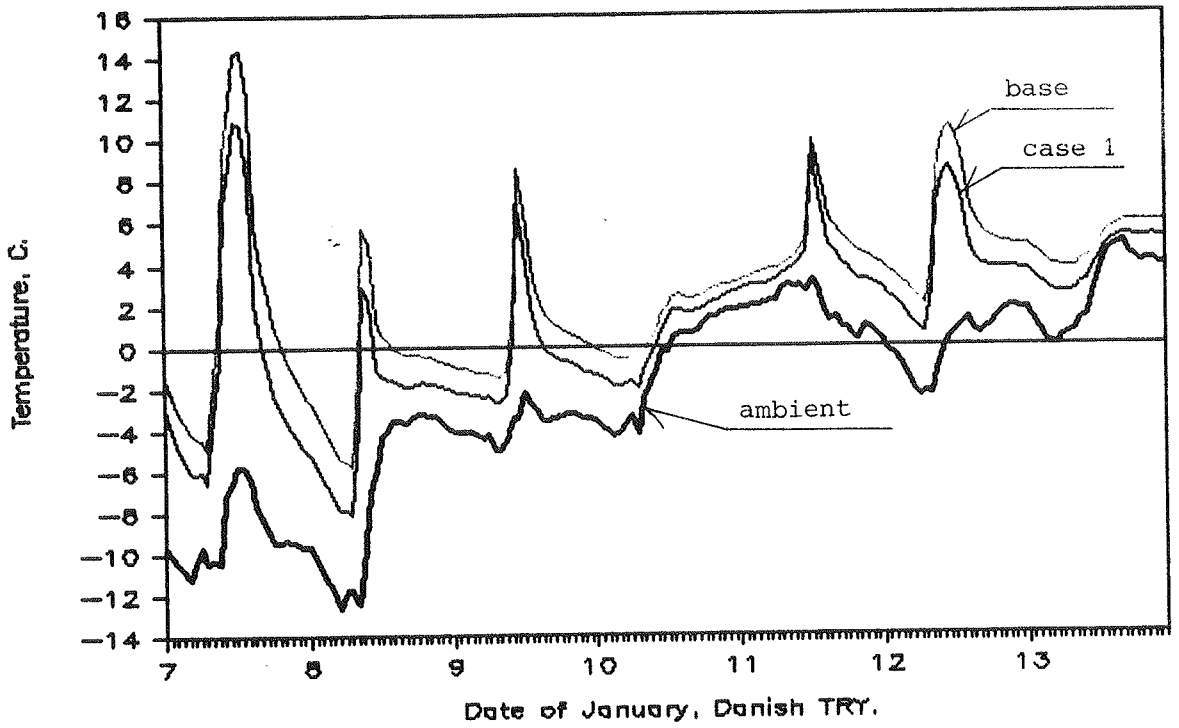

Fig. 7.17 Predicted temperature of sunspace with one layer of glass compared to base design temperature.

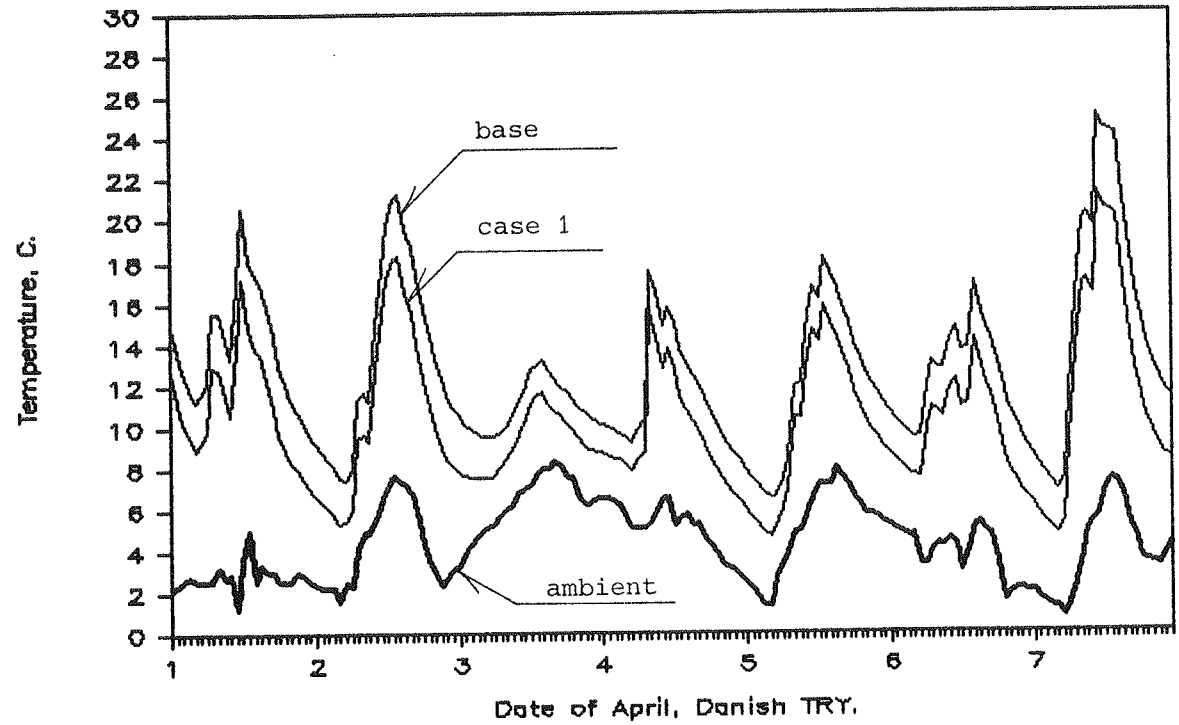

Fig. 7.18 Predicted temperature of sunspace with one layer of glass compared to base design temperature.

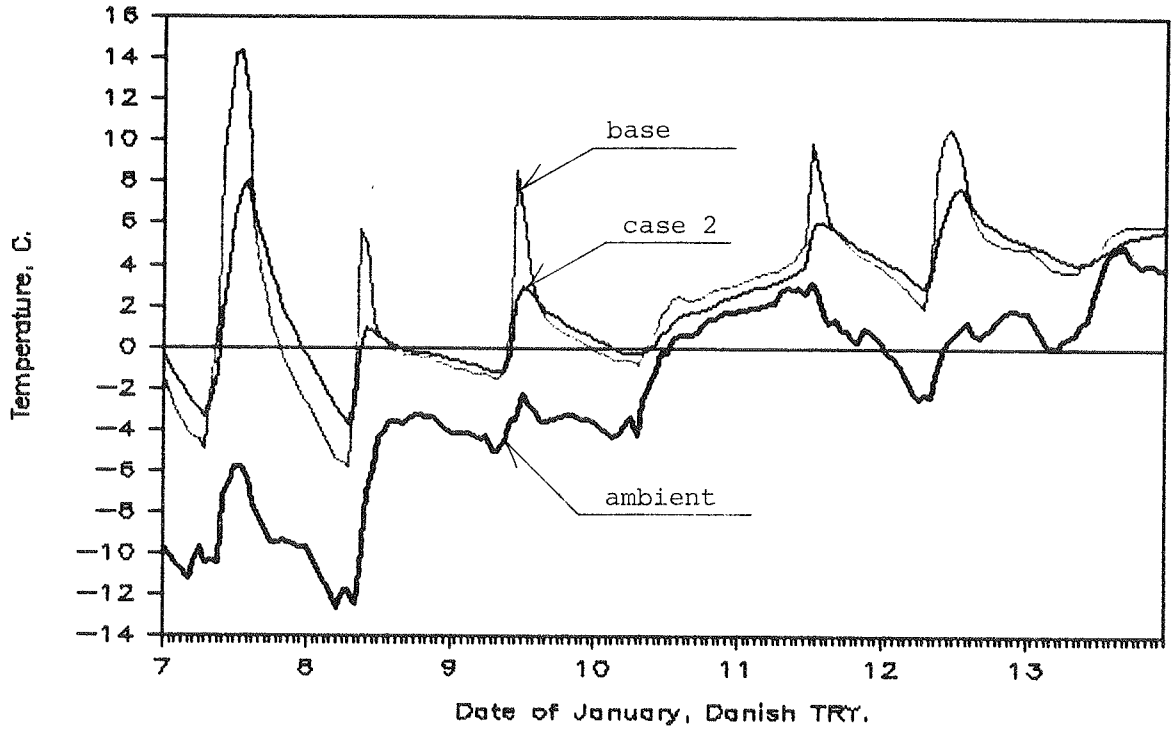

Fig. 7.19 Predicted temperature of sunspace with added mass (250 litres of water) compared to base design temperature.

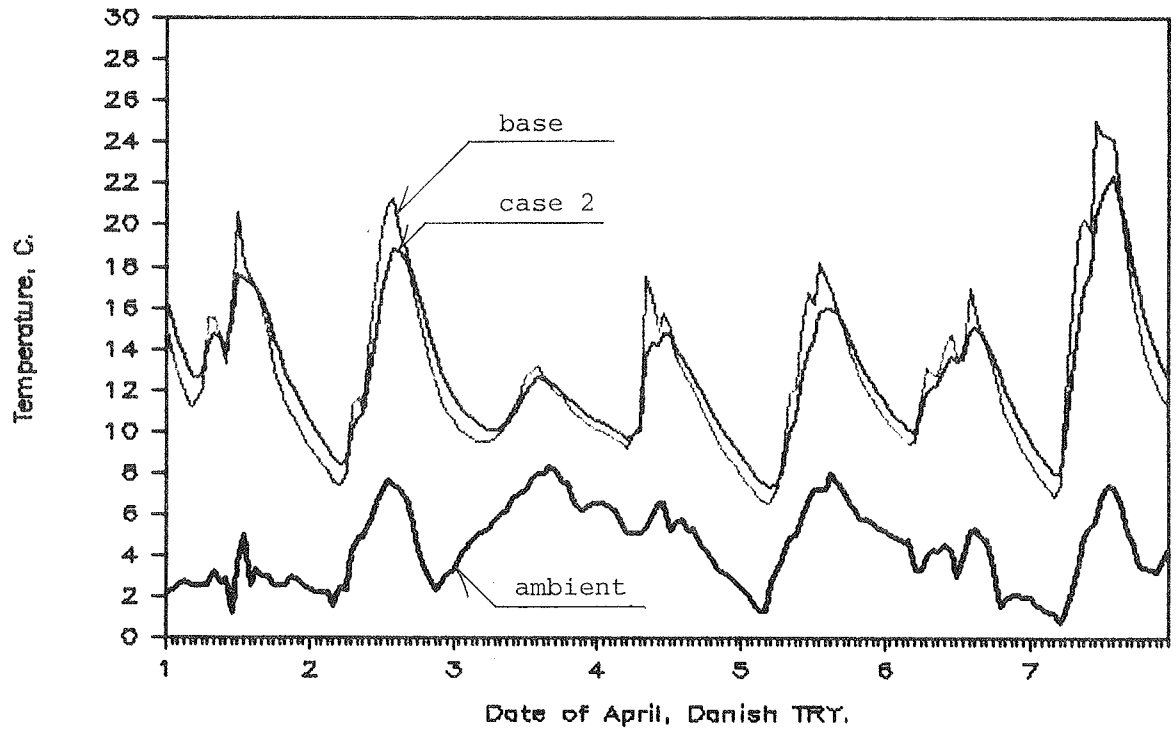

Fig. 7.20 Predicted temperature of sunspace with added mass (250 litres of water) compared to base design temperature.

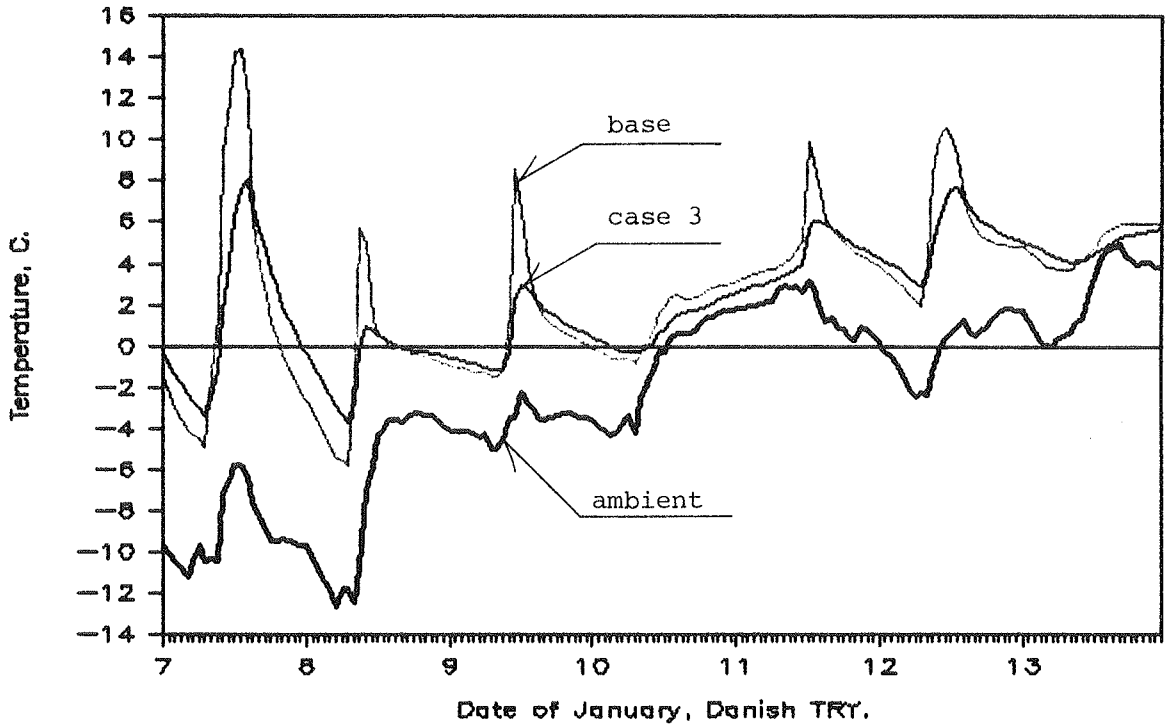

Fig. 7.21 Predicted temperature of sunspace with added mass (500 litres of water) compared to base design temperature.

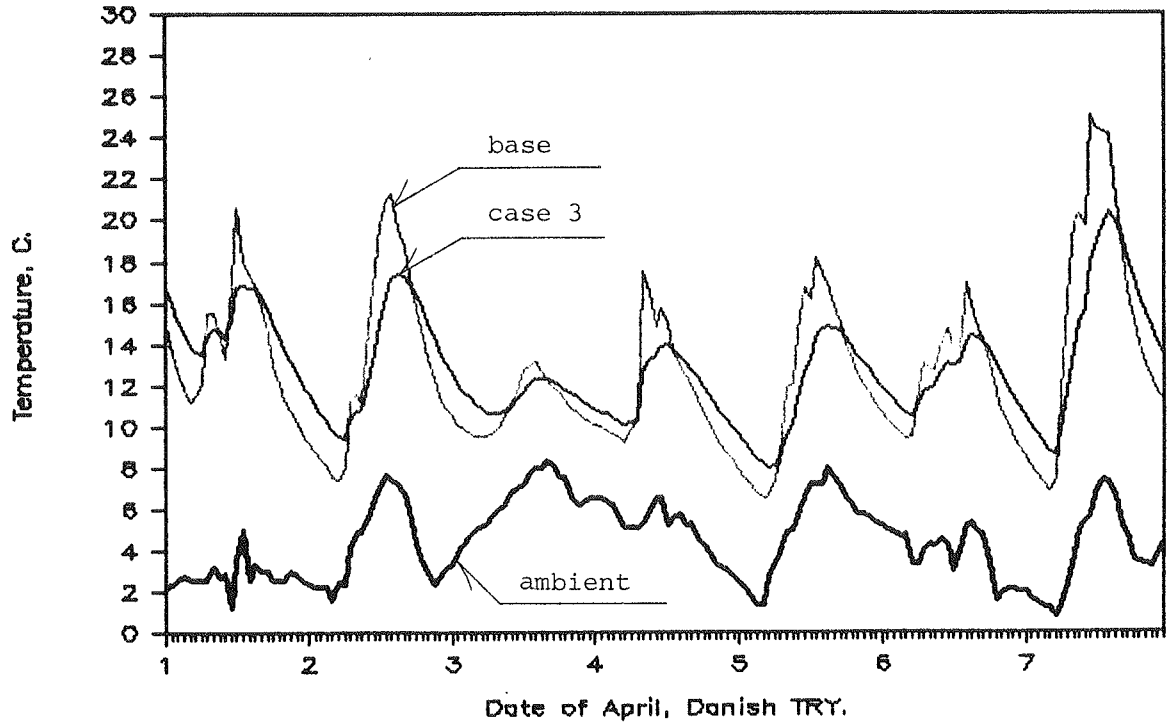

Fig. 7.22 Predicted temperature of sunspace with added mass (500 litres of water) compared to base design temperature.

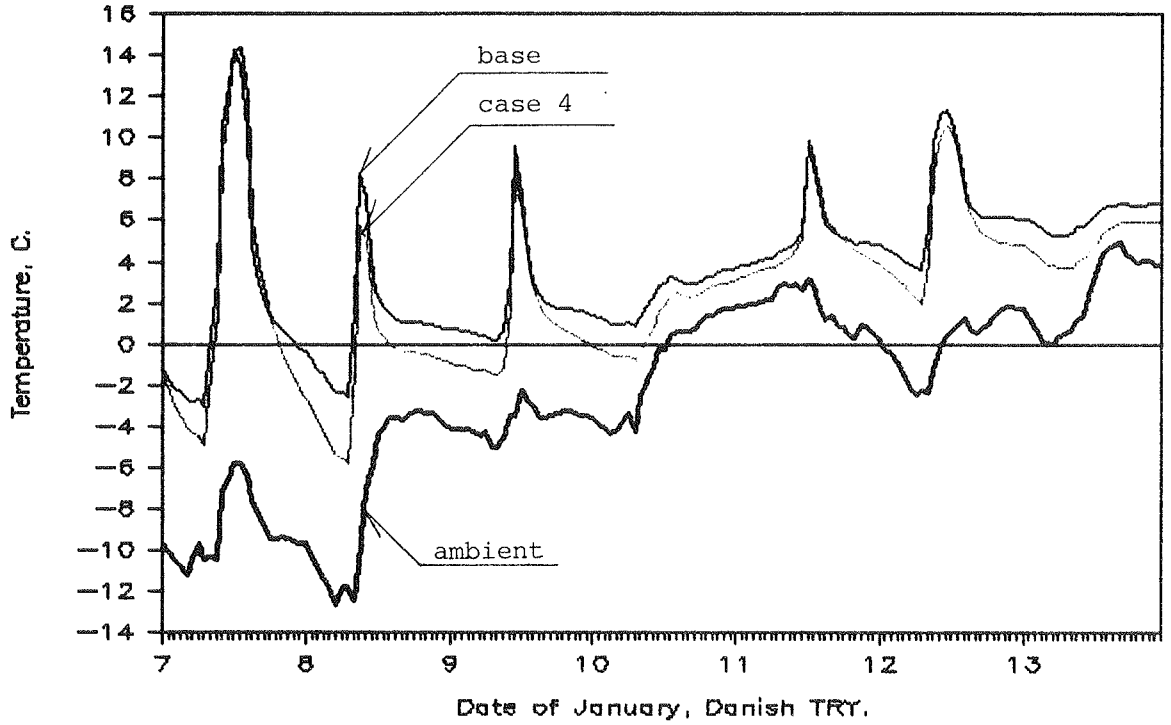

Fig. 7.23 Predicted temperature of sunspace with insulated end walls and unglazed part of ceiling compared to base design temperature.

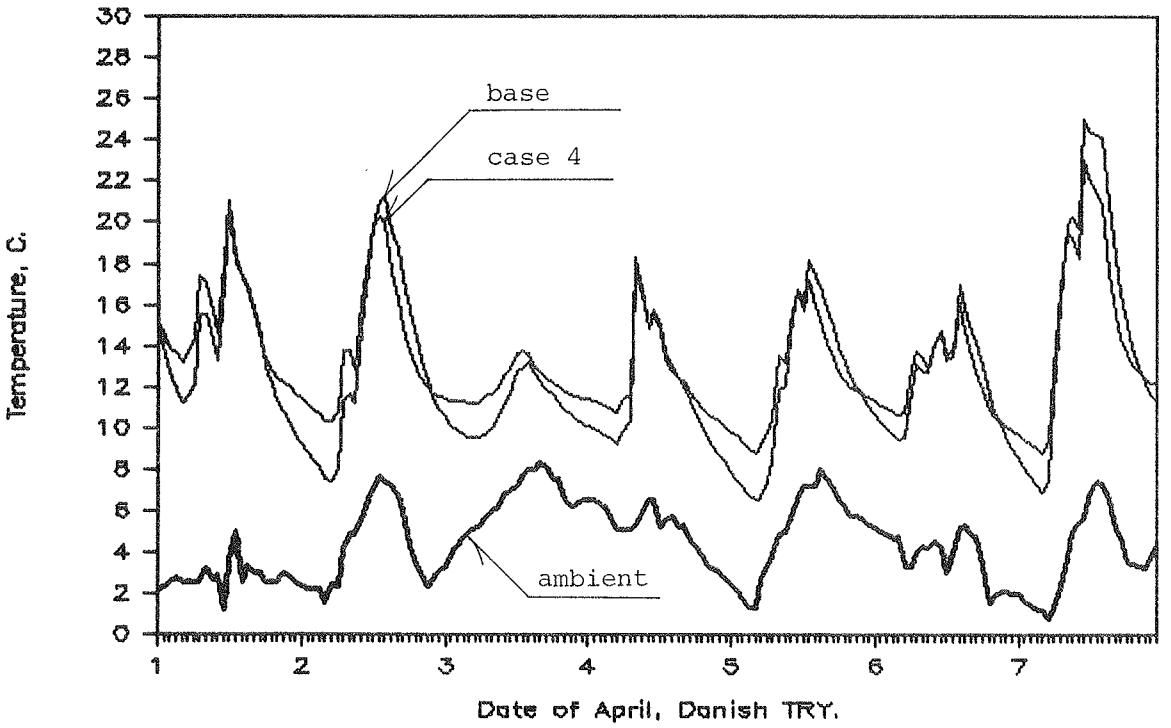

Fig. 7.24 Predicted temperature of sunspace with insulated end walls and unglazed part of ceiling compared to base design temperature.

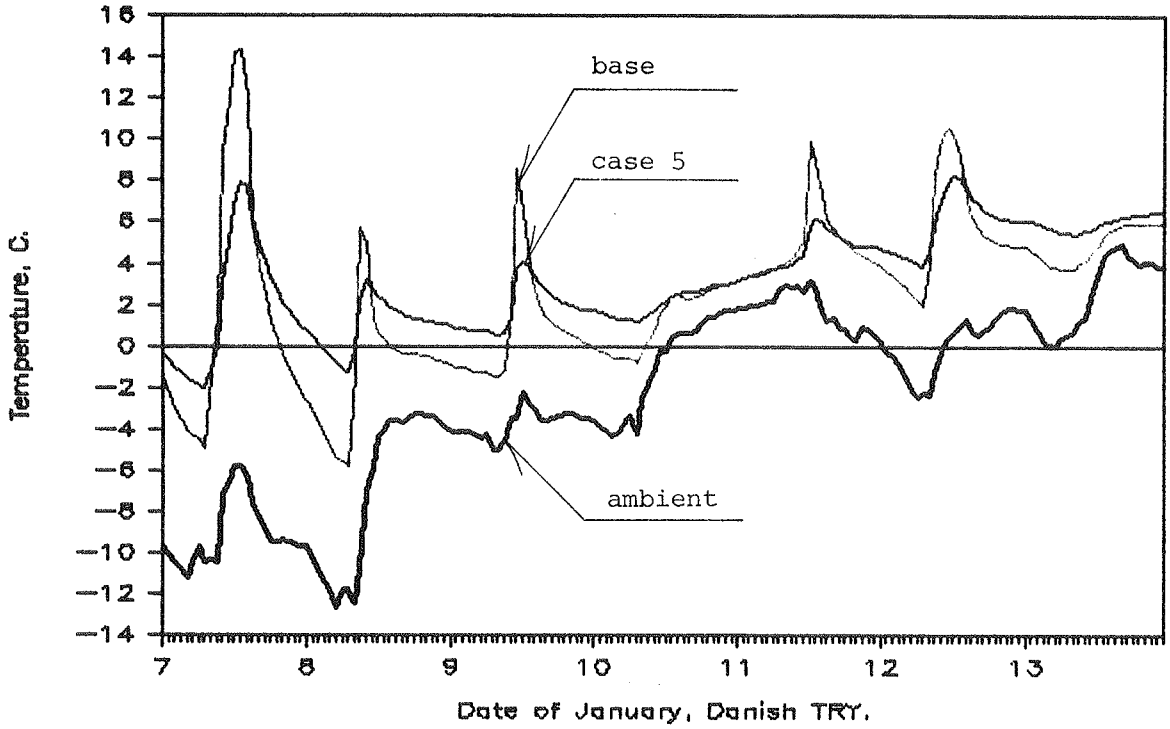

Fig. 7.25 Predicted temperature of sunspace with added mass and insulation compared to base design temperature.

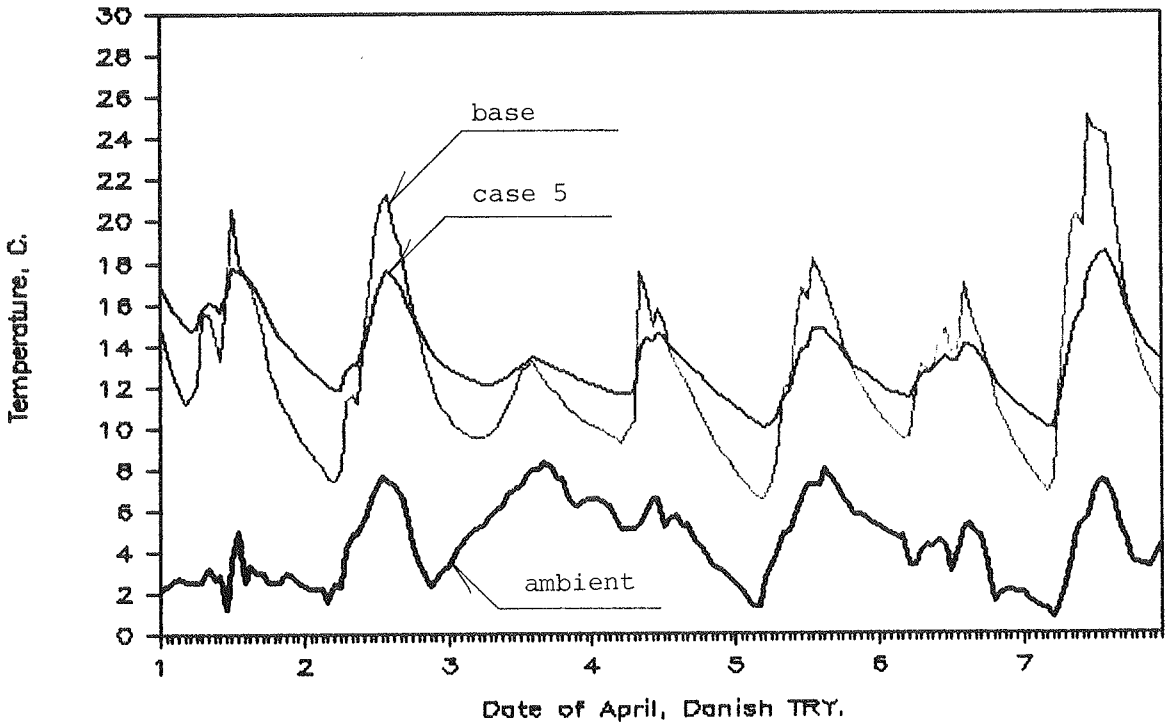

Fig. 7.26 Predicted temperature of sunspace with added mass and insulation compared to base design temperature.

8. CONCLUSION

The ability of mathematical simulation models to accurately predict the thermal performance of active as well as passive solar heating systems has been verified, not only by the validation studies performed in the course of the work presented in this document, but also by many other workers for different buildings and systems.

It has also been shown that the use of the simulation models is of extreme importance to the credibility of the results. The interpretation of the building or system, which is reflected in the choice of input data and parameters, is not always straightforward, and may lead to quite different results obtained by different users of the same program.

Consequently, the interface between the matematical simulation models and the users needs further development. This is true especially for programs intended for use by designers, who are without insight in the mathematics and the underlying assumptions of the programs.

With the rapid development of Computer Aided Design (CAD) and Computer Aided Engineering (CAE) programs follows an obvious opportunity for integrating thermal analysis capabilities within these programs.

The aim of this development will be to ease the work for the designer, making it possible to quickly assess the thermal implications of different design strategies at an early stage of the design process.

The interface between the CAD-system and the thermal simulation model therefore becomes the cornerstone of the development. Currently work is underway to develop an interface between the CAD-system SCRIBE and the thermal simulation program SERI-RES (Littler, 1984). In the coming years a large effort has to be put into the development of standardized interfaces and ways of storing intermediate data between the CAD-systems and the CAE-systems.

Another area of development for thermal simulation programs is to increase their ability to handle more complex systems. Very few of the larger thermal simulation programs can be used to model hybrid solar heating systems with natural convection charge or discharge of the thermal storage.

The final goal of these developments is to provide efficient tools for architects and designers, enabling them to create buildings and systems, which efficiently utilizes solar energy.

SAMMENFATNING

Matematiske modeller til simulering af solvarmesystemer introduceres som nødvendige og nyttige redskaber i såvel forsknings- som projekteringssammenhæng. Der lægges særlig vægt på fremgangsmåden for udvikling, evaluering og brug af simuleringsmodeller, og denne benyttes som underliggende tema for afhandlingen.

Udviklingsarbejdet for et computerprogram til simulering af solvarmesystemer, omfattende definition af det foreliggende system, opdeling i komponenter og fastlæggelse af grænsebetingelser beskrives. Der redegøres for udvalgte fysisk-teoretiske emner fra varmelæren, der benyttes som grundlag for modelopbygningen.

En sammenfatning af forfatterens tidligere arbejder med udvikling og validering af simuleringsprogrammer for aktive solvarmesystemer gives.

Udviklingen af et simuleringsprogram baseret på opbygningen af et termisk netværk beskrives. Der lægges særlig vægt på opdeling af den indfaldende solstråling i direkte og diffust sollys, på transmission og absorption i vinduer, samt på en korrekt simulering af kontrollen af opvarmningssystemet. Desuden præsenteres programmets opbygning.

Efter en kort introduktion til begrebet validering beskrives to forskellige empiriske valideringsforløb foretaget med den udviklede model. Modelberegningerne viser god overensstemmelse med målingsresultaterne, for dels en testbygning med direkte solindfald, og dels en glastilbygning.

Anvendelse af simuleringsmodeller illustreres ved tre forskellige eksempler: En parameterfølsomhedsanalyse, en sammenligning af direkte solindfalds- og solvægs-solvarmesystemer samt en undersøgelse af betydningen af konstruktionsændringer for

glastilbygningen, anvendt i valideringsarbejdet.

I de afsluttende bemærkninger skitseres mulighederne for projektering af solvarmesystemer ved anvendelse af simuleringsmodeller som en integreret del af fremtidens "Computer Aided Design" (CAD) systemer. Opmærksomheden henledes på, at forbindelsen mellem CAD-systemer og termiske simuleringsprogrammer er et kritisk nøgleområde for disse programkomplekser.

NOMENCLATURE

Roman letters

A	area
C	total system capacity
C_p	constant pressure heat capacity per unit mass
^oC	Celcius
F	free heat gain
F_R	collector heat removal factor
F_R'	correction factor for collector fin efficiency, collector flow rate and heat exchanger effectiveness
F_R''	$F_R' \cdot F_R$
F_S	storage temperature increase correction coefficient
G	global solar irradiation
G_b	beam solar irradiation
G_d	diffuse solar irradiation
h	film heat transfer coefficient
k	thermal conductivity
K	Kelvin
L	length
m	resistance
N_{Bi}	Biot number
Q	auxiliary heating, total heat transferred
Q_u	useful solar heat gain
S	transmitted and absorbed solar gain
T	temperature
U	overall heat transfer

U_L collector overall loss coefficient

V volume

Greek letters

α thermal diffusivity; solar radiation absorption

β slope angle from horizontal

ρ density; ground reflection coefficient

τ time constant; collector warm up period; solar radiation transmission

τ_c overall collector time constant

θ incidence angle of solar radiation

Mathematical symbols

$\underline{\underline{A}}$ matrix

$\underline{\underline{A}}_{|}$ column matrix

$\underline{\underline{A}}^{-1}$ inverse matrix

$\frac{\partial}{\partial t}$ partial derivative

Δ difference

∇^2 "Laplacian" operator

π pi = 3.14159...

REFERENCES

Barakat, S.A. (1982). Passive Solar Heating Studies at the Division of Building Research, Note 188. National Research Council Canada, Ottawa.

Duffie, J.A. and W.A. Beckman, (1980). Solar Engineering of Thermal Processes, Wiley, New York.

International Energy Agency (IEA), (1983). Implementing Agreement for a Programme to Develop and Test Solar Heating and Cooling Systems.

Hedstrom, J. (1981). Validation of Simulation Models using measured Performance Data from the Los Alamos Study Center. IEA Solar Heating and Cooling Programme, Task I. Los Alamos National Laboratory. LA-9028-MS.

Holtz, J.M. and F.D. Teller (1984). Parametric Sensitivity Study Base Buildings. IEA Task VIII, Subtask B. Architectural Energy Corporation, Col., U.S.A.

Jacoby, S.L.S. and J.S. Kowalik, (1980). Mathematical Modelling with Computers. Prentice Hall.

Judkoff, R., D. Wortman, B. O'Doherty and J. Burch, (1983). A Methodology for Validating Building Energy Analysis Simulations. SERI/TR-254-1508.

Jørgensen, O. (1979a). CEC Solar Energy R-D Programme, Project A. Modelling and Simulation Part. Thermal Insulation Laboratory, Technical University of Denmark.

Jørgensen, O. (1979b). CEC Solar Energy R-D Programme, Project A. Modelling and Simulation Part. Description of Simulation Codes and Monthly Tables. Thermal Insulation Laboratory, Technical University of Denmark.

Jørgensen, O. (1979c). Modelling and Simulation. IEA Solar Heating and Cooling Programme, Task I. Thermal Insulation Laboratory, Technical University of Denmark.

Jørgensen, O. and K. Mørkeberg (1980). Solar System Model Validation Using NBS Hot Water Systems. Thermal Insulation Laboratory, Technical University of Denmark, Internal Report.

Jørgensen, O. (1982a). Common Solar Simulation and Validation in Europe. Thermal Insulation Laboratory, Technical University of Denmark, Report No 119.

Jørgensen, O. (1982b). Simulation Program Validation using Domestic Hot Water System Data. IEA Solar Heating and Cooling Programme, Task 1. Thermal Insulation Laboratory, Technical University of Denmark, Report No 125.

Jørgensen, O. (1983a). Analysis Model Survey. IEA Solar Heating and Cooling Programme, Task VIII, Thermal Insulation Laboratory, Technical University of Denmark, Report No 143.

Jørgensen, O. (1983b). Subtask B Direct Gain Validation Exercise. IEA Solar Heating and Cooling Programme, Task VIII, Thermal Insulation Laboratory, Technical University of Denmark.

Jørgensen, O. (1984). Monitoring Programme for the Danish IEA building project SMÅKKEBO. Thermal Insulation Laboratory, Technical University of Denmark. Working Document.

Kennish, W.J. (1978). An Approach to the Validation of Computer Simulation Codes. Sandia Laboratories. SAND78-0433.

Klein, S.A. (1973). The Effects of Thermal Capacitance upon the Performance of Flat-Plate Solar Collectors. Master's Degree Thesis, University of Wisconsin.

Lawaetz, H. (1980). Solindfald og solvarmeanlæg - målt og beregnet. Thermal Insulation Laboratory, Technical University of Denmark, Report No 106.

Littler, G.F. (1984). London, Building Unit. Polytechnic of Central London, Building Unit. Private Communication.

Lund, H. (1985). Test Reference Years. Commission of the European Communities, EUR 9765.

Mørck, O. (1985). Simulation Program Validation using Passive Test Cell Data. IEA, Task VIII, Thermal Insulation Laboratory, Technical University of Denmark (To be published).

Mørck, O., M. Holtz, Å. Blomsterberg and T. Jacobsen (1985). Performance Evaluation Procedures for Subtask D Construction Projects. IEA Solar Heating and Cooling Programme, Task VIII. Interim report.

Orgill, J.F. and K.G.T. Hollands. Solar Energy, 19, 357 (1977). "Correlation Equation for Hourly Diffuse Radiation on a Horizontal Surface".

Palmiter, L. and T. Wheeling. SERI-RES, Version 1.0. Solar Energy Research Institute, Golden, Colorado.

Pedersen, P.V. and O. Jørgensen, (1979). Validation of the SVS Solar Heating System Simulation Code. Thermal Insulation Laboratory, Technical University of Denmark, Report No 95.

Pipes, A.P. and S.A. Hovanessian, (1969). Matrix-computer Methods in Engineering. John Wiley & Sons. New York. USA.

Steinmüller, B. The two-solarimeter method for insolation on inclined surfaces. Philips Gmbh Forschungslaboratorium Aachen.

Turlejski, S. (1985). Model of the Process of Heat-Exchange Indoors. Proceedings of First Danish-Polish Workshop on Modelling Heat Flow and Fluid Flow Problems, 53-71.

U.S. DOE (1981). Comparison of Load Determination Methodologies for Building Energy Analysis Program, IEA Energy Conservation in Buildings and Community Systems, Annex 1. (IEA Confidential).

Whitaker, S. (1983). Fundamental Principles of Heat Transfer. Robert E. Krieger. Florida, USA.

Wray, W.O. (1981). Design and Analysis of Direct Gain Solar Heated Buildings. Los Alamos Scientific Laboratory, LA-8885-MS.

BIBLIOGRAPHY

Butti, K. and J. Perlin (1980). A Golden Thread, Cheshire Books, Palo Alto, U.S.A.

Howell, H.R. and H.J. Sauer, Jr. (1980). Bibliography on Available Computer Programs in the General Area of Heating, Refrigerating, Air Conditioning and Ventilating. ASHRAE.

Jørgensen, O. (1983a). Analysis Model Survey. IEA Solar Heating and Cooling Programme, Task VIII, Thermal Insulation Laboratory, Technical University of Denmark, Report No 143.

Klein, S.A. (1983). Passive Solar Journal, 2,57, "Computers in the Design of Passive Solar Systems".

Morgan, E.M. (1961). Improvements in Solar Heated Buildings. Patent Specification 1,022,411, London. Patent Office - E1 A26; F4 U60.

D. Nordham (Ed.) (1981). Microcomputer Methods for Solar Design and Analysis. SERI/SP-722-1127.

A.V. Sebald (Ed.) (1979). Mathematical Models and Simulation in Solar Energy Research for Buildings, Pergamon Press. NY. USA.

SERI (1980). Analysis Methods for Solar Heating and Cooling Applications, 3rd Edition. SERI/SP-35-232R.

Versteegen, P.L. (1978). Survey of currently used simulation methods. Science Applications, Inc. US.DOE Contract EM-78-C-04-42651.

APPENDIX

Solar Energy Vol. 29, No. 2, pp. 175–176, 1982
Printed in Great Britain.

0038-092X/82/080175-02$03.00/0
Pergamon Press Ltd.

TECHNICAL NOTE

Collector heat capacity effect on solar system performance

O. C. JØRGENSEN†
Thermal Insulation Laboratory, Technical University of Denmark, Bld. 118, 2800 Lyngby, Denmark

(*Received* 7 *July* 1981; *accepted* 18 *November* 1981)

INTRODUCTION

The effects of collector heat capacity are often treated in two distinct parts. Duffie and Beckman[1]: "One part is due to the heating of the collector from its early morning low temperature to its final operating temperature in the afternoon. The second part is due to intermittent behaviour during the day whenever the driving forces such as solar radiation and wind change rapidly". The two effects are referred to as the "storage" effect and the "transient" effect. It has been shown[2] that the latter can be considered negligible. To estimate the reduction in useful energy gain because of the storage effect Duffie and Beckman[1] suggest multiplying the effective collector heat capacity by the temperature rise necessary to bring the collector to its inital operating temperature. However, this procedure does not account for the fact that the collector circuit pump is not switched on during the period of heating up of the collector to its operating temperature. To neglect this leads to erroneous estimations of the reduction in useful energy gain.

Time delay

Following Duffie and Beckman[1] the differential equation of the collector plate temperature can be simplified to

$$(mC)_e \frac{dT_p}{d\tau} = A_c[S - U_L(T_p - T_a)] \tag{1}$$

and with the assumption that S and T_a are constant for some period τ the solution to eqn (1) is

$$\frac{S - U_L(T_p - T_a)}{S - U_L(T_{p,\,\text{initial}} - T_a)} = e^{-(A_c U_L \tau/(mC)_e)}. \tag{2}$$

If the plate stagnation temperature (or equilibrium temperature)

$$T_s = (S + U_L T_a)/U_L \tag{3}$$

and the collector time constant

$$\tau_c = (mC)_e/A_c U_L \tag{4}$$

are introduced, eqn (2) can be rearranged to yield

$$T_s - T_p = (T_s - T_{p,\,\text{initial}})e^{-(\tau/\tau_c)}. \tag{5}$$

Equation (5) can be used not only to find the temperature of the absorber plate at the end of each time step when there is no flow in the collector, but also to find when the absorber plate reaches a certain temperature, e.g. the set point temperature for the controller to switch on the pump.

Applying the natural logarithm to both sides of eqn (5) and rearranging yields

$$\tau = \tau_c \ln[(T_s - T_{p,\,\text{initial}})/(T_s - T_p)]. \tag{6}$$

†Member of SEAS/ISES.

EXAMPLES

Using example 6.11.1 from Duffie and Beckman[1] as the basis, we have the following parameters and variables:

$(mC)_e$	$8000\ JC^{-1}$
U_L	$8\ Wm^{-2}\ C^{-1}$
A_c	$1\ m^2$
τ_c	$1000\ s$
F_R	0.8
$T_{p,\,\text{initial}}$	$25\ C$
$T_{p,\,\text{operating}}$	$40\ C$
S	$3.16\ MJm^{-2}/3600\ s = 878\ Wm^{-2}$
T_a	$2\ C$

The collector pump surely switches on in this hour, and the useful energy calculated by the simple non-capacity HWB equation is

$$0.8 \times [878 - 8(40 - 2)] \times 3600 = 1.65\ MJm^{-2}.$$

Following Duffie and Beckman[1] the reduction due to the storage effect is

$$8 \times 15 = 120\ kJm^{-2}.$$

If we instead use eqn (6) to find when the operating period begins

$$\tau = 1000 \ln (112 - 25)/(112 - 40) = 189\ s$$

the calculated useful energy has to be reduced by a factor of

$$189/3600.$$

The reduction calculated like this amounts to

$$1.65 \times 189/3600\ MJm^{-2} = 86\ kJ/m^{-2}.$$

It is seen that both estimates of the reduction are linearly proportional to the collector heat capacity. The dependence on solar irradiance, however, is not the same. Choosing a special example with $S = 337\ Wm^{-2}$ the useful energy calculated with no reduction becomes $120\ kJm^{-2}$. The reduction estimated following Duffie and Beckman will be the same as in the previous example $= 120\ kJm^{-2}$, resulting in a zero net energy gain. The correction calculated by the proposed method is $51\ kJm^{-2}$, resulting in a positive net energy gain equal to $69\ kJm^{-2}$.

The difference observed between the two approaches in these two examples is due to two different facts: While the collector is heated the losses are smaller than during the period of operation, and the solar gain heating the collector is not reduced by the collector heat removal factor.

DISCUSSION

In the above, the starting up effect of the collector heat capacity is treated. It is shown that the reduction in useful solar

gain will be somewhat overestimated by using the method proposed by Duffie and Beckman[1]. Since these examples in no way can be said to represent all situations and since the effect of the collector heat capacity when the collection stops is not considered here, no attempt shall be made to draw firm conclusions with respect to the importance of the collector heat capacity on the system performance on a dayly, monthly or yearly basis. Such conclusion would, in additon, take some investigations where the control temperature set points are taken into consideration.

NOMENCLATURE

$(mC)_e$ effective collector heat capacity, JC^{-1}
A_c collector area, m^2
S absorbed solar irradiance, Wm^{-2}
U_L overall collector loss coefficient, Wm^{-2}
T_p plate temperature, C
T_a ambient temperature, C
τ time, s
T_s plate stagnation temperature, C
τ_c collector time constant, s
F_R collector heat removal factor

REFERENCES

1. J. A. Duffie and W. A. Beckman, *Solar Engineering of Thermal Processes*, pp. 233–236. Wiley, New York (1980).
2. S. A. Klein, The effects of thermal capacitance upon the performance of flat-plate solar collectors. Master's Degree Thesis, University of Wisconsin (1973).

LICENTIATE DISSERTATIONS FROM THE THERMAL INSULATION LABORATORY

Rubinstein, Axel:
Metoder til bestemmelse af varmeledningstal, med særlig vægt på teorien for de instationære metoder samt nogle målinger med en termosonde af egent konstruktion. 1963.

Petersen, Erwin:
Solindfald gennem vinduer. 1966.

Lund-Hansen, Per:
Fugttransport i Byggematerialer. 1967.

Nicolajsen, Asta:
Fugttransportkoefficienter for gasbeton. 1973.

Nielsen, A.F.:
Fugtfordelinger i gasbeton under varme- og fugttransport. 1974.

Nielsen, Peter V.:
Strømningsforhold i luftkonditionerede lokaler. 1974.

Ravn-Jensen, Lars:
Vinduer og energi. 1977.

Lawaetz, Henrik:
Solindfald og solvarmeanlæg. Beregnet og målt. 1980.

Svendsen, S.:
Solfangeres effektivitet. Målt og beregnet. 1981.

Kielsgaard Hansen, Kurt:
Luftsolfangere og varmelagring i jord. 1982.

Furbo, Simon:
Varmelagring til solvarmeanlæg. 1984.